

Manuscript Number: CATENA6011R1

Title: Four-topic correlation between flood dendrogeomorphological evidence and hydraulic parameters (the Portainé stream, Iberian Peninsula)

Article Type: Research Paper

Keywords: Dendrogeomorphology; Fluvial geomorphology; Hydraulic modelling; Palaeoflood; Spanish Pyrenees.

Corresponding Author: Miss Ane Victoriano,

Corresponding Author's Institution: Facultat de Ciències de la Terra, Universitat de Barcelona

First Author: Ane Victoriano

Order of Authors: Ane Victoriano; Andrés Díez-Herrero; Mar Génova; Marta Guinau; Glòria Furdada; Giorgi Khazaradze; Jaume Calvet

Abstract: Torrential floods are hazardous hydrological phenomena that produce significant economic damage worldwide. Flood reconstruction is still problematic in mountainous ungauged areas due to the lack of systematic real data, so other indirect techniques are required. This paper presents an integrated palaeoflood study of a Pyrenean stream that combines fluvio-torrential geomorphology, dendrogeomorphology, palaeoflood discharges and flow hydraulics. The use of a total station and airborne LiDAR data has allowed obtaining a detailed topography for geomorphological mapping and for running a one-dimensional hydraulic model. Based on the height of scars on several damaged trees, we obtained palaeodischarges of 316 m³s⁻¹ and 314 m³s⁻¹ for the 2008 and 2010 floods. The hydraulic parameters were related to the geomorphic position of trees, showing a positive relation between most energetic geomorphic elements and flow depth and velocity values. The most intensely affected trees are located in intermediate energy geomorphic positions. Analysing variabilities in scar height and flow stage differences, we suggest that most reliable trees for peak discharge estimation correspond to those placed in areas related with fluvio-torrential processes of intermediate energy. This multidisciplinary palaeohydrological study relates flood hydrodynamics with the damages on trees and their geomorphological characteristics, focusing on the hydraulic parameters of the peak flow (depth, velocity and unit stream power), which has never been carried out elsewhere. The proposed approach shows a high potential for palaeoflood analysis in ungauged mountain catchments with scarce non-systematic data.



Barcelona, Juny 26th, 2017

Manuscript for *Catena*

Dear Editor Gert Verstraeten,

We would like to thank the three reviewers for their useful comments on our paper "**Four-topic correlation between flood dendrogeomorphological evidence and hydraulic parameters (the Portainé stream, Iberian Peninsula)**". All the comments were taken into account and incorporated in the reviewed version.

Enclosed you will find the following documents, which are the result of the thorough revision:

- Revision notes: point by point response to each editor's and reviewers' comment indicating how and where the changes have been introduced in the manuscript (pdf document entitled "Revision notes Victoriano_et_al"). We are aware that the extension of this document is longer than usual but this is because we received comments from the editor and three reviewers and we answered to all of them in detail.
- Revision, changes marked: the tracked-changes version of the manuscript that includes all the changes as a result of the revision (word document entitled "Revision changes marked Victoriano_et_al").
- Revision, unmarked: the new revised manuscript (word document entitled "Manuscript Victoriano_et_al").

This revision has improved the quality of the manuscript, hoping it is now suitable for publication in CATENA.

Sincerely,

Ane Victoriano and co-authors

Correspondence to: ane.victoriano@ub.edu

Departament de Dinàmica de la Terra i de l'Oceà

University of Barcelona

RISKMAT Research Group

REVISION NOTES

We thank the three reviewers for finding the paper interesting and for their useful revisions. We considered each comment made by the editor and the three reviewers, which considerably improved the quality of the manuscript. These corrections and suggestions have been incorporated in the new revised version of the manuscript, and can be easily identified in the marked version. A point-by-point response to each point of the reviewer's comments is presented here, and the changes are referred by indicating line numbers of the "Revision changes marked" document.

1. EDITOR

The authors thank the editor for his decision on the manuscript. Regarding missing methodology and inappropriate references, they have been corrected by properly detailing the dendrogeomorphological methods and avoiding inaccessible or unpublished literature. The structure of the paper has also been improved. Some contents from the results section have been moved to methods, and we have changed the structure of the methods section to be coherent with the four-topic correlation addressed in the introduction. See response to comments from the reviewers for further details.

2. REVIEWER 1

The paper relates fluvial geomorphology and dendrogeochronology for flood reconstruction and, as stated by the reviewer, this has been previously assessed. However, apart from building stronger evidence, it also contributes on the quantification of the relation of geomorphology and tree-ring series with the specific hydraulic parameters (water depth, velocity and stream power) by analysing these variables according to the different geomorphic positions. Moreover, the stream power obtained for hydraulic reconstruction (modelling) is used to estimate the mobilizable particle size, which is compared to field measures in order to assess its reliability. Considering reviewer comments and the above explanations, the goal of the paper has been rewritten in the introduction section, to better represent the contribution of this paper. Besides, taking into account reviewer's suggestion, we shortened the text to avoid unnecessary or repetitive information (e.g. introduction, study area and discussion sections) and we better explained some important ideas that required further details (e.g. methods for dendrochronological analysis and hydraulic modelling). The resulting manuscript is more direct.

Reply to Major points

- 1) The reviewer asks to justify the applications of a 1D model instead of a 2D one. A 1D hydraulic model was considered the best choice for this case study due to several factors.
 - *Geometric factors*: the 2D resolution of the topography (even integrating LiDAR total station data) does not allow obtaining an accurate terrain model, so a 2D model, instead improving the palaeoflood reconstruction results, would include more uncertainties. In fact, the study area is too large to be homogeneously surveyed with a high point-density using the total station, but small enough to acquire significant points at topographic breaklines, cross-sections and trees. We

have high-quality cross-sections measures in the field coinciding with tree locations, which provides appropriate input data for a 1D cross section based depth averaged calculations. Besides, 1D models have been outlined as the best option for narrow valleys with a length/width ratio higher than 3:1 (Desktop Review of 2D Hydraulic Modelling Packages, UK Environment Agency, 2009). Last but not least, the lack of bridges, dams or other features that cause contraction/expansion in the study area, characterized by a “natural” straight river reach, make a 2D model unnecessary, as there are not features along the channel producing changes in the flow.

- *Hydrodynamic factors*: the study reach is a steep gradient stream without floodplains showing primarily unidirectional flow patterns. That is, the flow does not spread considerably. Especially when high discharges (like the modelled ones), there is no split flow, and the flow is not divided (nor braided).
- *Other evidence*: an apparent parallelism between the scars heights and riverbed has been observed in the field. Therefore, a gradually variable unidimensional model is enough for the study case.

Other studies at mountain steep-gradient reaches showing the same configuration and characteristics as the Portainé stream, have used 1D hydraulic modelling and proved its suitability (Bodoque et al., 2011). In the revised manuscript, the choice of a 1D model and its justification has been included in the methods section (3.3. Palaeodischarge estimations and hydraulic modelling; line 330-338).

2) In the original manuscript, hydraulic parameters were related to the position of the damaged trees according to the geomorphic form in which they locate (previously a geomorphological survey, mapping and classification was done). The reviewer suggests relating hydraulic parameters to other characteristics of the trees and not only their geomorphic position. Other studies, like Ballesteros-Cánovas et al. (2016) have analysed the specific characteristics of the position of the trees, such as the channel reach morphology, position with respect to the channel and the degree of exposure of the tree. During the review process, we have looked at these tree in-situ characteristics for our study area and the results are presented below.

- *Reach morphology*: the study reach is a straight steep-gradient mountain stream without bends. All the channel can be considered as straight.
- *Tree position respect to the channel*: this characteristic is already considered in our study, as the hydraulic parameters (depth, velocity, stream power) are calculated for channel and both riverbanks. When comparing those parameters to the geomorphic position of the trees, we used the specific values of the specific tree position (e.g., the depth is calculated exactly for the point where the tree locates).
- *Tree exposure*: we have looked in detail if the scarred trees had any obstacle (large boulder or other trees) 5 m upstream from them. There are no significant obstacles in our study area, only two large boulders, but they are far away from the scarred trees and not affecting them. Therefore, all the scarred trees can be considered to be exposed to the flow in the same degree

Hence, in our study area these characteristics are not relevant and useful to compare the damaged trees with the hydraulic parameters. Therefore, we consider that for the

Portainé stream the best indicator is the determination of the specific geomorphic form on which each tree is located. In this sense, for the correlation of dendrochronology, geomorphology, discharges and flow hydraulics, we use the in-situ hydraulic parameters (given by both the geomorphic position and the specific position of the tree inside the cross-section). In the new manuscript, we have added in the methods section an explanation about the use of the geomorphic form as the best evidence for the tree relation with the flow hydraulics (line 320-324).

- 3) Some methods, regarding dendrogeomorphological analysis, were not accessible as still unpublished works were referenced. This has been amended and methodological details have been included in the methods section (3.2. Dendrogeomorphological analysis), such as sampling dates (line 268-269), the sampling strategy details and references (line 273-275), the species name (line 285-290) and dendrochronological analysis and dating steps and methods (line 298-309).
- 4) Considering that the different topics constitute the procedure for tree-ring-based palaeoflood assessment, the goal of the paper has been readdressed, changing the corresponding paragraph of the introduction section (line 103-111). In the new version, we first present what this paper deals with, then the main aim of the paper is outlined as quantifying the relation between flow hydrodynamics and geomorphological characteristics of damaged trees, and finally we mention the new contributions, which are the correlation between hydraulic parameters (flow depth and velocity) and the specific geomorphic features of damaged trees, and the improvement of flow hydrodynamics knowledge by estimating the mobilizable particle size from the stream power obtained from the palaeodischarge estimation using hydraulic modelling. In summary, the novel contribution of this study lies in relating the 4 disciplines (dendrogeomorphology, fluvial geomorphology, palaeodischarges and flow hydraulics) especially focussing in the flow hydrodynamics.

Reply to Specific comments

HIGHLIGHTS: Answering the question about if trees located in intermediate flow energy positions are the most suitable ones for discharge reconstruction, we point out that in our study area they are. On the one hand, riverbed trees (high flow energy) are destroyed in high discharge events so these cannot be used for palaeoflood reconstruction. In fact, it is noteworthy the scarcity of trees located in the riverbed area (only two of the 21 scarred trees used in this study). On the other hand, some trees located in both side slopes (low flow energy) do not record dendrogeomorphological evidence because the energy is insufficient to produce damage or because the flow does not arrive to that position. In the field, many of the trees on the slopes did not show external disturbances and therefore, they were not sampled. This has been better explained in the discussion section (5.1. Discussion on the results and new contributions; line 647-651).

INTRODUCTION: The statement “never before have been related the four elements: FDEs, geomorphological features, hydrological parameters and palaeodischarges” contained an error (hydrological should be hydraulic) has been replaced by another sentence that also provides missing reference (Ballesteros-Cánovas et al., 2016) relating

the topics introduced in that paragraph. In the new manuscript, it says “However, dendrogeomorphological evidence have rarely been associated to geomorphic forms and correlated with the position of the trees (Ruiz-Villanueva et al., 2010) and also to other characteristics (Ballesteros-Cánovas et al., 2016)” (line 91-94). The next paragraphs have also been rewritten according to these changes (see next point).

LINE 82-85: This sentence has been deleted and the paragraph rewritten, as the goal of the paper has been readdressed (see reply to 4th major point).

UNACCESSIBLE REFERENCE: The reference Génova et al. (under review) is not accessible and it has been deleted throughout the text. In order to provide details which were referenced to this still unpublished work, much further methodological details have been provided in the methods section (see reply to 3rd major point).

LINE 255-260: There are several reasons that explain why a 1D model was run in this study (see reply to 1st major point). Regarding topographic data, LiDAR data did not provide a good enough spatial resolution and elevation accuracy in the study area. Total station surveying could not provide a very high-resolution mesh because the area is too large for a homogeneous topographic survey (we focussed on breaklines and trees), but we could obtain very detailed cross-sections. Last, differential RTK GNSS methods could not be applied in the entire area due to the dense vegetation (we measured with high accuracy some control points out of dense forest). Furthermore, even combining LiDAR data and more dense and accurate total station topographic data, we could not get a very accurate DEM to be used as a basis of a 2D model. For all the reasons explained above, running a 2D hydraulic models in such a context would include many uncertainties associated to interpolation errors. Therefore, we chose a 1D model and the drawback about topographic data was overcome introducing accurate cross sections measured in the field. The choice of a 1D model has been explained in the new manuscript in the methods section (3.3. Palaeodischarge estimations and hydraulic modelling; line 330-338). Regarding the reviewer’s comment about uncertainties, we did not include any model distribution error (but we did include the absolute error of the scar height and the water table). First, the number of samples is too low for an error distribution analysis of the model, because it would just represent a numeric deviation not making sense due to the few trees. Second, in our 1D model there are not enough data to measure the model uncertainty (in a 2D model there would be, but that approach was not appropriate for our study areas, as explained in the reply to 1st major point).

LINE 271: We can affirm that these small waterfalls produce critical conditions (even during natural regime). Other studies on a similar mountain context working with steep-gradient reaches of the same characteristics as the Portainé stream have previously used these waterfalls as critical boundary conditions for the critical-depth method (Bodoque et al., 2011). Moreover, they are located in stable bedrock channel reaches. It is true that most of the studied stream is a mobile riverbed, but some stretches correspond to stable bed topography. Therefore, both for the stable nature and their critical flow conditions mentioned above, they are suitable for peak reconstruction, as they set good boundary conditions (critical sections), both for initial and final parameters for the hydraulic model. These specifications for cross sections’ suitability for the critical-depth method for peak discharge estimation have been included in this paragraph (line 380-385).

LINE 280-282: This choice of the scars for hydraulic modelling is based on the dendrogeomorphological evidence of the specific study area, such as the total amount of dated scars (41 scars) and the number of torrential flows which formed FDE (10 events). Among all the scars, we can only use external ones for peak reconstruction because their height gives information about the water stage. We only had external scars from 2000 (4 scars), 2006 (1 scar), 2008 (19 scars) and 2010 (6 scars) events. 2000 scars were almost closed, so they did not provide information about the height of the scar. In the case of 2006, we only had a scar, and a unique height data was not considered enough for water stage estimation. Therefore, only 2008 and 2010 could be reconstructed, because we had a representative number of scars and their height could be measured in detail. Therefore, we have deleted the threshold outlined in the old version and better explained how we chose the events for hydraulic modelling in the methods section (3.3. Palaeodischarge estimations and hydraulic modelling; line 392-398).

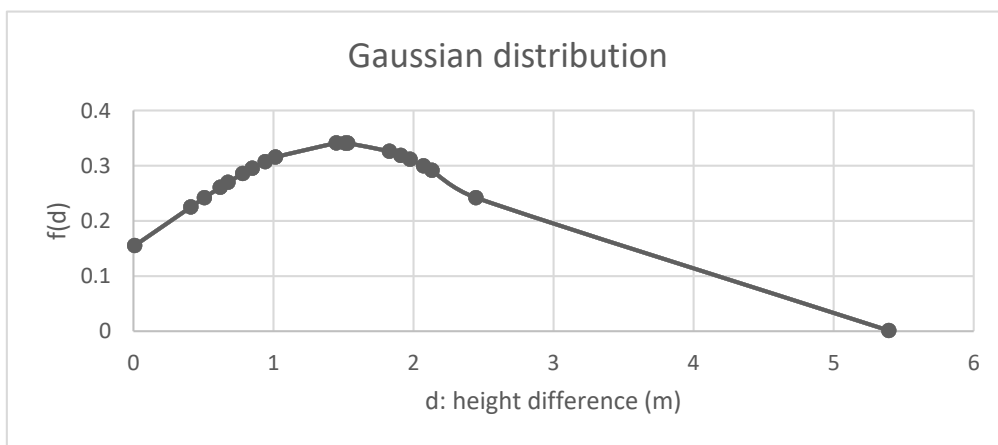
LINE 283-285: The reviewer says that this is a strong assumption that needs to be discussed and we agree that this was not well explained in the manuscript. This assumption is based on the historical documentation and the scar spatial and statistical distribution. The torrential events occurred in the 21st century are well documented. From 2006 to 2015, 10 events have occurred in the study area (see 2. Problematic study area and hazard section). There is detailed documentary information on these events, and also other studies about the recent torrential activity of the Portainé stream (e.g., IGC 2013a, Palau et al. 2017). All of them outline, and it is well known by the local authorities, that the most destructive ones in terms of damages were the 2008 and 2010 events. But, two events occurred in 2008 (September and November) and two in 2010 (July and August), and there are not coniferous species for Traumatic Resin Ducts for intra-annual detection (moreover, this analysis focused in external evidences without microscopic analyses). Considering these limitations and the lack of microscopic tree-ring analyses, we could not determine which event formed each scar, but the assumption has sense for both cases.

- 2008 (September and November): the September event was the most destructive event ever recorded in the study area (damages are recorded in all the road-channel crosses including the Montenartró bridge, located just upstream of the studied reach for where dendrogeomorphology was carried out), whereas the November event was a minor flow (it did not produced damages in the studied reach). Therefore, all the 2008 scars can be assumed to be formed by the September 2008 event.
- 2010 (July and August): they both were of intermediate magnitude and the recorded rainfall are of the same magnitude. But 9 sediment retention barriers were emplaced upstream of the study reach in 2009 (see 2. Problematic study area and hazard; 9 of the total 15 barriers were installed between 2008 and 2010). These barriers were filled during the first event after their installation, that is, in the July 2010 torrential event, when most of the material was accumulated in the barriers during that event, without reaching the study reach downstream. This means that the one in July did not transport material along the study reach because it was accumulated in recently emplaced sediment retention barriers (IGC, 2010b); so, the scars would correspond to the August event when the barriers were already filled and the flow transported high sediment load. Therefore, we can assume that the scars were formed by boulder or wood impact in 2010 correspond

to a unique event (the August 2010 one), as explained in the new version. Moreover, the normality test does not manifest any anomalous scar (that could be related to a different event), and the 6 scars show a uniform and a coherent scar height distribution.

In the new manuscript, this assumption has been better discussed and clarified considering the explanation mentioned (line 403-410).

LINE 288-289: In the field, orientation (facing towards the flow direction) of this anomalous scar suggested a fluvio-torrential origin, but its shape was rather anomalous and different to the rest of the scars. Afterwards, using the normality test, we almost confirmed that this scar is not related to the torrential event that formed the other 18 scars dated in 2008 scars. The normality test was applied to the variable d of equation 3, which is the difference between the maximum scar height and the water depth. The maximum scar height was chosen because indicates the minimum water elevation, so it can easily be compared to the modelled water elevation. This variable is represented as a Gaussian distribution in order to detect obvious anomalous scars that cannot be produced by the flow. A graph is included below that shows the results of the normality test for the 2008 case. The tail on the right corresponds to a tree showing a 2.45 m high scar (relative scar height) and a height difference of 5.39 m for the $Q=60\text{m}^3\text{s}^{-1}$. This height difference value is very high compared to the rest of the 18 scars, which show differences between 0 and 2.45 m. Therefore, this statistic analysis does not discretize suitable scars for palaeoflood reconstruction, but only detects a clear outlier which can hardly be attributed to the same torrential event as others. In fact, only one scar is discarded for 2008 and none for 2010. So, the normality test is not in contradiction with the sentence bridging the gap between dendrochronology and fluvial geomorphology, because it is only used to detect a scar that could not be formed by the impact of material transported during the 2008 high discharge event that formed the rest of the scars. Indeed, taking into account both the odd shape of the scar and its representation as an outlier when statistically comparing it to the rest of the scars, it is most likely related to a non-torrential process, so we did not use it as palaeostage indicator (PSI). Considering reviewer's comment, more information about the how the normality test was applied, to which specific variable and its significance has been included in the manuscript (line 412-417).



LINE 346: The geomorphic features were classified following Church et al. (2012), but also according to the formation energy of forms Villanueva et al. (2010). These two references are indicated in the methods section (line 233 and line 313), and we have avoided referring to the literature in the results section.

LINE 353: The degree of exposure in our study area is the same for all the scarred trees, as there are not significant obstacles upstream from them. This in-situ characteristic could not be considered in our study (see details in the reply to 1st major point). However, we have added two sentences in the manuscript to explain why this is not considered in our study and to justify the geomorphic position as the best characteristic in our study case (line 320-324).

LINE 374-377: This sentence has been moved to the methods section (3.3. Palaeodischarge estimations and hydraulic modelling; line 443-446), where an adequate justification of the use of a 1D model has also been incorporated (see reply to 1st major point).

LINE 391: We agree with the reviewer that stream power is highly correlated to velocity. The aim of the analysis of flow hydraulics presented in this study is not to relate these two variables among them, but to obtain and compare velocity and depth with the specific location and geomorphic position of the tree. The velocity and the stream power have the same value for each part (left bank, channel, right bank) of each cross section, but the depth changes depending on the specific location of the tree in the cross section. However, the values that were shown in table 3 are the outputs of the hydraulic model for each cross section, and not the specific values calculated for each tree according to their position. Therefore, table 3 has been removed from the text (we consider that the information is irrelevant for the paper goals) and included as supplementary material (see supplementary material; Table 1), and in order to meet reviewer's requirements, we have substituted it with a different table (Table 3). This new table and includes the specific hydraulic parameters calculated for each tree used for palaeodischarge estimation. The reviewer asks how the assessment of these variables was done. Regarding the velocity, we considered the value depending on the position of the tree inside the section (left bank, channel or right bank). The unit stream power was obtained by dividing the total stream power of each section part (left bank, channel or right bank), which is given by the hydraulic model, by the active width of the modelled flow at each cross section part. Last, the water depth is calculated considering the location of the tree in the cross section, and therefore subtracting the elevation of the base of the tree to the modelled water surface elevation at that cross section. Among these parameters, depth and velocity are calculated for each tree (4.4. Hydraulic parameters and mobilized particle size) and later on graphed for each specific tree geomorphic position (4.5. Relation between geomorphic forms, FDEs and flow hydraulics; Figure 9), and unit stream power is used to calculate the mobilizable particle size (4.4. Hydraulic parameters and mobilized particle size). For the particle diameter estimation for 2008, the values from the left bank of the Uc-Uc' section were used (using the overbank elevation value, not tree base elevations) because it corresponds to the cone apex and indicates the boulder size that could be mobilized and deposited at the debris cone formed in the left side of the channel, where field measures of real boulders are available. The values for these calculations ($w = 5221.92 \text{ Wm}^{-2}$; $d = 1.03 \text{ m}$) are shown in the results sections of the new manuscript (4.4. Hydraulic parameters and mobilized particle size; line 567-568) and all the explained above has been summarized and included in the methods section of new manuscript (3.4. Flow hydrodynamics; line 448-468). Also, a new table has been included (4.4. Hydraulic parameters and mobilized particle size; Table 3). Therefore, this reviewer's point has resulted in important changes in the methods and results sections.

LINE 399-417: This section has been revised and changed (see reply to previous point). Many of the text has been moved to the methods section (3.4. Flow hydrodynamics), especially explanations about the different particle size estimation approaches. The new results section only focusses in the objective results obtained from the application of the different equations (4.4. Hydraulic parameters and mobilized particle size; line 564-574).

SECTION 4.5: This section lies on the correlation of all the results obtained from the individual techniques (scar dating, geomorphological mapping, peak discharge reconstruction and flow hydrodynamics analysis). Even if other authors have already described frequent location of dendrogeomorphological evidence on trees, this correlation is not presented in any other previous work, especially the analysis of hydraulic parameters for each scarred tree according to its geomorphic position. We discuss why the geomorphic position is the best indicator in our study area in the reply to the 2nd major point. Regarding the reviewer's suggestion about deciphering the best locations for peak discharge reconstruction, we have payed attention to it. For that, we have analysed the height difference (EQ. 3) of 2008 scars (because it is the event reconstructed with higher reliability and lower errors) at each geomorphic position as an estimation of model uncertainty, and then we have calculated the mean height difference for each type of geomorphic form.

Cross section	Scar date	Height difference (m)	Geomorphic position
M-M'	2008	0.86	Right slope
K-K'	2008	0.49	Gravel bar
Kb-Kb'	2008	0.75	Terrace 1
Kc-Kc'	2008	1.04	Right slope
Kd-Kd'	2008	0.54	Terrace 1
Ke-Ke'	2008	0.31	Terrace 1
P-P'	2008	0.07	Terrace 2
O-O'	2008	0.07	In-channel
Nb-Nb'	2008	0.01	Right slope
Y-Y'	2008	0.46	Terrace 2
Xb-Xb'	2008	0.01	Artificial levee
D-D'	2008	0.82	Secondary channel of cone
F-F'	2008	0.04	Middle deposits of cone
F-F'	2008	0.28	Middle deposits of cone
C-C'	2008	0.10	Middle deposits of cone
C-C'	2008	0.41	Middle deposits of cone
G-G'	2008	0.07	Secondary channel of cone
G-G'	2008	0.00	Middle deposits of cone

Mean height differences for each geomorphic position:

- *In-channel* (1 tree): 0.07 m
- *Gravel bar* (1 tree): 0.49 m
- *Terrace 1* (3 trees): 0.53 m
- *Terrace 2* (2 trees): 0.26 m
- *Secondary channel of cone* (2 trees): 0.44 m

- *Middle deposits of cone* (5 trees): 0.17 m
- *Artificial levee* (1 tree): 0.01 m
- *Right slope* (3 trees): 0.63 m

Therefore, at a first glance, the best locations for peak discharge reconstruction seem to be in-channel and artificial levee. However, we only have 1 tree at each of these positions. Among the geomorphic forms where more than a unique tree is scarred, the best results are obtained for the terrace 2 and the middle deposits of the cone. This is in concordance with the results presented in the 4.5. subsection. This analysis has been included at the end of the results section of the new manuscript (4.5. Relation between geomorphic forms, FDEs and flow hydraulics; line 620-632). Also, the implications of these results for the reliability of peak discharge reconstruction is addressed in the discussion section and compared to Ballesteros-Cánovas et al. (2016) (line 729-733).

LINE 487: We have corrected this reference because the work de las Heras (2016) is indeed accessible. In the new manuscript, we have added the correct reference in the reference list (line 959-962), providing the link to the digital archive where it can be accessed from.

Reply to final comment

We have considered and included in the manuscript all the comments from the reviewer. Regarding the special recommendation on providing quantitative information about the suitability of individual trees for palaeodischarge estimations, we have carried out an analysis of the uncertainties on scars according to their geomorphic position (see reply to section 4.5.). The results suggest once again that, in our study area, the most reliable trees for palaeoflood reconstruction are located in geomorphic positions related to processes of intermediate energy.

New references:

Ballesteros-Cánovas, J.A., Stoffel, M., Spyt, B., Janecka, K., Kaczka, R.J., Lempa, M., 2016. Paleoflood discharge reconstruction in Tatra Mountain streams. *Geomorphology* 272, 92-101. doi:10.1016/j.geomorph.2015.12.004

Cook, E.R., Kairiukstis, L.A., 1990. *Methods of Dendrochronology. Applications in the Environmental Sciences*. Springer, Dordrecht, Netherlands. doi:10.1007/978-94-015-7879-0

Grissino-Mayer, H. D., 2001. Evaluating crossdating accuracy: a manual and tutorial for the computer program COFECHA. *Tree-Ring Research* 57 (2), 205–221.

RinnTech., 2003. *TSAP-Win Software for tree-ring measurement, analysis and presentation Product Information*, v. 0.53. RinnTech, Heidelberg, Germany, 2 pp.

Stoffel, M., Corona, C., 2014. Dendroecological dating of geomorphic disturbance in trees. *Tree-Ring Research*, 70 (1), 3-20. doi:10.3959/1536-1098-70.1.3

3. REVIEWER 2

The authors appreciate the reviewer's opinion considering that the paper has remarkable interest and potential.

Regarding the details of dendrogeomorphology, we have solved the problem in the new manuscript. The citation of an “under review” paper has been removed and specific methodological details on dendrogeomorphological sampling and analysis have been included, as explained in the reply to the first reviewer’s 1st major point. Therefore, details of the dendrogeomorphology are included in the methods section of the new revised version, which has been completely rewritten (3.2. Dendrogeomorphological analysis; line 268-309).

The reviewer says that we mention that different FDEs were dated (external and internal scars, decapitations and branch replacement, suppressions, growth releases and asymmetries) but no results are shown about the last ones. We want to clarify that the mesoscopic FDE (i.e., suppressions, releases and asymmetries) were only used as complementary data to date the torrential events, but they are not specifically analysed in this study. That is, they provided some additional information to more reliably date past events but they are not used for palaeoflood reconstruction, because they do not provide information on the minimum water surface elevation so they are not useful for peak discharge estimation. In order to be more clear and avoid confusion, we have avoided mentioning those FDE that are not used in this study by deleting that sentence and explaining that we only considered external growth disturbances in this study, and among them, scars were used for palaeoflood reconstruction (3.2. Dendrogeomorphological analysis; line 298 and line 306-309).

In terms of tree tilting, we should mention that tilting was not dated in this study. We only focussed on external disturbances on trees. Scars were dated and used as flood palaeostage indicators (PSIs), and their geomorphic position was also analysed. The rest of the used FDEs (i.e. decapitations, tilting and root exposure) were identified, located and their geomorphic positions analysed, in order to integrate it with the scars and compare the formation of external disturbances according to the geomorphic form on which the trees are located. Therefore, growth responses (e.g., suppressions, releases and asymmetries) were not used in this study and the old manuscript was rather confusing as it listed them even if they were then not used. Thus, in the revised manuscript, we have avoided mentioning types of growth responses and we have only explained the external disturbances used in this study (3.2. Dendrogeomorphological analysis; 303-309). This reply justifies why we did not mention other indicators as reaction wood.

We agree with the reviewer that there was missing information on the species used. We have included the name of the species that were both analysed (*Populus tremula* L., *Populus nigra* L., *Fraxinus excelsior* L., *Prunus avium* L., *Quercus petraea* (Matt.) Liebl., *Tilia platyphyllos* Scop., *Juglans regia* L., *Acer campestre* L. and *Salix caprea* L.) for dendrochronological dating (3.2. Dendrogeomorphological analysis; line 28-290), but also specifically the species of the scars that were finally used for the hydraulic modelling of 2008 and 2010 events (3.3. Palaeodischarge estimations and hydraulic modelling; line 417-420). This species information and the new dendrogeomorphological methods subsection have been highly improved in this sense. Among the sampled trees, there are no coniferous species, so Traumatic Resin Ducts were not used in this study. A sentence indicating that the trees used in this study are broadleaf species has been included in the study area and hazard section (line 175-176).

To sum it up, all the requirements of the reviewer have been considered and much further details of dendrogeomorphology have been included in the new manuscript, giving an adequate methodological description. That is, we no longer refer to the “in review” paper and we provide all the necessary details about the dendrogeomorphological study in the revised version.

4. REVIEWER 3

The reviewer considers that the paper is of high importance and interest, and we are thankful for these words. The comments and suggestions have been incorporated and the manuscript has improved a lot.

Reply to detailed comments

LINE 29: The time period of the events dated using tree-ring analysis is from 1957 to 2010. In the new manuscript, we have not included this information (we have deleted that sentence), because these are not the results obtained in this study, where we only reconstruct 2008 and 2010 events, and we consider that they are not necessary in the abstract.

LINE 31: We are sorry about the mistake in this sentence. The most intensely affected trees in our study area locate in intermediate energy geomorphic positions, which correspond to second level of alluvial terrace and alluvial cone, and not in high energy positions such as the channel and first level of alluvial terrace. The abstract has been corrected by deleting the “high” word (line 33).

ABSTRACT (LAST SENTENCE): The sentence has been rephrased to emphasize the contribution and innovativeness of the approach presented in this study. As the goal of the paper has been readdressed as a result of the revision (see reply to 4th major point of reviewer 1), two new sentences outline the combination of techniques with special detailed analysis of hydraulic parameters, which has not been carried out before elsewhere, and the application of such an approach (1. Introduction; line 108-111). Therefore, the last sentences of the abstract in the new manuscript are “This multidisciplinary palaeohydrological study relates flood hydrodynamics with the damages on trees and their geomorphological characteristics, focusing on the hydraulic parameters of the peak flow (depth, velocity and unit stream power), which has never been carried out elsewhere. The proposed approach shows a high potential for palaeoflood analysis in ungauged mountain catchments with scarce non-systematic data” (line 40-45).

LINE 55: The mistake has been correcting writing the word “lichenometric” properly and the word “or” has been added just before (line 70).

LINE 58-60: Worldwide references on different palaeohydrology approaches have been added in the new manuscript. On the one hand, we have included examples of peak discharge and flow hydraulics reconstruction (Chow, 1959; Lang et al., 2004; O’Connor and Webb, 1988; Webb and Jarrett, 2002). On the other hand, we have provided an adequate background on studies about palaeoflood occurrence and dynamics focussing in fluvial geomorphology (Baker and Pickup, 1987; Baker et al., 1988) and/or dendrogeomorphology (Gottesfeld, 1996; Kundzewicz et al., 2014; Malik and Matyja, 2008; Sigafos, 1964; Yanosky and Jarrett, 2002; Zielonka et al., 2008). All these

references have been added in the introduction section. Besides, we have also rewritten and shortened the two paragraphs providing worldwide references because it was somehow repetitive. Therefore, the new manuscript provides an adequate, clear and precise background (line 57-70).

LINE 61: Following the reviewer's suggestion, we have added a new paragraph in the introduction section that explains the limitations and restriction of the application of each individual method in mountain areas (line 96-102). These limitations are the justification of the approach of this study, based on combination of all the techniques (line 103-104), which overcomes the specific drawbacks of the results obtained from isolated methods by relating all the results.

LINE 63: We agree with the reviewer that some global references were missing regarding flood reconstruction using dendrogeomorphology. We have searched for worldwide studies on this theme and added them (see reply to line 58-60 and new references). In this way, we have included dendrogeomorphological works applied to palaeofloods in the introduction section (line 67-69).

LINE 82-84: The text in parenthesis refers to the specific works carried out in our study area, but not to the definition of the research disciplines. In order to avoid confusion, we have deleted the text in parenthesis and changed the sentence (line 103-104).

LINE 91: It is true that our study has its limitations as explained in the discussion section, and that is the reason because we combine the four techniques for a better comprehension of the torrential dynamics and system behaviour. Following reviewer's suggestion, we have deleted the word "realistic" and rephrased the sentence as "allows us to obtain an improved knowledge about fluvio-torrential dynamics in areas with few source data" (line 108-111).

LINE 121-125: We have corrected the writing of species along the text. The species are written with their complete scientific writing name in latin (e.g. *Populus tremula* L.) when they appear for the first time in the text in the methods section (3.2. Dendrogeomorphological analysis; line 286-290) and in their abbreviated way (e.g. *P. tremula*) when mentioned later (3.3. Palaeodischarge estimations and hydraulic modelling; line 417-419).

FIGURE 3: We have changed the figure to be coherent with the paper structure. In the new figure the methodological procedure of the four palaeohydrology subdisciplines has been indicated separately and their combination has been better represented. Mainly, we have divided the "hydraulic modelling" input (which is not really an input, but a method) in two different ones, which are "palaeodischarge estimation" and "flow hydrodynamics" (Figure 3). This change has also been made in the methods section text, where a subsection (see reply to editor comments). At the bottom of the figure, boxes have changed to better illustrate the combination of the different topics; e.g. relation between tree characteristics and hydraulic parameters and mobilizable particle size estimation (Figure 3).

CHAPTER 3: The methods section structure has been changed, so in the new manuscript there are four subsections, each one corresponding to one the disciplines. This makes it easier to follow the paper and is coherent with the title and with the introduction. The

new version is structured in the following methods subchapters: 3.1. Geomorphological analysis and mapping; 3.2. Dendrogeomorphological analysis; 3.3. Palaeodischarge estimations and hydraulic modelling; 3.4. Flow hydrodynamics. The combination of all of them is presented in the results section, where first results of each of the technique are shown (subsections 4.1. to 4.4.) and then the results obtained from their relation and integration (4.5. Relation between geomorphic forms, FDEs and flow hydraulics).

LINE 167-168: The total station surveying was mainly carried out during a first field campaign in March 2014, but some topographic points to locate sampled trees were also acquired in March 2015 and September 2015. The surveyed area covered 4850 m². The collected point dataset consisted of 1118 points, from which 853 are ground points (terrain + cross sections) and 265 are tree data (tree base location + height of scars and decapitations). These details about the topographic data acquisition using a total station have been added to the methods section (3.1. Geomorphological mapping and analysis; line 223-231).

LINE 177: For the integration of the different topographic data sources, we first assumed that total station data is the most reliable one (because it focused on *in situ* topographic breaklines, geomorphic elements and trees). For total station points we created a buffer (0.5 m in steep areas and 1 m in flat areas) and intersected it with LiDAR points. For each LiDAR point falling within a total station-based buffer, a maximum elevation difference was established as a threshold for its acceptance or rejection (0.5 m). Those points showing higher differences in elevation were removed. Therefore, we only used LiDAR points that fell outside the buffer or inside the buffer but below the threshold. Finally, selected LiDAR points and total station ground points (excluding those of FDE heights) were merged into a point dataset, which was then used to generate the TIN. Details about this topographic data integration explained here have been included in the manuscript (line 362-369).

LINE 191-192: The main mapped geomorphological elements are itemized in the last sentence of this paragraph. However, we have changed the paragraph and moved the list of the geomorphological elements to the previous paragraph about geomorphological field mapping (line 234-237). After describing the geomorphic features, we mention the digitization of them in a GIS environment. The new version is clearer.

LINE 195-196: The date of the geomorphological mapping fieldwork campaigns are March 2014, March 2015, September 2015 and June 2016 (note that the topographical data acquisition to create the geomorphological map was performed in March 2014, and the rest of campaigns were based on just identifying changes along the channels without taquimetric survey). The performance of four multi-temporal field surveys, explaining that topographic data was only acquired in the first one and that a single geomorphological map is created, has been added (line 231-243).

LINE 205: When we give a brief definition of dendrogeomorphology we just introduce the concept of dendrogeomorphological evidence, without itemizing which kind of evidence can be formed. We have deleted part of this sentence and we have listed the different type of FDE found and sampled in the study later on (line 272-273).

LINE 212-213: The subsection about dendrogeomorphological analysis was rather confusing in the old version, as we mentioned some FDE that were not explicitly used in this study. In fact, the growth responses to which this reviewer's comment refers were just a general itemization, but none of them were analysed in this study. This paper is focussed on the external disturbances on trees without any mesoscopic or microscopic analysis or techniques. Among external disturbances, we dated scars, which were then used as palaeostage indicators for peak discharge reconstruction. Decapitations, tilting and root exposure were localized in the field and their position was used for establishing their relation with geomorphic forms, in order to correlate the formation of external disturbances due to torrential events according to the different geomorphologic features. Therefore, in the revised manuscript, we have avoided mentioning types of growth responses and we have only explained the external disturbances used in this study (3.2. Dendrogeomorphological analysis; line 268-273). This reply justifies why we did not mention other indicators as reaction wood. Regarding traumatic rows of resin ducts, we did not use them because there are not coniferous in the study area.

LINE 221-222: The sampling was carried out during three field surveys, in March 2014, March 2015 and September 2015. The sampled species were *Populus tremula* L., *Populus nigra* L., *Fraxinus excelsior* L., *Prunus avium* L., *Quercus petraea* (Matt.) Liebl., *Tilia platyphyllos* Scop., *Juglans regia* L., *Acer campestre* L., *Salix caprea* L. and *Betula pendula* Roth. In the revised manuscript, we have made important changes to the subsection of dendrogeomorphological analysis methods (see reply to 3rd major point of reviewer 1), and information of sampling dates (line 268-269) and species (line 286-290) has been included in the new version. Also methodological details on dendrogeomorphological sampling, analysis and dating are present in the new manuscript (3.2. Dendrogeomorphological analysis).

LINE 228: Yes, these samples are wedges with callus portion. That is, we extracted wedges in some trees showing callus overgrowing and covering part of the scar. In our study area, callus are well-defined so the dating of wedges was very useful for the subsequent dating of the scar or start of callus formation, because they provided more reliable results than cores. We have specified in the manuscript that "some wedges were extracted from overgrown callus in scarred trees" (line 282-283). We have also added the number of wedges dated for each of the modelled years (line 418-420).

LINE 228: Cross-sections and wedges were processed in the same way as cores, that is, (i) sample air-drying, high-precision sanding and preparing; (ii) tree ring counting and width measuring using a LINTAB table (with 1/100 mm accuracy) and the associated software TSAPWin (RinnTech, 2003); (iii) representation of tree ring series; (iv) cross-dating using visual and statistical techniques (Cook and Kairiukstis, 1990); and (v) quality check using the Cofecha software (Grissino-Mayer, 2001). This laboratory dendrochronological analysis procedure has been detailed in the new manuscript, and we have indicated that all the samples (i.e. cores, wedges and sections) were processed in the same way (3.2. Dendrogeomorphological analysis; line 298-299). Regarding the death year, it was estimated by dating the last ring. This ring was dated by comparing the tree-ring series with other living trees of the same specie using visual and statistical techniques and cross-dating, as explained above. For the modelled years, only two samples from 2008 were from dead trees and their last ring was dated from 2012 and 2013. However,

the death year can be uncertain, as some trees can be alive without forming rings during an undetermined time, but we at least are able to cross-check tree-ring series to date the scar year. Details on the procedure of dead trees dating has been included in the methods section (3.2. Dendrogeomorphological analysis; line 304-305).

LINE 231-232: The text about the age of the analysed trees has been removed because it is not relevant for this study.

LINE 233-234: The citation of the paper in review has been removed and specific methodological details on dendrogeomorphological sampling and analysis have been described in the new manuscript (see reply to 1st major point of reviewer 1). Therefore, details of the dendrogeomorphology are included in the methods section of the new revised version, which has been completely rewritten (3.2. Dendrogeomorphological analysis).

LINE 235-237: Considering both this comment and reviewer 2 ones, we have avoided mentioning growth releases releases, suppressions and asymmetries at this point of the paper, because these FDE are not used for the hydraulic modelling of this study (see reply to reviewer 2). Therefore, we have deleted that sentence and added another one explaining that we only considered external growth disturbances in this study (those shown in Figure 8 and Table 6), and among them scars were used for palaeoflood reconstruction (3.2. Dendrogeomorphological analysis; line 298 and line 306-307). The use of only external disturbances is because they are the best indicators of fluvio-torrential activity and can vary depending on the geomorphic position of the tree. Tree-ring growth anomalies or asymmetries can be related to other factors and do not indicate the occurrence of an event by themselves.

LINE 253-254: The third parameter for running the hydraulic model are discharges, and those are obtained using the maximum height of tree scars as palaeostage indicators (PSIs). That is, the height of the scar indicates the water elevation for that tree and the discharge is obtained by a trial-and-error approach based on searching for the minimum standard deviation between the modelled water level and the scar height. This is explained in the fourth paragraph of the 3.3. subsection. However, in order to be easy to understand that this paragraph refers to the third parameter for hydraulic modelling (discharge), we have changed the first sentence and indicated that “Palaeodischarges were calculated using external scars as palaeostage indicators (PSIs)” (line 386-388).

LINE 257: This sentence was not clear enough so we have changed it and better explain why we run two different hydraulic models. The issue here is that each topographic data source has its strengths and limitations. On the one hand, total station data (total station data acquisition is explained in subsection 3.1.) is the most reliable one because it includes sharp topographic changes with high accuracy (see reply to comment line 177), but the point density is not enough for a good terrain model. On the other hand, the inclusion of LiDAR data provided a higher point density and allows to create much more cross sections, but these points do not represent sharp changes of the terrain, and moreover, the elevation accuracy in mountain areas makes it less reliable than total station data. Therefore, we decided to run two models: one using only total station data, and another one using the integration of LiDAR and total station data. The two different hydraulic models run in this study and the justification for it have been better explained in the revised manuscript (line 342-355).

LINE 279: It is true that the use of the scar height as an indicator of the minimum water stage (palaeostage indicator, PSI) has its limitations. In this study, we use the maximum scar heights, which has been indicated in the new manuscript (line 759-761) because it was not explained. The main limitations or uncertainties of this method are: (i) the scar could be formed by boulders or woody material accumulated upstream from the tree, so the scar height would be higher than the flood stage and the discharge would be overestimated (Ballesteros-Cánovas et al., 2010); (ii) the scar could be partially closed, so the maximum height measured in the field would be lower than the height at the formation time and the discharge would be underestimated (Guardiola-Albert et al., 2015); and (iii) the scar could be formed by bedload material instead of floating boulder or wood, so the discharge would be underestimated (Ballesteros-Cánovas et al., 2010). These limitations have been included in the discussion section, also including references (5.2. Limitations of the data sources; line 763-770).

LINE 280: This choice of the scars for hydraulic modelling is based on the dendrogeomorphological evidence of the specific study area, such as the total amount of dated scars (41 scars) and the number of torrential flows which formed FDE (10 events). Among all the scars, we can only use external ones for peak reconstruction because their height gives information about the water stage. We only had external scars from 2000 (4 scars), 2006 (1 scar), 2008 (19 scars) and 2010 (6 scars) events. 2000 scars were almost closed, so they did not provide information about the height of the scar. In the case of 2006, we only had a scar, and a unique height data was not considered enough for water stage estimation. Therefore, only 2008 and 2010 could be reconstructed, because we had more than one scar and their height could be measured in detail. Therefore, we have deleted the threshold outlined in the old version and better explained how we chose the events for hydraulic modelling in the methods section (3.3. Palaeodischarge estimations and hydraulic modelling; line 392-398).

LINE 283-285: The reviewer says that this is a strong assumption that needs to be discussed and we agree that this was not well explained in the manuscript. This assumption is based on the historical documentation and the scar spatial and statistical distribution. The torrential events occurred in the 21st century are well documented. From 2006 to 2015, 10 events have occurred in the study area (see 2. Problematic study area and hazard section). There is detailed documentary information on these events, and also other studies about the recent torrential activity of the Portainé stream (e.g., IGC 2013a, Palau et al. 2017). All of them outline, and it is well known by the local authorities, that the most destructive ones in terms of damages were the 2008 and 2010 events. But, two events occurred in 2008 (September and November) and two in 2010 (July and August), and do not have coniferous species for Traumatic Resin Ducts for intra-annual detection (moreover, this analysis focused in external evidences without microscopic analyses). Considering these limitations and the lack of microscopic tree-ring analyses, we could not determine which event formed each scar, but the assumption has sense for both cases.

- 2008 (September and November): the September event was the most destructive event ever recorded in the study area (damages are recorded in all the road-channel crosses including the Montenartró bridge, located just upstream of the studied reach for where dendrogeomorphology was carried out), whereas the November event was a minor flow (it did not produced damages in the studied reach).

Therefore, all the 2008 scars can be assumed to be formed by the September 2008 event.

- 2010 (July and August): they both were of intermediate magnitude and the recorded rainfall are of the same magnitude. But 9 sediment retention barriers were emplaced upstream of the study reach in 2009 (see 2. Problematic study area and hazard; 9 of the total 15 barriers were installed between 2008 and 2010). These barriers were filled during the first event after their installation, that is, in the July 2010 torrential event, when most of the material was accumulated in the barriers during that event, without reaching the study reach downstream. This means that the one in July did not transport material along the study reach because it was accumulated in recently emplaced sediment retention barriers (IGC, 2010b); so, the scars would correspond to the August event when the barriers were already filled and the flow transported high sediment load. Therefore, we can assume that the scars were formed by boulder or wood impact in 2010 correspond to a unique event (the August 2010 one) , as explained in the new version. Moreover, the normality test does not manifest any anomalous scar (that could be related to a different event), and the 6 scars show a uniform and a coherent scar height distribution.

In the new manuscript, this assumption has been better discussed and clarified considering the mentioned explanations (line 401-410).

LINE 336: In the new manuscript, the date of the geomorphological field campaigns (March 2014, March 2015, September 2015 and June 2016) is mentioned in the methods section when presenting data collected in the field (3.1. Geomorphological analysis and mapping. We have also clarified that the topographic data acquisition was performed in the first survey (March 2014), and the following field campaigns consisted in identifying changes on the channel and mapping them. Therefore, a unique geomorphological map was created for the study area, even if changes along the channel were mapped during the following fieldwork (March 2015, September 2015 and June 2016). Moreover, the geomorphic position of the trees, presented in the paper, did not change in time. The second paragraph of the 3.1. subsection has been rewritten in the new manuscript to make it clear when and how the geomorphological analysis and mapping was carried out (line 231-240). Please note that dendrogeomorphological sampling was only carried out during the first three field campaigns (March 2014, March 2015 and September 2015). This has also been indicated (3.2. Dendrogeomorphological evidence; line 268-269).

LINE 336-343: We have made changes in the manuscript regarding this point. In fact, the old version said that four geomorphological maps were created but it was a mistake. Only one geomorphological map was obtained based on the topographic survey in March 2014, and in the following surveys, changes along the channels were marked in the field above the geomorphological map, without creating a map for each survey (line 237-240). Moreover, the geomorphic position of the trees, presented in the paper, did not change in time. Therefore, we consider that including a maps for each survey marking the changes is not necessary for this study, and that the geomorphological map shown in figure 5a is enough.

FIGURE 5: Tree codes are not usually indicated if they do not provide any information by themselves. However, in this figure (an only in this figure) we indicated the ID codes

of trees because they help to identify each photo in the map of figure 5a. As the aim of the figure is illustrating the different geomorphic positions of the trees, their code helps to identify them in the geomorphological map, where different geomorphic elements are shown.

LINE 361-362: This sentence has been removed because it is not a result and it is previously explained in the methods section.

FIGURE 6: We have considered adding the discharges calculated based on the total station to the figure, but this is not feasible. The total station data mean squared errors are much lower (0.099 to 0.078 m) than the TIN-based errors displayed in the figure (0.249 to 0.232). Therefore, when we display both lines in the same graph, the Y axis of the graph ranges between 0.249 to 0.078, and the lines are smoothed so the estimated palaeodischarges (the ones corresponding to the minimum MSE) can not be visualized and the graph does not provide useful information visually. The TIN-based and total station-based discharges should be represented in two different graphs, but we think that two graphs are excessive and that including just one example (the TIN-based 2008 palaeodischarge calculation) is enough.

LINE 374-376: This sentence has been moved to the methods section, but also other contents of this paragraph (see reply to reviewer 1 comment line 399-417). In fact, the critical overflow discharges were not explained in the methods and first mentioned in the results. In the new manuscript, the approach for bank overflow discharge estimation is presented in the methods (3.3. Palaeodischarge estimations and hydraulic modelling; line 443-446) and the obtained discharges in the results section (4.3. Flood discharges; line 532-538).

FIGURE 7: The scale has been added to the figure, but also the coordinate system specifications.

LINE 402-404: In the field, we selected 10 boulders that were representative of the boulders forming the deposits of the alluvial cone. In fact, the boulder size in the deposit is rather homogenous. However, we chose samples of different size (from largest ones to smallest ones) to obtain the most representative measures. The obtained mean size shows a variance of 0.06 for intermediate axes. This low value confirms the suitability of the measured boulders as an enough number of boulders for the study area.

LINE 407: this paragraph has been almost completely moved to the methods (see reply to reviewer 1 comment line 399-417), avoiding the reference in the results.

TABLE 4: The relative size of the boulders was determined according the field observations, so, we did not use any general methodology. Therefore, the different relative sizes established in this study are based on the deposit of the Portainé alluvial cone, and cannot be used for other study areas. The most common boulder size observed in the field is between 20-30 cm (medium relative size). For this study, we named “small” those blocks with less than 20 cm length, and “big” if they were larger than 30 cm. However, these threshold are for the common sized particles, but there are also few particularly small (<10 cm) or big (> 1 m) ones. Considering the variety of particle size and in order to get a good representation of the deposit, we considered 5 medium-sized,

2 small/big and 1 very small/very big particles, obtaining a total of 10 representative measures. The mentioned relative size classification can be summarized as follows:

- Very small: <10 cm length. 1 measure.
- Small: 10-20 cm. 2 measures.
- Medium: 20-30 cm. 5 measures.
- Big: 30-100cm. 2 measures.
- Very big: > 1m. 1 measure.

This procedure for establishing thresholds has been included in this response to the reviewer but we consider that it is not necessary including it in the manuscript, because it is just a local approach not based in any existing methodology.

TABLE 6 / FIGURE 8: We agree with the reviewer that Table 6 and Figure 8 should be reduced because they represent the same data. Therefore, in the new version, we have deleted the table and included it as supplementary material. However, following the suggestions from this reviewer for Figure 8 (see next point), we have made changes into this FDE-geomorphology relation, by dividing the number of each FDE type at each geomorphic position by the number of trees; that is, representing the number of FDE per tree. These new calculations have been included both in the table (supplementary material; Table 2) and figure (Figure 8). Thus, the new manuscript has been reduced by deleting the table.

FIGURE 8: This figure has been modified considering the reviewer's suggestions. We have modified the variable to represent in the figure by dividing the number of each FDE type at each geomorphic position (old representation) by the number of trees (new representation); that is, representing the number of FDE per tree. Also, some results of the total of FDE (sum of the four different external FDE) per tree for geomorphic positions have been included in the results section (4.5.Relation between geomorphic forms, FDEs and flow hydraulics; line 596-598) to support the results that “most intensely damaged tree concentrate on the geomorphological elements related to processes of intermediate energy (second terrace and alluvial cone)”. The number of FDE per tree have been grouped in 5 categories, and the size of the symbol in the figure indicates it, from low to high as follows:

- < 0.5
- [0.5-1)
- [1-1.5)
- [1.5-2)
- ≥ 2

We have also added to the figure a legend that allows easily identifying the graphical results in this qualitative way (Figure 8).

LINE 453-454: We are aware that the number of scars depends on the number of trees at each geomorphic form (see reply to previous point). However, we want to clarify that we sampled all the trees showing indicators of damage in the field. That means that the quantity of samples is also related to the real disturbances recorded on trees, and therefore, the number of dated scars for each geomorphic position is a pretty good representation of scar formation due to torrential events for our study area. We have added a sentence in the new manuscript indicating that all the tree showing scars were sampled (4.5. Relation

between geomorphic forms, FDEs and flow hydraulics; line 617), so the concentration of scars in the alluvial cone is not conditioned by the sampling strategy.

LINE 459: The word “novel” has been avoided. In fact, this long sentence has been shortened by deleting repetitive text (5.1. Discussion on the results and new contributions; line 636-640).

LINE 463-465: As explained in the reply to reviewer 2 and reply to reviewer 3 line 453-454, the external FDE are the only one used in this study, and never internal ones like growth releases, suppressions or asymmetries. Therefore, when we say that “formation of different dendrogeomorphological evidence (FDEs) depends on the geomorphic position of the affected trees” we refer to external disturbances (i.e. decapitation, scars, tilting and root exposure), but not to other FDE. In order to be clear about the FDE analysed and used in this study, we have avoided mentioning other FDE throughout the text and we have focussed in the external disturbances, as explained in the methods section (3.2. Dendrogeomorphological evidence; line 298).

LINE 437: This contradiction has been amended by deleting “high” in the abstract, which was an error. The new manuscript has been unified, and the position of the most intensely damaged tree is indicated as being the geomorphic elements related to torrential processes of intermediate energy.

LINE 547-554: Limitations of the topographic data could not be eliminated due to the availability of source data. Regarding the limitation “(i)”, there is only LiDAR data from 2011 and the first total station surveying was carried out in 2014. Point “(ii)” could not be solved because there is no data prior to 2011 so the exact topography of the cone for 2008 cannot be obtained. Concerning “(iii)”, we consider that the obtained terrain model is a good representation of the main features of the topography. At last, the accuracy limitation outlined in “(iv)” was overcome in this study with the acquisition of high-accuracy and high-resolution cross section in the field using total station. A sentence explaining how the limitation was overcome has been introduced in the manuscript (line 783-785).

LINE 571: As explained in the methods section (3.3. Palaeodischarge estimations and hydraulic modelling; line 392-398), the 2008 and 2010 events were the only one that could be modelled because the rest of the years (2000 and 2006) showing any external scars were not reliable. Scars dating of 2000 were almost closed and the height was unknown. From 2006, there was only 1 scar so we only had information about the water elevation at one point, which can introduce significant uncertainties. However, from 2008 and 2010 events we had 6 and 19 scars respectively, which allows us to reconstruct flood using multiple scar height information and therefore, allows a deviation analysis to a palaeodischarge approach. The sentence mentioned by the reviewer has been changed according to the new justification of the choice of the 2008 and 2010 for hydraulic modelling (5.2. Limitations of the data sources; line 772-774).

CONCLUSIONS: We have rewritten the first part of the conclusions to emphasize the findings and new contributions of this study (line 848-860).

New references:

- Baker, V.R., Pickup, G., 1987. Flood geomorphology of the Katherine Gorge, Northern Territory, Australia. *Geol. Soc. Am. Bull.* 98, 635-646. doi:10.1130/0016-7606(1987)98<635:FGOTKG>2.0.CO;2
- Gottesfeld, A.S., 1996. British Columbia flood scars: maximum flood stage indicators. *Geomorphology* 14, 319-325. doi:10.1016/0169-555X(95)00045-7
- Guardiola-Albert, A., Ballesteros-Cánovas, J.A., Stoffel, M., Díez-Herrero, A., 2015. How to improve dendrogeomorphic sampling: variogram analyses of wood density using XRCT. *Tree-Ring Research* 71 (1), 25-36. doi:10.3959/1536-1098-71.1.25
- Kundzewicz, Z., Stoffel, M., Kaczka, R., Wyźga, B., Niedźwiedź, T., Pińskwar, I., Ruiz-Villanueva, V., Łupikasza, E., Czajka, B., Ballesteros-Cánovas, J., Małarzewski, Ł., Choryński, A., Janecka, A., Mikuś, P., 2014. Floods at the northern foothills of the Tatra Mountains—a Polish–Swiss research project. *Acta Geophys.* 62 (3), 620–641. doi:10.2478/s11600-013-0192-3
- Lang, M., Fernandez-Bono, J.F., Recking, A., Naulet, R., Grau-Gimeno, P., 2004. Methodological guide for paleoflood and historical peak discharge estimation, in: Benito, G., Thorndycraft, V.R. (Eds.), *Systematic, Palaeoflood and Historical Data for the Improvement of Flood Risk Estimation: Methodological Guidelines*. CSIC, Madrid, Spain, pp. 43-53. ISBN:84-921958-3-5
- Malik, I., Matyja, M., 2008. Bank erosion history of a mountain stream determined by means of anatomical changes in exposed tree roots over the last 100 years (Bila Opava River–Czech Republic). *Geomorphology* 98, 126-142. doi:10.1016/j.geomorph.2007.02.030
- Sigafoos, R.S., 1964. Botanical evidence of floods and flood-plain deposition. United States Geological Survey Professional Paper 485-A.
- Webb, R.H., Jarrett, R.D., 2002. One-dimensional estimation techniques for discharges of paleofloods and historical floods, in: House, P.K., Webb, R.H., Baker, V.R., Levish, D.R. (Eds.), *Ancient Floods, Modern Hazards: Principles and Applications of Paleoflood Hydrology*. American Geophysical Union, Washington, DC, pp. 111–125. doi:10.1029/WS005p0111
- Zielonka, T., Holeksa, J., Ciapala, S., 2008. A reconstruction of flood events using scarred trees in the Tatra Mountains, Poland. *Dendrochronologia* 26, 173-183. doi:10.1016/j.dendro.2008.06.003

Four-topic correlation between flood dendrogeomorphological evidence and hydraulic parameters (the Portainé stream, Iberian Peninsula)

Ane Victoriano^{a,*}, Andrés Díez-Herrero^b, Mar Génova^c, Marta Guinau^a, Glòria Furdada^a, Giorgi Khazaradze^a, Jaume Calvet^a

^a RISKINAT Group, Geomodels Research Institute, Dpt. de Dinàmica de la Terra i de l'Oceà, Facultat de Ciències de la Terra, Universitat de Barcelona (UB), ~~Martí i Franquès s/n~~, 08028 Barcelona (Spain).

^b Geological Hazards Division, Geological Survey of Spain (IGME), ~~28003~~ Madrid (Spain).

^c Dpto. de Sistemas y Recursos Naturales, Universidad Politécnica de Madrid (UPM), ~~28040~~ Madrid (Spain).

* Corresponding author

E-mail addresses: ane.victoriano@ub.edu (A. Victoriano), andres.diez@igme.es (A. Díez-Herrero), mar.genova@upm.es (M. Génova), mguinau@ub.edu (M. Guinau), gloria.furdada@ub.edu (G. Furdada), gkharzar@ub.edu (G. Khazaradze), jcalvet@ub.edu (J. Calvet).

Abstract

Torrential floods are hazardous hydrological phenomena that produce significant economic damage worldwide. Flood reconstruction is still problematic in mountainous ungauged areas due to the lack of systematic real data, so other indirect techniques ~~need to be applied~~ are required. This paper presents an integrated palaeoflood study of a Pyrenean stream that combines fluvio-torrential geomorphology, dendrogeomorphology, palaeoflood discharges and flow hydraulics. The use of a total station and airborne LiDAR data has allowed obtaining a detailed topography for geomorphological mapping and for running a one-dimensional hydraulic model. ~~Peak discharges were estimated by searching for the minimum deviation between height of scars on trees and the modelled water stage. Based on the height of scars on several damaged trees, W~~we obtained palaeodischarges of $316 \text{ m}^3 \text{ s}^{-1}$ and $314 \text{ m}^3 \text{ s}^{-1}$ for the 2008 and 2010 floods events. The hydraulic parameters ~~obtained from the 1D model~~ were related to the geomorphic position of ~~analysed~~ trees, showing a positive relation between most energetic geomorphic elements and flow depth and velocity values. ~~Geomorphology was also combined with flood dendrogeomorphological evidence (FDEs). A total of 15 events were identified by the dendrochronological dating. We identified the geomorphic forms showing the highest amount of external disturbances on trees.~~ The most intensely affected trees are located in intermediate ~~high~~ energy geomorphic positions. Analysing variabilities in scar height and flow stage differences, we suggest that most reliable trees for peak discharge estimation correspond to those placed in areas related with fluvio-torrential processes of intermediate energy, ~~which is discussed to be the result of the destruction of the most exposed trees, such as those located in the main active channel. This multidisciplinary approach shows a high potential for palaeoflood analysis in ungauged mountain catchments, and relates four palaeohydrology subdisciplines for the first time in a selected study area. This multidisciplinary palaeohydrological study relates flood hydrodynamics with the damages on trees and their geomorphological characteristics, focusing on the hydraulic~~

43 parameters of the peak flow (depth, velocity and unit stream power), which has never
44 been carried out elsewhere. The proposed approach shows a high potential for
45 palaeoflood analysis in ungauged mountain catchments with scarce non-systematic data.

46 *Keywords:* Dendrogeomorphology, Fluvial geomorphology, Hydraulic modelling,
47 Palaeoflood, Spanish Pyrenees.

48 1. Introduction

49 Hydrometeorological phenomena are one of the most recurrent causes of natural
50 disasters worldwide that annually produce significant economic damages and fatalities
51 losses of human life (Gaume et al., 2009). Flood disasters, ~~including flash floods, river~~
52 ~~floods and coastal floods,~~ are increasing in number and damages in the last few decades
53 in Europe (Barredo, 2007). In mountainous areas of Catalonia (Spain), flash floods and
54 debris flows cause severe socioeconomic and geomorphologic impacts due to their
55 sudden occurrence, torrential behaviour and high sediment load involved (Portilla et al.,
56 2010).

57 Flood hazard assessment is often based on conventional statistical magnitude-
58 frequency analyses, which are difficult to apply in areas with scarce rainfall data and ~~no~~
59 lack of flow gauging stations. Palaeohydrology is a useful method in active torrential
60 basins with ~~no gauging station~~ non-systematic records, ~~and that~~ consists on the study of
61 past floods especially focusing on ancient extraordinary events, and encompasses
62 different research lines depending on the palaeoflood data and working methodology
63 (Baker, 2008; Benito and Díez-Herrero, 2015; Lang et al., 2004; Webb and Jarrett,
64 2002) (Baker, 2008; Benito and Díez-Herrero, 2015). Extreme flood reconstruction has
65 been carried out using a variety of data sources and evidence, such as sedimentological
66 (Benito et al., 2003, 2015; Kochel and Baker, 1982), geomorphological (Baker et al.,
67 1988; Baker and Pickup, 1987), dendrochronological (Ballesteros-Cánovas et al., 2016;
68 Gottesfeld, 1996; Kundzewicz et al., 2014; Malik and Matyja, 2008; Sigafos, 1964;
69 Yanosky and Jarrett, 2002; Zielonka et al., 2008) ~~(Ballesteros-Cánovas et al., 2015;~~
70 ~~Benito and Díez-Herrero, 2015), and lichenometric~~ lichenometric indicators (Gob et al.,
71 2003) ~~—indicators. Palaeoflood hydrology encompasses different research lines~~
72 ~~depending on the palaeoflood data and working methodology (Baker, 2008; Benito and~~
73 ~~Díez-Herrero, 2015). Some studies focus on the estimation of flood discharges and flow~~
74 ~~hydraulic parameters, while others are focused on the morphodynamics and chronology~~
75 ~~using disciplines as fluvial geomorphology or dendrogeomorphology. However, each~~
76 ~~method has its own strengths and limitations, so the combination of techniques provides~~
77 ~~a better knowledge about to past rare events.~~

78 Many authors have reconstructed palaeoflood using dendrogeomorphology, which
79 provides information about past events recorded in flood dendrogeomorphological
80 evidence (FDE) in riverbed and riverbank trees. ~~FDEs have been used to obtain flood~~
81 ~~discharges (Ballesteros et al., 2011; Ballesteros-Cánovas et al., 2013; Bombino et al.,~~
82 ~~2015, among others; see compilation reviews from~~ Ballesteros-Cánovas et al., 2015b
83 and Benito and Díez-Herrero, 2015), but also other hydraulic parameters like flow
84 velocity, depth and power by means of hydrodynamic modelling (Ballesteros-Cánovas
85 et al., 2010, 2015a). Numerous studies relate flood discharges with flow hydraulics with
86 different empirical equations (Bagnold, 1980; Chanson, 2004; Chow, 1959; Costa,

87 1983; Ferguson, 2005). Some other works deal with flow hydraulics and fluvial
 88 geomorphology from different perspectives: flood geomorphology (Baker et al., 1988),
 89 the stability of geomorphological elements (Nicholas and Walling, 1997; Ortega and
 90 Garzón, 1997) or past flood discharges and deposits (Baker, 1987; Kochel and Baker,
 91 1982; Sánchez-Moya and Sopena, 2015). However, dendrogeomorphological evidence
 92 have rarely been associated to the geomorphic ~~forms and correlated with the~~ position of
 93 the trees (Ruiz-Villanueva et al., 2010), or other local characteristics of the river reach
 94 (Ballesteros-Cánovas et al., 2016); and never before have been related the four
 95 elements: FDEs, geomorphological features, hydrological parameters and
 96 palaeodischarges.

97 However, these methods tend to have some limitations in mountains areas.
 98 Dendrogeomorphological studies are conditioned by the number of trees of the study
 99 area, which is limited in some cases. High-resolution geomorphological mapping is
 100 difficult to carry out in remote areas. Palaeodischarge reconstructions in ungauged
 101 catchments require an adequate topographic data for hydraulic modelling, which is
 102 usually scarce in forested mountain catchments. Regarding flow hydrodynamics, the
 103 calculation of hydraulic parameters depends on the estimated peak discharge.

104 This paper reconstructs flood events combining all the above mentioned disciplines
 105 (Fig. 1). The aim of this paper is to quantify the relation between flood hydrodynamics
 106 and the geomorphological characteristics of damaged trees. Flow hydraulics are
 107 analysed according to the specific geomorphic position of trees and the obtained stream
 108 power from hydraulic modelling is used to estimate the mobilizable particle size, which
 109 is compared to field measures to assess its reliability. Such a multidisciplinary analysis
 110 specially focusing on hydraulic parameters has never been carried out before in a
 111 selected study area, and allows us to obtain an improved knowledge about fluvio-
 112 torrential dynamics in areas with few source data.

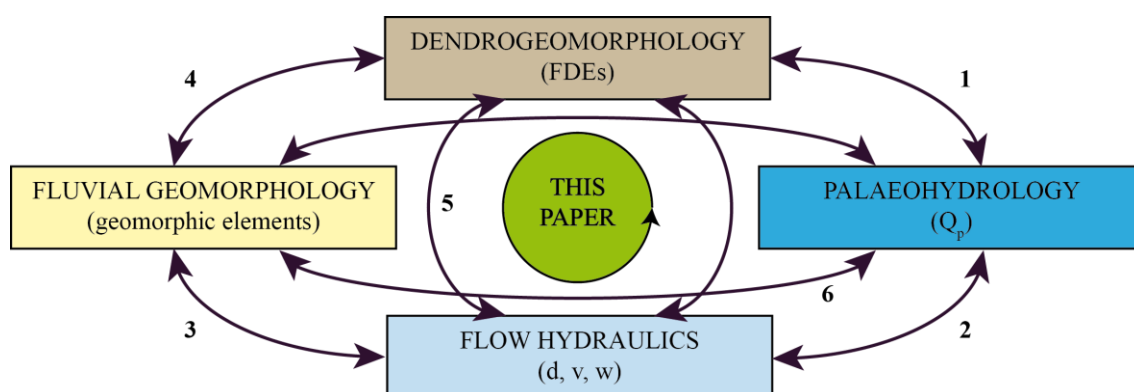


Figure 1. Conceptual diagram of the disciplines and methods combined ~~for the first time~~ in the present study. Numbers indicate some of the groups of existing studies relating different research topics: 1, Dendrogeomorphology vs Palaeohydrology -(see reviews from Ballesteros-Cánovas et al., 2015b, and Benito and Díez-Herrero, 2015)(Ballesteros et al., 2011; Ballesteros-Cánovas et al., 2013; Bombino et al., 2015); 2, Palaeohydrology vs Flow Hydraulics (Bagnold, 1980; Chanson, 2004; Chow, 1959; Costa, 1983; Ferguson, 2005); 3, Flow Hydraulics vs Fluvial Geomorphology (Nicholas and Walling, 1997; Ortega and Garzón, 1997, ~~2009~~; Sánchez-Moya and Sopena, 2015); 4, Fluvial Geomorphology vs Dendrogeomorphology (Ballesteros-Cánovas et al., 2016; Ruiz-Villanueva et al., 2010); 5, Dendrogeomorphology vs Flow Hydraulics (Ballesteros-Cánovas et al., 2010, 2015a); 6, Palaeohydrology vs Fluvial Geomorphology (Baker, 1987; Baker et al., 1988; Kochel and Baker, 1982).

113 ~~The aim of this paper is to reconstruct torrential flood events by putting together all~~
114 ~~these research topics in a detailed study that combines dendrogeomorphology~~
115 ~~(dendrochronological dating and geomorphic position of affected trees), fluvial~~
116 ~~geomorphology (detailed topography and geomorphological mapping), flow hydraulics~~
117 ~~(1D hydraulic modelling) and palaeoflood discharge estimations (Fig. 1). This is~~
118 ~~achieved by estimating peak discharges and hydraulic parameters from~~
119 ~~dendrogeomorphological evidence (sears), and relating flow hydraulics of past flood or~~
120 ~~debris flood events with the geomorphic position of affected trees. Such a~~
121 ~~multidisciplinary analysis has never been carried out before in a selected study area and~~
122 ~~bridges the gap between the previous applications of specific methods. This study~~
123 ~~allows us to obtain a realistic knowledge of the torrential dynamics of the system by~~
124 ~~better reconstructing past events in areas with few source data.~~

125 2. Problematic Study area and hazard

126 The multidisciplinary approach presented in this paper was performed in the 5.72
127 km² Portainé drainage basin (Pallars Sobirà County, Catalonia, Spain), located in the
128 Eastern Pyrenees (Fig. 2a). ~~The Portainé basin is a 5.72 km² mountainous area.~~
129 ~~Maximum altitude is 2439 m a.s.l. (Torreta de l'Orri). A ski resort, called Port Ainé, is~~
130 ~~situated in the headwaters.~~ Two main streams drain the basin towards the north, the
131 Portainé stream (5.7 km long) and its tributary the Reguerals stream (3 km long), ~~the~~
132 ~~latter being a tributary of the former.~~ Their confluence is placed at 1285 m a.s.l. and
133 then, the Portainé stream flows until its confluence with the Romadriu ~~or Santa~~
134 ~~Magdalena~~ River (part of the Ebro River Basin, ~~draining to the Mediterranean Sea~~) at
135 950 m a.s.l., ~~where the Vallespir hydroelectric power station is located~~ (Fig. 2c). An
136 access road to the Port-Ainé ski station crosses both streams at various points. The
137 climate ~~of the study area~~ is Alpine Mediterranean, with a mean annual rainfall of 800
138 mm and 5-7 °C mean annual temperature (Meteocat, 2008).

139 From a geological perspective, the Portainé basin is located in the Pyrenean Axial
140 Zone (Fig. 2b). In the study area, the bedrock is composed of highly folded and
141 fractured Cambro-Ordovician metapelites and sandstones with quartzite intercalations.
142 Wide surficial colluvial materials irregularly cover large parts of the terrain. ~~In addition,~~
143 ~~torrential deposits are found in the stream bottom and margins.~~ Due to the highly
144 fractured bedrock and the unconsolidated surficial deposits, materials are easily eroded
145 and mobilized along the streams. Geomorphologically, ~~the present landscape of the~~
146 ~~Pyrenees is mostly the result of the Upper Pleistocene last glacial period. Valleys were~~
147 ~~excavated into Neogene high planation surfaces, presently found above 2000 m a.s.l.~~
148 ~~(Ortuño et al., 2013). Partly due to these processes, the Portainé basin~~ catchment
149 can be divided in two sectors (IGC, 2013). The southern one corresponds to the headwaters
150 ~~previously occupied by a glacial cirque,~~ and shows lower gradients (less than 25°, but
151 usually around 10-20°) and a poorly entrenched drainage network. The northern sector
152 shows higher gradients (more than 25°) ~~and the streams are strongly~~ entrenched
153 streams (Fig. 2c).

154 ~~Vegetation of the area includes a variety of tree species, including *Populus tremula*~~
155 ~~(common aspen), *Populus nigra* (black poplar), *Fraxinus excelsior* (ash), *Prunus avium*~~
156 ~~(wild cherry), *Quercus petraea* (sessile oak), *Tilia cordata* (littleleaf linden), *Juglans*~~

157
158

~~regia (common walnut), Acer campestre (field maple), Salix caprea (goat willow) and Betula pendula (silver birch).~~

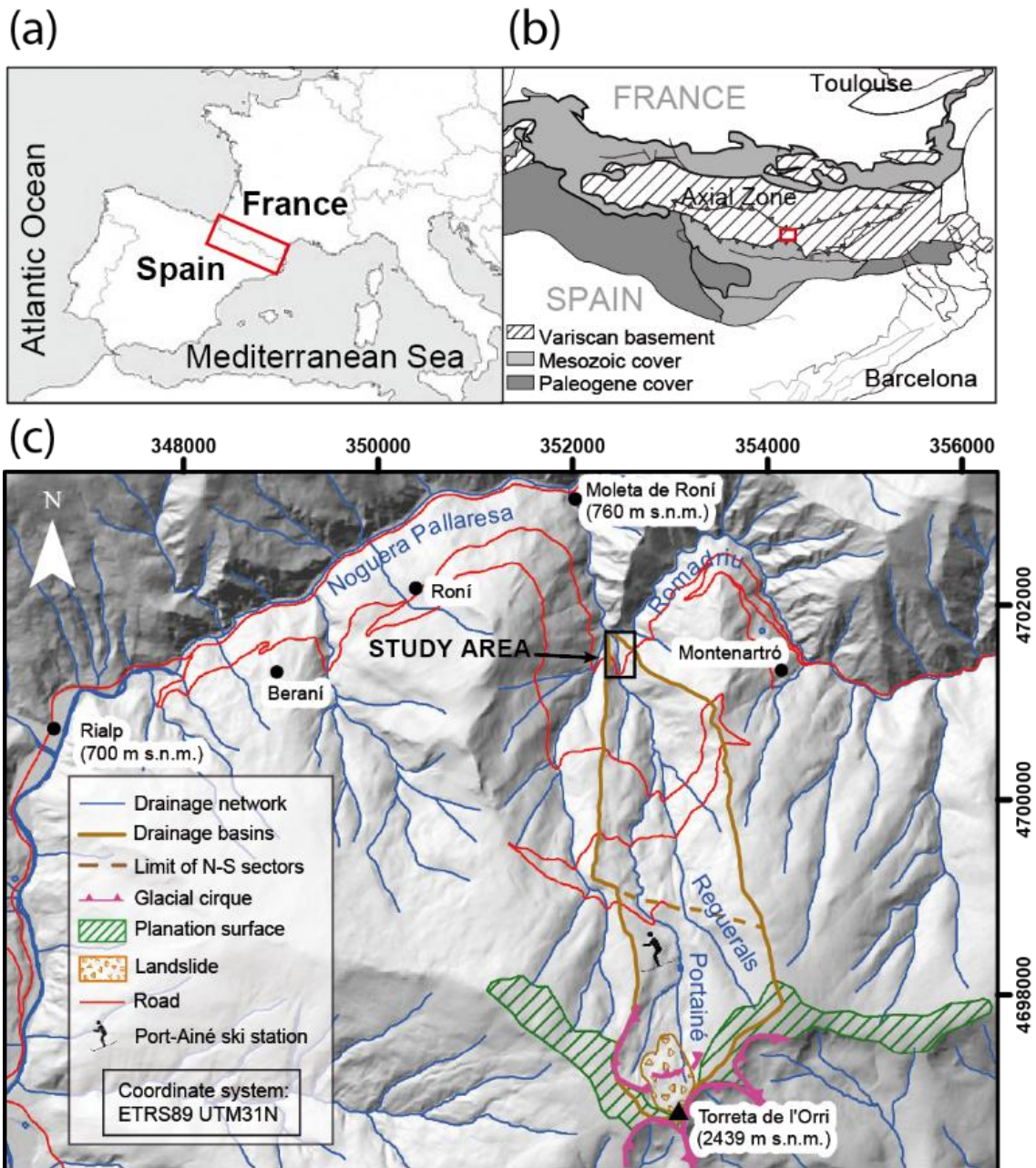


Figure 2. (a) Geographic setting, with the Pyrenees marked with a red square. (b) Geological setting of the study area, located in the Axial Pyrenees, and the area of Fig. 2c marked with a red square. (c) Geomorphological context of the Portainé basin and the specific study area marked with a ~~red-black~~ square, corresponding to the most downstream reach ~~of the Portainé stream.~~

159
160
161
162
163
164
165

The Portainé and the Reguerals streams are characterized by a high torrential activity especially since 2006, as debris flood, hyperconcentrated flow and/or debris flow events produce significant losses in infrastructures, mainly where the ~~access~~ road ~~to the Port-Ainé ski station~~ crosses the streams. From 2006 to 2015, ten events have occurred in this area (FGC and ICGC, 2015; IGC, 2008, 2010a, 2010b, 2011, 2013b; IGC et al., 2013; Portilla et al., 2010; Palau et al., 2017), even without extraordinary rainfall values. In addition, dendrogeomorphological studies have proved the occurrence

166 of previous torrential events, even if their frequency is much lower (Furdada et al.,
 167 2016; García-Oteyza et al., 2015). In order to reduce these impacts, 15 sediment
 168 retention barriers were installed along the channels since 2009 as a hydrological
 169 correction measure (Luis-Fonseca et al., 2011; ~~Raimat et al., 2010, 2013~~). However, the
 170 problem remains, ~~as torrential events still occur frequently~~ and the increasingly
 171 entrenched streams show a significant erosive tendency (Victoriano et al., 2016).

172 The specific study area corresponds to the most downstream 500 m-long reach of
 173 the Portainé stream. In the confluence with the Romadriu River, an alluvial elongated
 174 debris cone has ~~been~~ formed, mainly composed of sub-rounded to sub-angular
 175 decimetric boulders. High sediment load torrential events change the morphology ~~and~~
 176 ~~the geomorphic forms~~ of the mobile riverbed ~~and the cone~~ easily, also affecting the
 177 riverbank trees. In general, the vegetation of the area constitutes a deciduous broadleaf
 178 forest with a variety of species.

179 3. Material and methods

180 The ~~methodology applied in methodological approach~~ of this study is synthesized in
 181 Fig. 3, showing ~~for each research topic the main data sources, the techniques of analysis~~
 182 ~~and the preliminary results, but also and~~ the integration of the methods for final results.

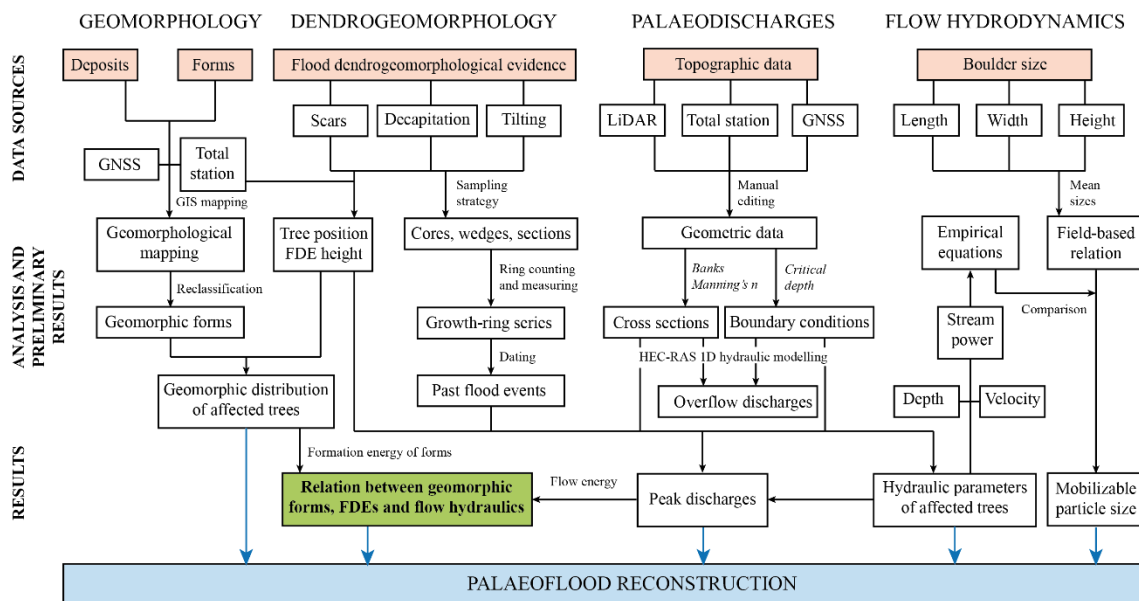


Figure 3. Flow diagram showing the multidisciplinary methodology applied in this study for palaeoflood reconstruction, from data sources to results, following four main disciplines: geomorphology, dendrogeomorphology, paleodischarge estimation and flow hydrodynamics.

183 3.1. Topographic data acquisition and Triangulated Irregular Network generation

184 Topographic data from different sources were combined to obtain the most suitable
 185 bare earth digital elevation model (DEM) of the area, in fact, integrating: (i) airborne
 186 LiDAR data, and (ii) total station surveying.

187 The potential of LiDAR (Light Detection and Ranging) data for terrain mapping and
 188 creating high resolution DEMs has been widely accepted (Day et al., 2013; Roering et
 189 al., 2013; Tarolli, 2014), and this technique has already been applied for a variety of
 190 environments (Abermann et al., 2010; Bizzi et al., 2016; Jaboyedoff et al., 2012).

191 ~~However, their accuracy and resolution decreases in mountain areas, characterized by~~
192 ~~significant gradients and dense vegetation. LiDAR data used in this study were~~
193 ~~collected with the aircraft Cessna Caravan 208B and the topographic LiDAR sensor~~
194 ~~Leica ALS50 II, owned by the Cartographic and Geological Institute of Catalonia~~
195 ~~(ICGC), obtaining an altimetric accuracy of <15 cm mean squared error (MSE). In the~~
196 ~~forested area, the accuracy is estimated to show <50 cm MSE. The point cloud was~~
197 ~~georeferenced and filtered using the TerraScan software (Terrasolid, 2016), but the~~
198 ~~classification was latter manually verified and corrected. This airborne LiDAR data~~
199 ~~provided a good coverage of the area but not a high-resolution topography (0.63~~
200 ~~points/m² for ground points). This deficiency was overcome by the use of topographic~~
201 ~~data obtained in the field using a total station.~~

202 ~~Detailed topographic data acquisition was carried out using a Leica TC 1700 total~~
203 ~~station. These taquimetric surveys focused in localizing and defining topographic sharp~~
204 ~~changes (breaklines), geomorphic elements and trees, therefore collecting a complete~~
205 ~~point dataset (Keim et al., 1999). In addition, very detailed topographic cross sections~~
206 ~~were obtained where trees showing external FDEs are located. Differential RTK GNSS~~
207 ~~methods were used to accurately measure the absolute coordinates of some control~~
208 ~~points (Khazaradze et al., 2016), used to georeference the dense measurements obtained~~
209 ~~by the total station.~~

210 ~~The integration of LiDAR and total station data reveals some adjacent points with~~
211 ~~significant differences in elevation. This was due to (i) small but detectable erosion and~~
212 ~~accumulation reflected in the 2011 LiDAR and 2014-2016 total station data sets; and~~
213 ~~(ii) the morphology of the real steep terrain (e.g. stream entrenchment, steep slopes and~~
214 ~~escarpments). To overcome these limitations, a manual point editing process was~~
215 ~~carried out, using objective criteria of congruence and acceptability. It consisted on~~
216 ~~detecting erroneous points by comparing their coordinates with the surrounding points.~~
217 ~~Stablishing a tolerance threshold of 0.5 m for the differences on elevation, incoherent~~
218 ~~data were deleted. Finally, a bare-earth Triangulated Irregular Network (TIN) was~~
219 ~~created with the selected terrain points.~~

220 *3.2.3.1. Geomorphological mapping and analysis and mapping*

221 ~~A detailed geomorphological study and mapping of the features associated to the~~
222 ~~Portainé stream was carried out based on the topographic data and field observations.~~
223 ~~This analysis had two steps, (i) the topographic and geomorphological fieldwork, and~~
224 ~~(ii) GIS mapping.~~

225 ~~Detailed topographic data acquisition was carried out in March 2014 using a Leica~~
226 ~~TC 1700 total station. This taquimetric survey was focused on localizing and defining~~
227 ~~topographic sharp changes (breaklines), of geomorphic elements and tree positions in~~
228 ~~order to collect a complete point dataset (Keim et al., 1999) consisting of 1118 points~~
229 ~~(853 ground points and 265 tree points) in a 4850 m² area. In addition, in places where~~
230 ~~trees showing external FDE were identified we also obtained detailed topographic cross~~
231 ~~sections. Differential RTK GNSS methods were carried out to accurately measure the~~
232 ~~absolute coordinates of certain control points (Khazaradze et al., 2016) used to~~
233 ~~georeference the dense measurements obtained with the total station. Regarding~~
234 ~~geomorphological mapping, dduring the first-mentioned topographic field survey, main~~

235 geomorphological elements were identified following the proposal of Church et al.
236 (2012) and their limits were measured with the total station. Main geomorphological
237 elements and deposits were roughly classified as: functional channel, distributary
238 channels of the cone, gravels and boulders; in addition, alluvial terraces were identified,
239 as well as other features like levees, escarpments and flow paths. During subsequent
240 field surveys carried out in March 2015, September 2015 and June 2016, morphological
241 changes in landforms, elements and facets (different parts of the elements) were
242 recognized, which mainly occurred along the channels and did not alter the position of
243 riverbed and riverbank trees and measured.

244 The deposits and forms were mapped using the ArcGIS 10.2.2 software (ESRI,
245 2014), creating ~~four a detailed geomorphological maps, one from each survey~~
246 ~~campaign. Main geomorphological elements and deposits have been roughly classified~~
247 ~~as: functional channel, distributary channels of the cone, gravels and boulders; in~~
248 ~~addition, alluvial terraces have been identified, as well as other features like levees,~~
249 ~~escarpments and flow paths.~~

250 3.3.3.2. Dendrogeomorphological analysis

251 Dendrogeomorphology is a palaeohydrological data source that provides
252 information about past torrential events recorded ~~in different types of evidence (FDEs)~~
253 ~~in trunks, branches and roots of~~ riverbed and riverbank trees (Díez-Herrero, 2015).
254 ~~FDEs, formed by significant torrential events, may be identified in trunks, branches and~~
255 ~~roots of trees. Dendrogeomorphological techniques have~~ Tree-ring analysis been widely
256 applied for fluvio-torrential processes in flood studies (see reviews from Ballesteros-
257 Cánovas et al., 2015b and Benito and Díez-Herrero, 2015), ~~by analysing the tree ring~~
258 ~~widths to study the frequency and magnitude of past flood and debris flow events~~
259 ~~(Benito and Díez-Herrero, 2015; Bollschweiler and Stoffel, 2010; Díez-Herrero et al.,~~
260 ~~2013b; Génova et al., 2015). The most frequent and used external evidence are scars in~~
261 ~~tree bark, stem decapitation (usually with branch replacement), tree tilting, root~~
262 ~~exposure, bark erosion and stem burial. These disturbances produce reactions in trees,~~
263 ~~such as growth reduction (or suppression), growth release and asymmetries. The~~
264 ~~dendrogeomorphological study carried out in Portainé, following the proposal of Díez-~~
265 ~~Herrero et al. (2013a) can be divided in two complementary tasks, (i)~~
266 ~~dendrochronological study, and (ii) geomorphological analysis of the tree positions. The~~
267 ~~dendrogeomorphological study carried out in Portainé is divided in three~~
268 ~~complementary tasks, (i) dendrochronological sampling, (ii) tree-ring analysis and FDE~~
269 ~~dating, and (iii) geomorphological analysis of the tree positions.~~

270 Dendrochronological sampling was carried out in March 2014, March 2015 and
271 September 2015, and the strategy was based on the field recognition of external
272 ~~disturbances on trees (Fargas, 2015; García-Oteyza et al., 2015). The~~ Especially,
273 selected trees were those showing evidence most probably produced by the impact of
274 boulders and/or large wood transported by the flow, mainly injured, decapitated and
275 tilted trees (Fig. 4), but also few trees with exposed roots. Trees were sampled following
276 dendrogeomorphological procedures (Stoffel & Bollschweiler, 2008; Díez-Herrero et
277 al., 2013, Stoffel & Corona, 2014). A total of 67 trees from 10 different species were
278 sampled, providing a multievidence population (Génova et al., under review). The

279 geographic position of each tree was measured using a total station, and also the height
 280 of scars and decapitation nodes. Additional information was also ~~noted and~~ collected,
 281 such as an identifier code, ~~the~~ sampling date, species, description of the tree (height and
 282 perimeter), description of the FDE (type, height and size), description of the sample
 283 (height) and photos of the tree. Cylindrical samples (cores) were obtained using a
 284 Pressler increment borer of 5 mm diameter. Some wedges were also extracted from
 285 overgrowing callus in scarred trees and ~~in some death trees~~ cross sections were cut in
 286 some death trees. ~~A total of 144 samples were obtained but 10 trees were rejected due to~~
 287 ~~rotten cores or indistinguishable rings; so finally~~ We analysed 57 trees from 9 different
 288 species (151 samples) were analysed providing a multievidence population of *Populus*
 289 *tremula* L. (common aspen), *Populus nigra* L. (black poplar), *Fraxinus excelsior* L.
 290 (ash), *Prunus avium* L. (wild cherry), *Quercus petraea* (Matt.) Liebl. (sessile oak), *Tilia*
 291 *platyphyllos* Scop. (largeleaf linden), *Juglans regia* L. (common walnut), *Acer*
 292 *campestre* L. (field maple) and *Salix caprea* L. (goat willow). ~~The average age of the~~
 293 ~~analysed trees is 52 years, with the oldest one being 86 years old, and the dating~~
 294 ~~allowed to detect 15 past events from 1957 to 2011. The sampling strategy and the~~
 295 ~~methodology for dendrochronological and dendrogeomorphological analysis is~~
 296 ~~described in detail in Génova et al. (under review). Different FDEs were characterized~~
 297 ~~and dated (external an internal scars, decapitations and branch replacement,~~
 298 ~~suppressions, growth releases and asymmetries) and all this information was compiled~~
 299 ~~in a dendrogeochronological database.~~

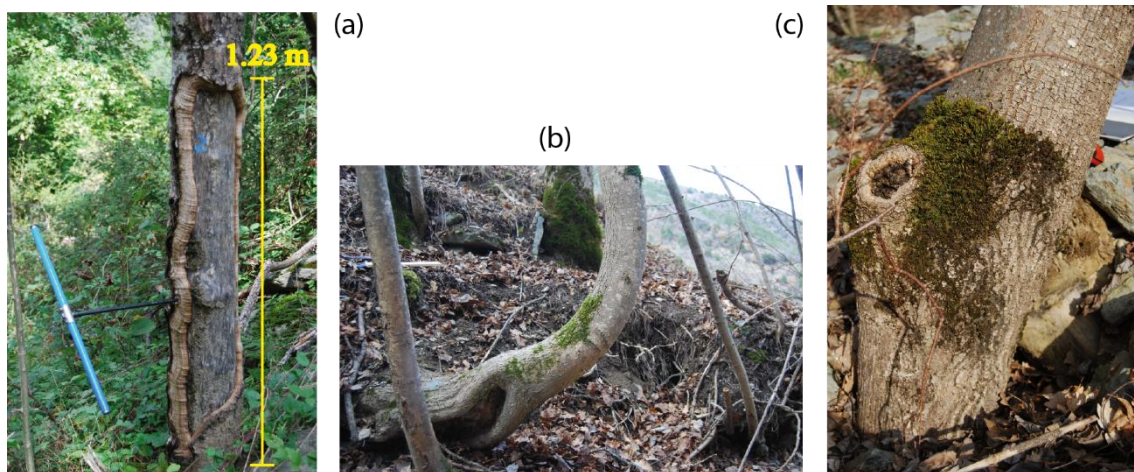


Figure 4. External disturbances on trees located in the riverbanks of the Portainé stream. (a) Scar formed in 2008. (b) Stem tilting. (c) Decapitated tree.

300 In this study, we only considered external evidence on trees. In the laboratory, tree-
 301 ring analysis of cores, wedges and sections consisted in (Génova et al., 2015): (i)
 302 sample air-drying, cutting or sanding; (ii) tree-ring width measuring using a LINTAB
 303 table (with 1/100 mm accuracy) and the associated software TSAPWin (RinnTech,
 304 2003); (iii) cross-dating using visual and statistical techniques (Cook and Kairiukstis,
 305 1990); and (iv) quality check using the Cofecha software (Grissino-Mayer, 2001). This
 306 process let us to date scars in tree-ring series and consequently, torrential events. The
 307 last ring of dead trees was dated by comparing tree-ring series with other living trees of
 308 the same species. For palaeoflood reconstruction, the scars' formation year (dated
 309 following the mentioned procedure) and their height (measured in the field) were used.

310 Additionally we considered the location of decapitated trees, tilted trees and exposed
311 roots for the geomorphic analysis. This information was compiled within a
312 dendrogeochronological database.

313 The inclusion of the dendrogeochronological database into a GIS environment,
314 using ArcGIS 10.2.2 software (ESRI, 2014), allowed to study the geomorphological
315 setting of disturbed trees. Based on the geomorphological mapping and tree positions,
316 geomorphic features were reclassified according to their formation energy (Ruiz-
317 Villanueva et al., 2010), ~~considering the specific elements identified in the field.~~ This
318 lead to a considerably more elaborated classification of the geomorphic forms, elements
319 and facets. Moreover, the detailed geomorphic position of each tree was determined in
320 the field, and trees were classified according to the geomorphic form (e.g. riverbed),
321 element (e.g. gravel bar) or facet (e.g. bar tail) in which they were located, obtaining the
322 spatial distribution of de FDE according to the formation energy of the geomorphic
323 form on which they locate. Other geomorphological characteristics (e.g. channel reach
324 morphology and tree exposure to the flow) were not considered in this study because
325 they were equal for all the scarred trees (straight channel and exposed trees). Therefore,
326 the geomorphic position according to geomorphic units was the best evidence to relate
327 flow hydrodynamics and FDE formation.

328 3.4.3.3. Palaeodischarge estimations and hydraulic modelling*Hydrodynamic* 329 *modelling*

330 Palaeofloods were reconstructed using the one-dimensional hydraulic simulation
331 software HEC-RAS 4.0 from the US Army Corps of Engineers (USACE, 2008). This
332 ~~1D numerical hydrodynamic~~ model was used to obtain palaeoflood discharges and other
333 hydraulic parameters as stage, water depth, velocity and stream power. It was run a 1D
334 model instead of a 2D one due to the following groups of factors: a) channel geometric
335 characteristics (lack of high-resolution and high-accuracy 2D topographic data; detailed
336 cross-sections coinciding with tree locations measured with total station; narrow valley
337 with length/width ratio >3:1; and lack of anthropic features, such as bridges or culverts,
338 along the channel); b) hydrodynamic factors (unidirectional flow patterns during floods;
339 limited secondary transversal flows due to the narrowness of the valley and the steep
340 gradient with waterfalls and rapids); and c) other evidence (scar height-riverbed
341 parallelism suggesting a sub-uniform to gradually variable flow). The required
342 parameters and conditions to run the hydraulic model were: (i) geometric data, (ii)
343 boundary conditions, and (iii) discharges.

344 Regarding geometric data, HEC-RAS works with transversal cross sections (XS
345 sections). Topographic data from two different sources were available for the study
346 area: total station and airborne LiDAR (Light Detection and Ranging). Total station data
347 was acquired in the field (see section 3.1.) and provided high accuracy but slightly low
348 point-density. LiDAR data was collected with the aircraft Cessna Caravan 208B and the
349 topographic LiDAR sensor Leica ALS50-II, owned by the Cartographic and Geological
350 Institute of Catalonia (ICGC), and the point cloud was georeferenced and filtered using
351 the TerraScan software (Terrasolid, 2016). The potential of LiDAR data creating high-
352 resolution elevation models has been widely accepted (Tarolli, 2014). However, in our
353 mountain study area with steep slopes and dense vegetation, the LiDAR dataset

354 provided a good coverage but a low elevation accuracy (about 50 cm RMSE) and not
355 very high-resolution topography (0.63 ground point/m²). Taking into account that for
356 this study we had different topographic data sources (LiDAR and total station), Taking
357 into account the mentioned strengths and limitations of data sources, two hydraulic
358 models with different geometric data were run. ~~First~~The first one, manually introducing
359 the cross sections measured with the total station in the field ~~survey~~ (23 XS sections).
360 The second one, combining both topographic data. LiDAR points were added into the
361 total station dataset and carefully analysed in order to assess its suitability. Some
362 adjacent points showed significant differences in elevation, which were attributed to (i)
363 small but detectable erosion and accumulation between the 2011 LiDAR and 2014 total
364 station data; and (ii) the real morphology of the steep terrain (e.g. stream entrenchment,
365 escarpments and steep slopes). In order to overcome these limitations, a manual point
366 editing process was carried out using objective criteria of congruence and acceptability,
367 consisting in detecting erroneous points by comparing their coordinates with the
368 surrounding points. This was done by creating 0.5 m (in steep areas) or 1 m (in flat area)
369 buffers for total station points and intersected with LiDAR ground points. Establishing a
370 maximum tolerance threshold of 0.5 m for the differences on elevation between both
371 topographic data sources, incoherent LiDAR points were deleted. Finally, a bare-earth
372 Triangulated Irregular Network (TIN) was created with the selected terrain points and
373 sections were extracted from it , and second, extracting sections from the TIN that
374 combines both topographic data sources (35 XS sections), using HEC-GeoRAS 10.2
375 extension (USACE, 2012) for ArcGIS. The advantage of the TIN-based model is that it
376 allowed the input of additional transversal profiles ~~not measured in the field, coinciding~~
377 ~~with the position of others trees with dated scars~~, but its weakness is that LiDAR data
378 can distort and smooth the detailed sharp topography obtained in the field. In addition,
379 the stream centreline, banks and levees were added. The limits of the riverbanks were
380 defined coinciding with roughness changes, so that a Manning's *n* value for the left
381 bank, channel and right bank was established for each cross section. The roughness
382 coefficient was obtained from field observations, based on Arcement and Schneider
383 (1989).

384 Boundary conditions upstream and downstream from the modelled reach were
385 critical depth because both boundary sections correspond to small waterfalls (more than
386 2 m high) in stable bedrock riverbed, identified in the field. These are hydraulic jumps
387 with a critical flow (Froude number = 1); especially during flood events, so they are
388 suitable for the critical-depth method (Bodoque et al., 2011). The model was run as a
389 steady flow, as the input were peak discharge values; and the flow regime modelled as
390 supercritical.

391 Palaeodischarges were calculated using external scars ~~For the palaeohydraulic~~
392 ~~reconstructions of this study, dendrogeomorphological evidence were used as~~
393 ~~palaeostage indicators (PSIs). External scars were considered the evidence that~~These
394 evidence provide the most precise information of both the date and the magnitude of the
395 event, as they allow knowing both the precise year in which they were formed by
396 dendrochronological dating and the minimum water depth of the flow by measuring the
397 height of the scar and/or its absolute altitude. In our study, we dated external scars from
398 2000 (4 scars), 2006 (1 scar), 2008 (19 scars) and 2010 (6 scars) events. Scars from
399 2000 were almost closed and did not provide information about the water stage.

400 Regarding the trees scarred in 2006, there was a unique evidence so it was not
401 considered enough as a palaeostage indicator. Therefore, only 2008 and 2010 events
402 could be reconstructed, as they provided a representative number of scars and their
403 height could be reliably measured in the field~~Only those years that showed at least five~~
404 ~~scars were considered to have enough evidence to be adequately reconstructed by~~
405 ~~hydrodynamic modelling. Only 2008 and 2010 met this requirement,;~~ which-but are also
406 the last most destructive documented events. Although two high discharge events
407 occurred in 2008 (September and November) and two others in 2010 (July and August),
408 we assume that the scars were formed by ~~the higher magnitude a unique~~ event for each
409 year. In fact, scars from 2008 were all formed in the high-magnitude torrential flood
410 occurred in September, which produced documented damages in a bridge located just
411 upstream of the study reach (IGC, 2013), whereas the low-magnitude event occurred in
412 November did not produce any effect at that point. Regarding scars from 2010, the one
413 in July did not transport material along the study reach because it was accumulated in
414 recently emplaced sediment retention barriers (IGC, 2010b); so, the scars would
415 correspond to the August event when the barriers were filled and the flow transported
416 high sediment load. We selected ~~from the FDE database (Génova et al., under review)~~
417 the trees showing scars corresponding to those events years ~~(25 trees)~~ in different
418 geomorphic positions (25 trees). For each year, we carried out a normality test to height
419 differences (d; Eq. 3) in order to detect outliers, comparing the samples with a normal or
420 Gaussian distribution. This process allowed us to detect an anomalous scar for 2008,
421 which indeed, showed an odd shape in the field. Therefore, its origin may not be
422 torrential and it was deleted before simulating the discharge values. At last, 18 scars (6
423 *P. tremula*, 6 *P. nigra*, 2 *F. excelsior*, 2 *P. avium*, 1 *Q. petraea* and 1 *A. campestre*)
424 were considered for 2008 modelling (9 of them dated from wedges) and 6 scars (2 *P.*
425 *tremula*, 2 *F. excelsior*, 1 *Q. oetraea* and 1 *T. platyphyllos*) for 2010 (1 dated from a
426 wedge). Peak discharges for analysed palaeofloods were calculated using the step-
427 backwater method (Ballesteros-Cánovas et al., 2010; O'Connor and Webb, 1988), by
428 increasingly introducing peak discharge input values in the model and finding the best
429 fit water surface elevation for the height of the scars. For each event and each input
430 geometric data (XS section), the trial-and-error technique was used towe estimated the
431 peak discharge (with a precision of $1 \text{ m}^3\text{s}^{-1}$), by finding the value that showed the
432 minimum mean absolute error (σ or MAE) and mean squared error (MSE) in the heights
433 (difference between scar altitude and modelled water stage), defined as

$$\sigma = \frac{\sum_i^n d_i}{n} \quad (1)$$

$$MSE = \frac{\sum_i^n d_i^2}{n}$$

434 where n is the number of scars and d is the absolute value of the difference between the
435 height of the scar and the water stage, estimated by the expression

$$d = |Z_{FDE} - Z_Q| \quad (3)$$

436 where Z_{FDE} is the altitude of the scar in meters (m) and Z_Q is the water surface elevation
437 for the modelled peak discharge in meters (m), both measured in the cross section where
438 the scar is located.

439 The peak discharges were finally calculated as the weighted arithmetic mean
 440 between the discharges obtained ~~from with~~ the two geometric data, ~~one the model based~~
 441 ~~on the TIN and the other one using taquimetric sections~~, which was estimated by the
 442 following equation:

$$Q_{2008} = \frac{\left(\frac{1}{\sigma_{TIN}^2} Q_{TIN}\right) + \left(\frac{1}{\sigma_{TS}^2} Q_{TS}\right)}{\frac{1}{\sigma_{TIN}^2} + \frac{1}{\sigma_{TS}^2}} \quad (4)$$

443 σ_{TIN} and σ_{TS} being the absolute error of the TIN-based model and the one with total
 444 station data respectively, and Q_{TIN} and Q_{TS} being the estimated peak discharges in m^3s^{-1} .

445 As the flow in the alluvial cone can be difficult to simulate using a 1D model, we
 446 also calculated the minimum peak discharge for bank overflow. This is the threshold for
 447 cone flooding and consequently, marks a change in the distribution of the flow
 448 discharge. This critical overflow discharge was obtained from the cross section located
 449 in the cone apex.

450 3.4. Flow hydrodynamics

451 ~~In addition to palaeoflood discharges, w~~We extracted other hydraulic parameters
 452 from HEC-RAS results for each cross section, such as water depth, velocity and ~~unit~~
 453 total stream power (also called specific stream power). These parameters were then
 454 obtained for the relative-specific position (left margin, channel or right margin) of each
 455 tree containing a scar used for the hydrodynamic modelling. Depth was calculated
 456 subtracting the elevation of the base of the tree from the water surface elevation. For the
 457 velocity value, we considered the value of the cross section part in which the tree was
 458 located (left bank, channel or right bank). The unit stream power was obtained dividing
 459 the total stream power obtained by the active width of the flow at the specific cross
 460 section part.

461 ~~Moreover, the~~The knowledge of flow hydraulics allowed us to estimate the particle
 462 size that might be mobilized by the flow. These calculations were carried out for the
 463 2008 event and in the deposit of the alluvial cone, because discharge estimation is more
 464 reliable and accurate than for 2010 event. We also measured in the field the maximum
 465 (length), medium (width) and minimum (height) axes of a representative population of
 466 boulders deposited in the alluvial cone~~Boulder size was also measured in the field,~~
 467 allowing us to compare the results obtained by empirical relations with the real
 468 ~~diameters of the~~ deposited material. The diameter of the transported boulders was
 469 calculated using different empirical equations. The mobilizable particle size is a
 470 function of the critical unit stream power, so the hydraulic parameters needed for these
 471 equations were obtained from the upstream cross section of the alluvial cone because
 472 the flow in the study site is supercritical. The three applied relations were:

$$\omega_c = a \cdot D^b \quad (5)$$

473 where ω_c is the critical unit stream power in W/m^2 , a and b are numerical constants
 474 depending on the author (Costa, 1983; Gob et al., 2003; Jacob, 2003; Williams, 1983),
 475 and D is the particle diameter in millimeters (mm),

(6)

$$\omega_c = c_1 \cdot D^{1.5} \cdot \log_{10} \left(\frac{c_2 \cdot d}{D} \right)$$

476 d being the water depth and c_1 and c_2 being numerical constants determined by different
 477 authors (Bagnold, 1980; Ferguson, 2005), and

$$C_d = \left(\frac{0.6}{\left(\frac{d}{H}\right)\left(\frac{L}{B}\right)} \right) + 0.9 \quad (7)$$

478 where C_d is the drag coefficient, assumed to be 0.95, and H , B and L are the diameters
 479 corresponding to the main three main axes of the particles; ~~which are~~ height
 480 (minimum), width (intermediate) and length (maximum), respectively (Carling et al.,
 481 2002). In fact, ~~Carling et al. (2002) come up with an~~ this equation ~~that~~ assumes the
 482 morphometry of the particle being dependent on the water depth. They propose that the
 483 mobilized boulders should be considered according to ~~as~~ relation of ~~their diameter in~~ the
 484 three axes, which depends on several factors, such as the lithology, internal structure
 485 and fractures of the material.

486 4. Results

487

488

4.1. Geomorphological mapping and geomorphic forms

489 A geomorphological map of the torrential system was obtained based on the March
 490 2014 topography for each field survey campaign: March 2014, March 2015, September
 491 2015 and June 2016. These maps Multi-temporal field campaigns (2014-2016) showed
 492 that the distribution and morphology of the geomorphological elements and deposits
 493 changes in time, especially those associated to the riverbed, and therefore the Portainé
 494 stream is very dynamic. These changes are mostly visible in the functional channel, ~~in~~
 495 ~~the riverbanks and levees~~ and in the lowest level of alluvial terraces. In general, the
 496 stream shows an erosive tendency, which is reflected on the backward motion of the
 497 bank escarpments that delimit the channel. In the alluvial cone area, the flow tends to
 498 deposit the boulders transported during debris flow and flood events.

499 ~~The geomorphological mapping and field observations enabled the identification of~~
 500 13 types of geomorphic forms, elements and facets were identified and mapped, which
 501 are. These are ordered according to their formation energy ~~following the literature~~, as:
 502 in-channel (functional active channel), gravel bars, terrace 1 (low terrace), terrace 2
 503 (high terrace), natural levee, main inactive channel of cone, secondary inactive channels
 504 of cone, upper deposits of cone, middle deposits of cone, lower deposits of cone,
 505 artificial levee (dyke), left-side slope and right-side slope (Table 1 and Fig. 5).

506

4.2. Dendrogeomorphological evidence

507

508

Regarding external disturbances we identified 10 decapitations, 41 external scars, 25
tilted trees and 3 trees with exposed roots.

509

510

511

The determination of the geomorphic position of the trees allows relating the spatial
 distribution of FDE along the torrent with the geomorphological elements (Fig. 5).
 Table 1 shows the geomorphic position of all the analysed trees and of ~~only~~ the scarred

512 | trees used for hydraulic modelling. Analysed trees locate on ~~1213~~ different geomorphic
513 forms, indeed, on all of the identified forms except for natural levees. Most of them are
514 located in the alluvial cone (58%), alluvial terraces (16%) and slopes (14%).

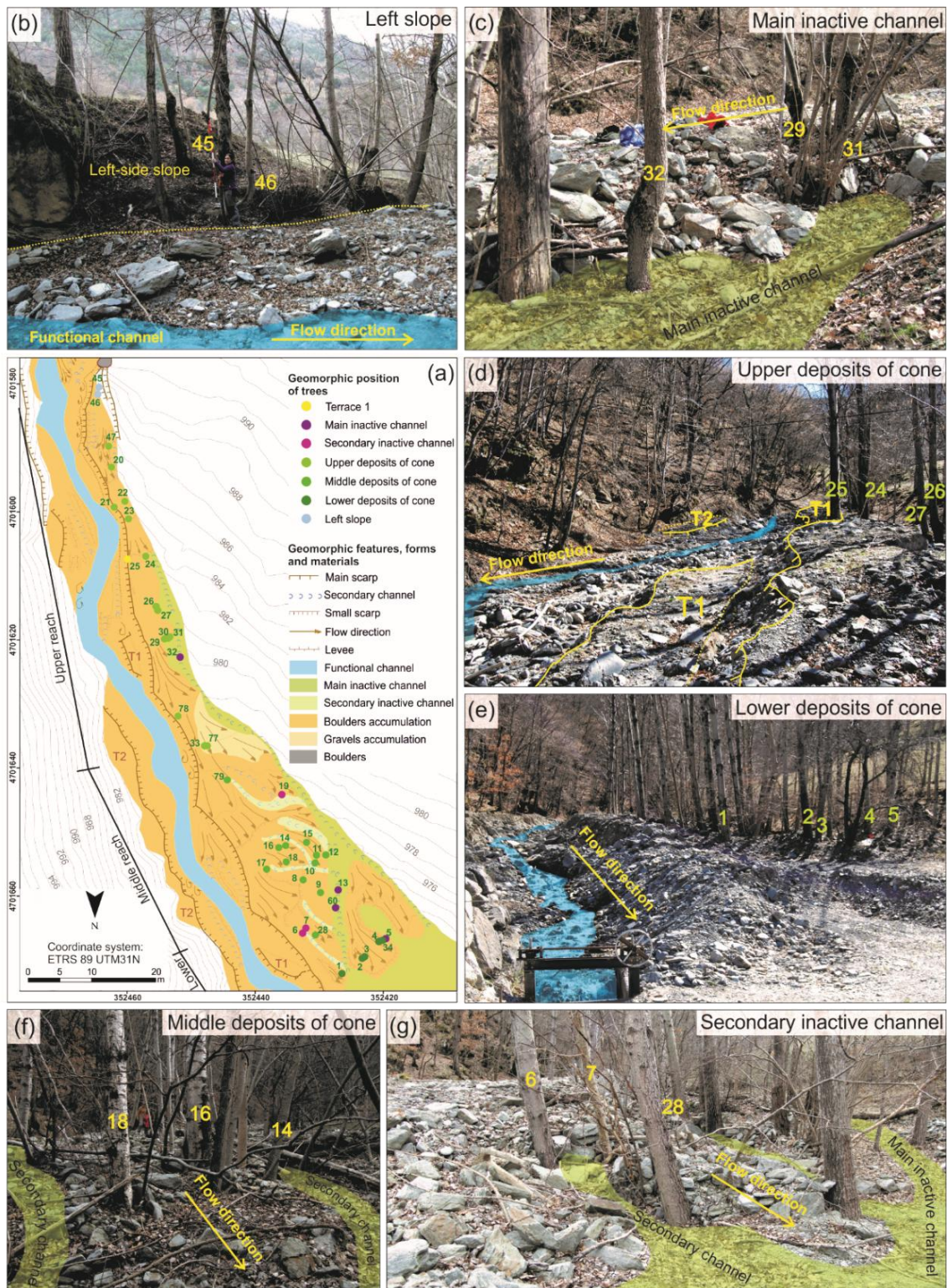


Figure 5. (a) Detailed geomorphological mapping (September 2015) of the alluvial cone showing the main geomorphological features, forms, deposits and the position of the trees that have been sampled for the dendrogeomorphological analysis; where trees are colored by the geomorphic position. (b), (c), (d), (e), (f), (g) Pictures showing examples of different geomorphologic positions identified in the study area.

516 **Table 1.** Geomorphic position of the trees analyzed and dated by dendrochronological techniques and the
517 number of trees with external scars used for hydrodynamic modelling of 2008 and 2010 events.

Geomorphic form		Trees with FDE	Scarred trees
Riverbed	In-channel	1	1
	Gravel bar	1	1
Alluvial terraces	Terrace 1	4	3
	Terrace 2	5	4
Levees	Natural levee	0	0
	Artificial levee	5	1
Alluvial cone	Main channel	3	0
	Secondary channel	3	2
	Upper deposits	14	1
	Middle deposits	8	6
Slope	Lower deposits	5	2
	Left-side	4	0
	Right-side	4	3

518
519

4.3. Flood discharges

520 ~~Palaeodischarges were estimated using HEC RAS hydraulic modelling, based on~~
521 ~~dendrogeomorphological evidence used as palaeostage indicators, as explained in 3.4.~~

522 The obtained peak discharges for 2008 and 2010 are presented in Table 2. For each
523 case, the value that minimized both absolute and mean squared error was considered.
524 For 2008, the calculated discharges were $300 \text{ m}^3\text{s}^{-1}$ from the TIN topography (Fig. 6)
525 and $321 \text{ m}^3\text{s}^{-1}$ from the total station topography. These results were weighted according
526 to their errors (Eq. 4), obtaining a peak discharge of $316 \text{ m}^3\text{s}^{-1}$ ($\sigma = 0.18 \text{ m}$). Given that
527 for 2010 there were only 4 scars corresponding to cross sections measured with total
528 station ~~in the field~~, the $314 \text{ m}^3\text{s}^{-1}$ discharge ($\sigma = 0.7 \text{ m}$) obtained from the TIN-based
529 model was considered as the best-most reliable peak discharge value.

530 ~~The flow dynamics in the alluvial cone can be difficult to simulate using a one-~~
531 ~~dimensional model, so the minimum peak discharge for bank overflow was first~~
532 ~~calculated. This is the threshold for cone flooding and therefore, marks a change in the~~
533 ~~distribution of the flow discharge. This critical overflow discharge was calculated in the~~
534 ~~cross-section located in the cone apex. For the critical overflow discharge, we~~
535 ~~obtained a $43 \text{ m}^3\text{s}^{-1}$ value of initial overbank and formation of crevasse splays, named~~
536 ~~partial overbank discharge. However, the complete flooding of the cone does not occur~~
537 ~~until the flow exceeds the total critical overbank discharge, estimated to be $58 \text{ m}^3\text{s}^{-1}$ for~~
538 ~~Portainé. Therefore, higher peak discharges produce the inundation of the debris cone~~
539 ~~and water also flows along distributary channels. These are considered extraordinary~~
540 ~~events, like those in 2008 and 2010.~~

541 **Table 2.** Estimation of flood peak discharges using hydraulic modelling based on scars as
542 dendrogeomorphological palaeostage indicators.

Year	Geometric data source	Peak discharge, Q_p (m^3s^{-1})	Absolute error, σ (m)	Mean squared error, MSE	Variance (m)
------	-----------------------	---	------------------------------	-------------------------	--------------

		(m)			
2008	TIN	300	0.35	0.23	0.11
	Total station	321	0.21	0.08	0.04
2010	TIN	314	0.7	0.35	0.04
	Total station	-	-	-	-

543

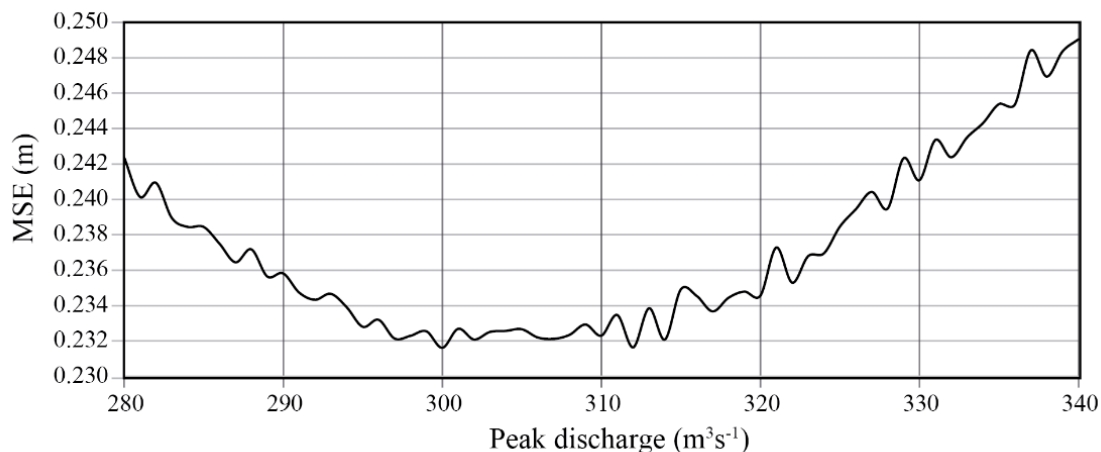


Figure 6. Peak discharge estimation for 2008 from the TIN-based hydraulic modelling based on the TIN topography. The accepted value corresponds to the minimum mean squared error obtained from the average of the squared errors of 18 tree scars.

544 *4.4. Hydraulic parameters and mobilized particle size*

545 Considering the discharge values obtained for 2008 and 2010 events, the flow
 546 hydraulics was similar in both cases. Fig. 7 shows the flooded area and the water depth
 547 in the most downstream part of the study area for 2008 event. This past flood produced
 548 almost the total flooding of the alluvial cone, generating scars in trees due to the impact
 549 of boulders and floating large wood.

550 The hydraulic parameters obtained from hydrodynamic modelling are water depth
 551 (d), flow velocity (v) and unit stream power (ω) for the left bank, channel, and right
 552 bank of each cross section (see results in supplementary material Table 1)-(Table 3). In
 553 situ hydraulic parameters for the specific position of each scarred tree are shown in
 554 Table 3.

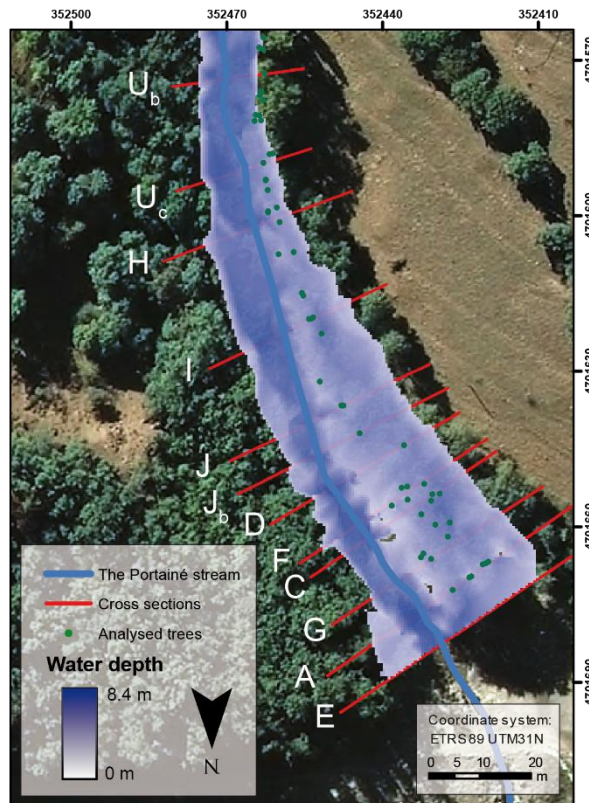


Figure 7. Bathymetric map of the flooded area for the 2008 event, corresponding to the alluvial cone.

555

Table 3. Hydraulic parameters calculated for the specific location of the trees.

Tree				Hydraulic parameters		
Cross section	Bank location	Elevation	Scar date	Water depth (m)	Velocity (ms⁻¹)	Unit stream power (Wm⁻²)
<u>M-M'</u>	<u>Right</u>	<u>1029.42</u>	<u>2008</u>	<u>2.17</u>	<u>12.18</u>	<u>4542.02</u>
<u>K-K'</u>	<u>Channel</u>	<u>1019.13</u>	<u>2008</u>	<u>1.32</u>	<u>15.07</u>	<u>3291.31</u>
<u>Kb-Kb'</u>	<u>Channel</u>	<u>1015.45</u>	<u>2008</u>	<u>1.75</u>	<u>14.52</u>	<u>6403.48</u>
<u>Kc-Kc'</u>	<u>Right</u>	<u>1015.24</u>	<u>2008</u>	<u>0.96</u>	<u>6.15</u>	<u>1775.85</u>
<u>Kd-Kd'</u>	<u>Channel</u>	<u>1013.60</u>	<u>2008</u>	<u>1.43</u>	<u>14.02</u>	<u>5338.19</u>
<u>Ke-Ke'</u>	<u>Channel</u>	<u>1012.49</u>	<u>2008</u>	<u>1.21</u>	<u>13.55</u>	<u>3541.88</u>
<u>P-P'</u>	<u>Left</u>	<u>1008.98</u>	<u>2008</u>	<u>1.65</u>	<u>5.15</u>	<u>1899.26</u>
<u>O-O'</u>	<u>Channel</u>	<u>1007.51</u>	<u>2008</u>	<u>1.88</u>	<u>14.98</u>	<u>7375.25</u>
<u>O-O'</u>	<u>Left</u>	<u>1007.98</u>	<u>2010</u>	<u>1.48</u>	<u>6.02</u>	<u>1826.440</u>
<u>O-O'</u>	<u>Left</u>	<u>1007.98</u>	<u>2010</u>	<u>1.48</u>	<u>6.02</u>	<u>1826.440</u>
<u>Nb-Nb'</u>	<u>Right</u>	<u>1007.11</u>	<u>2008</u>	<u>1.22</u>	<u>4.37</u>	<u>362.72</u>
<u>Y-Y'</u>	<u>Left</u>	<u>995.25</u>	<u>2008</u>	<u>0.27</u>	<u>4.81</u>	<u>1365.61</u>
<u>Xb-Xb'</u>	<u>Left</u>	<u>993.14</u>	<u>2008</u>	<u>0.55</u>	<u>4.35</u>	<u>1294.98</u>
<u>Uc-Uc'</u>	<u>Left</u>	<u>985.80</u>	<u>2010</u>	<u>0.75</u>	<u>12.12</u>	<u>5476.54</u>
<u>Jb-Jb'</u>	<u>Left</u>	<u>978.70</u>	<u>2010</u>	<u>1.10</u>	<u>11.02</u>	<u>915.50</u>
<u>D-D'</u>	<u>Left</u>	<u>977.53</u>	<u>2008</u>	<u>1.12</u>	<u>9.08</u>	<u>592.94</u>
<u>F-F'</u>	<u>Left</u>	<u>976.75</u>	<u>2008</u>	<u>0.70</u>	<u>8.13</u>	<u>886.59</u>
<u>F-F'</u>	<u>Left</u>	<u>976.21</u>	<u>2008</u>	<u>1.24</u>	<u>8.13</u>	<u>886.59</u>
<u>C-C'</u>	<u>Left</u>	<u>975.75</u>	<u>2008</u>	<u>1.32</u>	<u>7.75</u>	<u>539.47</u>

<u>C-C'</u>	<u>Left</u>	<u>975.51</u>	<u>2008</u>	<u>1.56</u>	<u>7.75</u>	<u>539.47</u>
<u>G-G'</u>	<u>Left</u>	<u>975.19</u>	<u>2008</u>	<u>0.30</u>	<u>8.74</u>	<u>753.42</u>
<u>G-G'</u>	<u>Left</u>	<u>974.88</u>	<u>2008</u>	<u>0.61</u>	<u>8.74</u>	<u>753.42</u>
<u>A-A'</u>	<u>Left</u>	<u>973.75</u>	<u>2010</u>	<u>0.73</u>	<u>6.91</u>	<u>336.96</u>
<u>A-A'</u>	<u>Left</u>	<u>973.18</u>	<u>2010</u>	<u>1.30</u>	<u>6.91</u>	<u>336.96</u>

556

557 ~~Flow hydraulics is used to estimate the particle size that might be mobilized by the~~
558 ~~flow. These calculations were carried out for 2008 event and in the deposit of alluvial~~
559 ~~cone, because the estimation of the flood discharge is more reliable and accurate than~~
560 ~~for 2010 event/s. In our study area, we also measured in the field the maximum (length),~~
561 ~~medium (width) and minimum (height) axes of boulders deposited in the alluvial cone~~
562 ~~(Table 4). This allowed us establishing the following field-based diameter relationships:~~
563 ~~$B=0.74L$, where B is width and L length; and $H=0.43L$, H being height. These relations~~
564 ~~were used to calculate the maximum particle size according to Carling et al. (2002).~~

565 ~~The rest of the empirical equations use different numerical constants (a , b , e_1 and e_2)~~
566 ~~and are based on the critical unit stream power, so the hydraulic parameters should be~~
567 ~~obtained from the upstream cross section of the alluvial cone because the flow is~~
568 ~~supercritical in the study site. Therefore~~For the empirical equations for particle size
569 estimation, the water depth and unit stream power values ~~for particle size estimation~~
570 were those corresponding to left bank of the section at the apex of the cone (section U-
571 Uc'), for the ~~peak discharge of 2008~~ peak discharge estimated as $316 \text{ m}^3 \text{ s}^{-1}$. These values
572 were 1.03 m and 5221.92 Nm^{-2} . ~~Regarding the unit stream power, it was calculated by~~
573 ~~dividing the total stream power obtained from the hydraulic modelling by the width of~~
574 ~~the flow in the left bank.~~The boulder size mobilized by the flow and deposited in the
575 cone was also obtained from the measures of the three axes (Table 4). This allowed us
576 establishing the following field-based diameter relationships: $B=0.74L$, where B is
577 width and L length; and $H=0.43L$, H being height. Table 5 collects the particle
578 diameters calculated for the Portainé alluvial cone, considering the relations proposed
579 by different authors.

580 **Table 4.** Field measurements and relationships among the length (L), width (B) and height (H) of
581 boulders accumulated in the alluvial cone.

Boulder number	Relative size	Length (m)	Width (m)	Height (m)	B/L ratio	H/L ratio
1	Big	0.67	0.48	0.3	0.72	0.45
2	Very big	1.52	0.88	0.92	0.58	0.61
3	Big	0.54	0.32	0.15	0.59	0.28
4	Medium	0.26	0.17	0.05	0.65	0.19
5	Medium	0.27	0.13	0.08	0.48	0.30
6	Small	0.17	0.15	0.08	0.88	0.47
7	Small	0.15	0.15	0.05	1.00	0.33
8	Very small	0.09	0.07	0.06	0.78	0.67
9	Medium	0.21	0.18	0.08	0.86	0.38
10	Medium	0.21	0.17	0.13	0.81	0.62

Average	Medium	0.29	0.21	0.12	0.74	0.43
---------	--------	------	------	------	------	------

582 **Table 5.** Estimation of the mobilized particle size, obtained from equations proposed by different authors.
583 Costa, Williams, Jacob and Gob et al.: intermediate axis of maximum boulders; Bagnold: intermediate
584 axis of mode size (medium) boulders; Carling et al: maximum axis of average size (medium) boulders.

Author	Equation	Numerical constants	Particle diameter (m)
Costa (1983)	Eq. 5	$a=0.09$ $b=1.686$	2.62
Costa (1983) for coarse material	Eq. 5	$a=0.03$ $b=1.686$	1.28
Williams (1983)	Eq. 5	$a=0.079$ $b=1.27$	6.24
Jacob (2003)	Eq. 5	$a=0.025$ $b=1.647$	1.70
Gob et al. (2003)	Eq. 5	$a=0.0253$ $b=1.62$	1.91
Bagnold (1980), adapted by Ferguson (2005)-and Parker et al.-(2011)	Eq. 6	$c_1=2860.5$ $c_2=12$	1.63
Carling et al. (2002)	Eq. 7	$C_d=0.95$ $L-H-B$ (field)	0.27

585

586 4.5. Relation between geomorphic forms, FDE and flow hydraulics

587 All the aspects analysed ~~aspects~~ in the above previous sections ~~were related to each~~
588 ~~other have been linked together~~ to obtain a more complete knowledge of ~~the link~~
589 ~~between~~ the hydrodynamics of the Portainé stream, the behaviour of the riverbank trees
590 and the morphology of the area.

591 The formation of ~~different dendrogeomorphological evidence (FDEs), but especially~~
592 ~~the external dendrogeomorphological~~ disturbances, depends on the geomorphic position
593 of the trees. 103 disturbances (decapitations, scars, stem tilting and root exposure) in 12
594 geomorphic positions were analysed in our study area from 57 different trees. The
595 number of evidence per tree was calculated for each geomorphic form (total FDE /
596 number of trees for each geomorphic position), shown in Fig. 8 (see results in
597 supplementary material Table 2). Table 6 and Fig. 8 show the geomorphological
598 ~~location of the dendrogeomorphological evidence of the study area.~~ There are few FDE
599 in the riverbed trees (in-channel and gravel bars), although these are the most energetic
600 positions. This is due to the lower number of trees in these geomorphic positions and
601 therefore, little number of samples for dendrochronological analysis. Most ~~of~~ FDEs
602 locate in the alluvial cone, both in the main or secondary inactive channels (2.7 FDE per
603 tree) or in the deposit area (2 FDE per tree) (Fig. 8). Therefore, in the Portainé study
604 area, the most intensely damaged trees concentrate on the geomorphological elements
605 related to processes of intermediate energy (second terrace and alluvial cone).

606 ~~Table 6. Dendrogeomorphological evidence in the study area for each geomorphic position.~~

Geomorphic form	Decapitations	Scars	Tilting	Root exposure	Total
-----------------	---------------	-------	---------	---------------	-------

In-channel	0	1	1	0	2
Gravel bar	0	1	0	0	1
Terrace 1	0	5	1	0	6
Terrace 2	1	7	1	0	9
Main channel of cone	1	4	3	0	8
Secondary channel of cone	0	6	2	0	8
Upper deposits of cone	6	11	4	0	21
Middle deposits of cone	0	11	5	0	16
Lower deposits of cone	0	2	3	0	5
Artificial levee	1	6	1	1	9
Left slope	0	4	3	0	7
Right slope	1	7	1	2	11

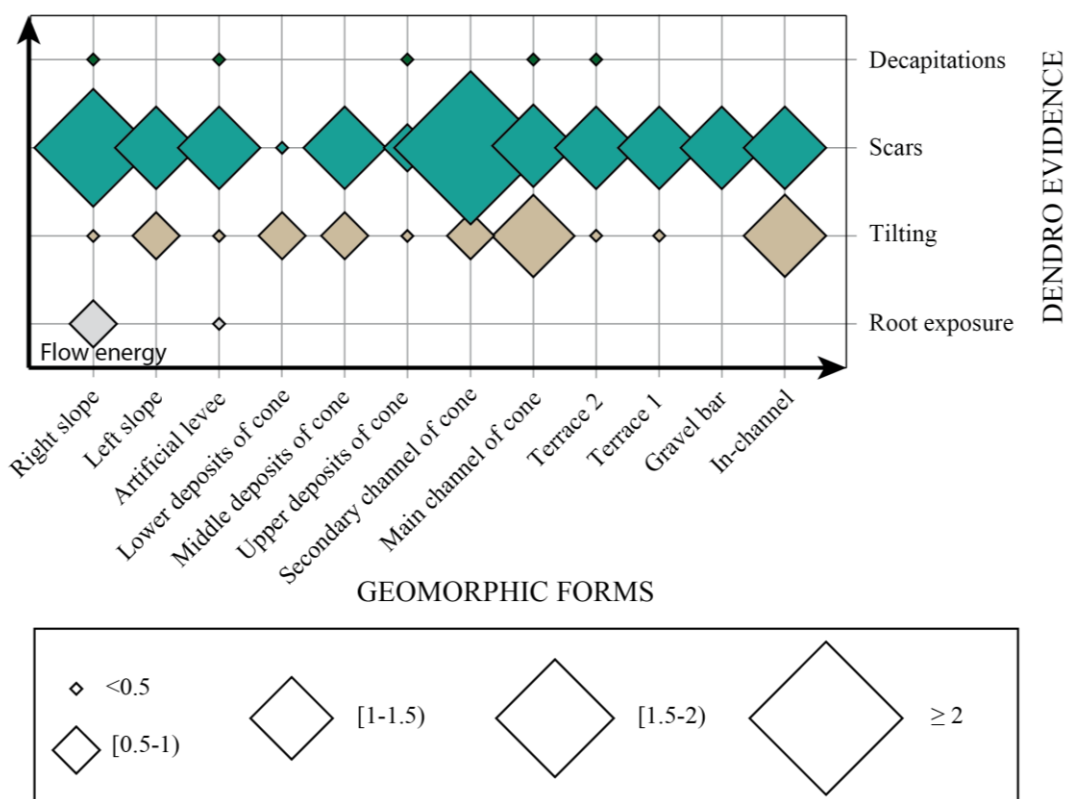


Figure 8. Relation between dendrogeomorphological evidence and geomorphic forms, organized by the increase of the flow energy. The size of the symbols represents the number of FDE per tree.

607

608 The geomorphological features of the valley bottom are ~~Geomorphology is~~ also
609 related to flow hydraulics, and in this specific case, the stability of geomorphic forms
610 associated to torrential processes depends on the energy of the water. The
611 hydrodynamic modelling allowed us to determine the specific velocity and water depth
612 values for the ~~tree scars of the modelled years~~ scarred trees. These hydraulic parameters
613 were then associated to the geomorphic element in which each tree ~~containing a scar~~
614 was located. Fig. 9 is the representation of the relation between the energy of flow,
615 affectionation on trees and geomorphology. Higher velocity and depth values indicate areas

616 where torrential processes are more intense, and therefore correspond to energetic
 617 geomorphic forms. These most energetic geomorphological elements are close to the
 618 riverbed (in-channel and gravel bars). Far from the riverbed, there is a decrease on the
 619 flow energy, both in terms of hydraulic parameters and in the intensity of the torrential
 620 processes associated to the geomorphic features (Fig. 9). In addition, the largest number
 621 of scars are located in the alluvial cone, which corresponds to torrential processes of
 622 intermediate intensity. Taking into account that every scarred trees of the study area was

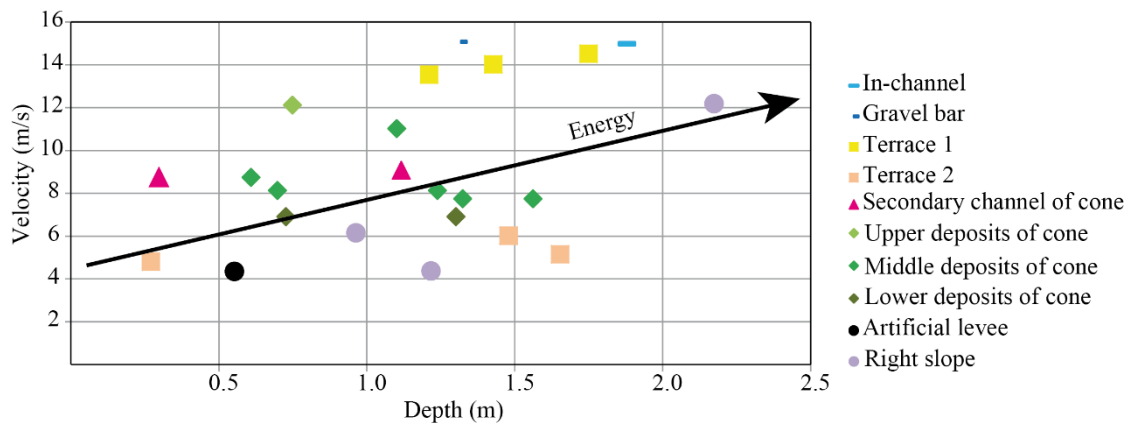


Figure 9. Flow velocity – depth diagram for the formation of scars, classified by the geomorphic form in which they are located. The arrow indicates the increase of the flow energy.

623 sampled, the number of samples does not condition the concentration of scars in the
 624 alluvial cone and it represents the geomorphic form where more trees are affected
 625 during torrential events.

626 The relation of scars, geomorphic forms and flow hydrodynamics can be assessed
 627 by comparing the differences between scar height and the modelled water stage (Eq. 3)
 628 of the trees according to their geomorphic position. We analysed the 2008 event because
 629 it provided a larger population of scars and lower errors in discharge estimation, and we
 630 obtained mean height differences for each geomorphic form: 0.07 m in-channel (1 tree),
 631 0.49 m in gravel bars (1 tree), 0.53 m in terrace 1 (3 trees), 0.26 m in terrace 2 (2 trees),
 632 0.44 m in secondary channels of the cone (2 trees), 0.17 m in middle deposits of the
 633 cone (5 trees), 0.01 m in artificial levees (1 tree) and 0.63 m in right-side slopes (3
 634 trees). The lowest variability in scar heights was located inside the channel and in an
 635 artificial levee, but these geomorphic forms only contain one tree. If we consider
 636 geomorphic positions with more than a single tree, the lowest variabilities corresponded
 637 to trees located on terrace 2 or middle deposits of the cone, which are intermediate
 638 energy positions. Highest variabilities occurred in the right-side slope.

639 5. Discussion

640

641 5.1. Discussion on the results and new contributions

642 This paper presents a combined—detailed palaeoflood studymultidisciplinary
 643 approach in an ungauged mountain stream (Portainé, Spanish Pyrenees) based on the
 644 novel multidisciplinary methodology that consisted on—the four-topic correlation of

645 geomorphology, dendrogeomorphology, flood discharge and flow
646 ~~hydraulics~~ hydrodynamics.

647 Detailed geomorphological mapping from total station data contributed to a good
648 correlation between damaged trees and geomorphic forms. The formation of different
649 dendrogeomorphological evidence (FDE), depends on the geomorphic position of the
650 ~~affected~~ trees. Usually the most energetic disturbances are found in trees located in
651 energetic geomorphic forms (e.g. Ruiz-Villanueva et al., 2010). Nonetheless, in our
652 study area, most ~~of the~~ FDEs locate in geomorphic positions of intermediate energy.
653 This is explained by (i) the ~~inexistence of many~~ scarcity of trees on the riverbed (most
654 energetic positions) because high discharge events, with significant stream power, pull
655 and transport them, and (ii) the scarcity of external disturbances on slopes (less
656 energetic positions) due to the flow not having enough energy to produce damages on
657 those trees farther from the active channel, or even the flow not reaching those areas.

658 The estimation of peak discharges was possible thanks to the detailed ~~topography~~
659 ~~and~~ cross sections measured in the field. LiDAR data was not accurate enough for the
660 application of hydraulic models due to the dense vegetation and therefore, insufficient
661 ~~and inaccurate~~ ground points. The methodology for palaeodischarge calculation for
662 2008 and 2010 was adapted from Ballesteros-Cánovas et al. (2010). Comparing the two
663 reconstructed years ~~and considering the values of the hydraulic parameters,~~ it seems that
664 their ~~values magnitudes~~ were similar ~~and they had the same order of magnitude~~; but the
665 2008 event has been reported as the most severe one ~~in the last decade~~ (IGC, 2013).
666 This discrepancy could be explained by the difference in the real pre-event topography:
667 ~~In this study, as~~ we used the same topographic data for hydraulic modelling in both
668 cases, which includes boulder accumulation in the alluvial cone during extraordinary
669 events. Therefore, the pre-2008 topography would be lower than the pre-2010 one, and
670 the water stage for scar formation ~~the generation of the injuries~~ higher, leading to an
671 ~~This leads to the~~ underestimation of the 2008 event.

672 Overbank critical discharges calculated at the apex of the alluvial cone indicate the
673 minimum discharge for the overflow of the left bank. However, this minimum discharge
674 not necessarily involves water flowing all along the cone, as it may return to the
675 functional channel. In order to validate the estimations, we checked for the discharge
676 that, apart from overflowing the bank, showed water continuity along the distributary
677 channels of the cone. Therefore, two overbank flow discharges were estimated: partial
678 overbank critical discharge associated to levee breach and formation of crevasse splays
679 (43 m³s⁻¹), and total overbank critical discharge and cone flooding (58 m³s⁻¹).

680 Peak discharges for different return periods were calculated for the Portainé basin by
681 other authors using hydrologic modelling (de las Heras ~~et al.~~, 2016). Comparing those
682 results with ~~both~~ palaeodischarge values obtained ~~in the approach presented~~ in this
683 study, for 2008 event (316 m³s⁻¹) and 2010 event/s (314 m³s⁻¹), both ~~discharges events~~
684 would correspond to return periods higher than 500 years. This makes no sense, as
685 torrential or debris events are recorded almost every year ~~or every two years~~ since 2006.
686 Moreover, the obtained overbank critical discharge in the downstream part of the
687 Portainé stream would correspond to about ~~the~~ 500-year return period ~~value~~. This means
688 that (i) the discharges estimated in this study may be overestimated; and (ii) the

689 discharges with different return periods from de las Heras (2016) could be
690 underestimated. ~~In our study, t~~This is due to the high sediment load ~~of the torrential~~
691 ~~flows,~~ not considered in the palaeohydrologic and palaeohydraulic analyses. As outlined
692 by Bodoque et al. (2011), the estimated peak discharges are the result of the
693 combination, not only the sum, of water and sediment load. This is very common in
694 steep mountain streams with high torrential activity.

695 Regarding the calculation of the particle size transported for a specific flow, the best
696 approach is the one proposed by Carling et al. (2002) because we adapted it for the
697 study case ~~by establishing a relation between the three diameter axes of the deposited~~
698 ~~boulders.~~ The obtained relation of maximum ~~(length)~~, medium ~~(width)~~ and minimum
699 ~~(height)~~ diameters of boulders is in agreement with the typology of the bedrock, which
700 is composed of highly fractured metapelites. This leads to the formation of boulders
701 with two similar axes and a considerably shorter one. However, results obtained from
702 Carling et al. (2002) correspond to the most common size of deposited boulders
703 (medium size in the study area), as the relation between diameter axes was established
704 for the average of the field measurements. Bagnold (1980) also considers the most
705 common size ~~(mode)~~, so the obtained results are clearly overestimated. All the other
706 authors come up with equations for the intermediate axis estimation of the maximum
707 transported boulder, so the obtained results should be compared with the width of
708 biggest boulders identified in the field (Table 4, boulder number 2). Among these
709 equations, the one proposed by Costa (1983) for coarse material is considered the most
710 suitable ~~one~~ in our case.

711 In general, the ~~The~~ results obtained for the Portainé alluvial cone using empirical
712 relations (Table 5) are higher than the boulder size measured in the field (Table 4). The
713 causes for this can be that: (i) they are empirical relations calculated for biphasic flows
714 with Newtonian behavior, and some debris flows are uniphase; (ii) equations work with
715 the mobilizable particle size, but boulders of this dimension are not always available to
716 be moved in the river bottom, in part due to the lithology of the source area (even
717 though this does not seem to occur in the study case), or because they could be
718 fragmented during the transport; (iii) ~~water depth and velocity~~ stream power values are
719 averaged for the channel or margins (using a 1D hydraulic model that only distinguishes
720 three zones in each cross section), but they could not be representative of some specific
721 positions; and (iv) the ~~used 1D~~ model works with Newtonian flows of clean water so the
722 calculated discharges may be overestimated due to the higher viscosity of the more
723 dense real flow (which includes sediment), leading to a real transport capacity of
724 smaller boulders. Considering these limitations, the results obtained by empirical
725 relations are coherent with real torrential processes in the Portainé study area. The
726 equation proposed by Williams (1983) is the exception and does not work for the
727 studied stream, ~~as suggests a mobilizable particle size of more than 6 meters, which is~~
728 ~~completely illogical.~~

729 ~~Overbank critical discharges calculated at the apex of the alluvial cone indicate the~~
730 ~~minimum discharge for the overflow of the left bank. However, this minimum discharge~~
731 ~~not necessarily involves water flowing all along the cone, as it may return to the~~
732 ~~functional channel. In order to validate the estimations, we checked for the discharge~~
733 ~~that, apart from overflowing the bank, showed water continuity along the distributary~~

734 ~~channels of the cone. Therefore, two overbank flow discharges were estimated: (i)~~
735 ~~partial overbank critical discharge associated to levee breach and formation of crevasse~~
736 ~~splays ($43 \text{ m}^3 \text{ s}^{-1}$), and (ii) total overbank critical discharge and cone flooding ($58 \text{ m}^3 \text{ s}^{-1}$).~~

737 The uncertainty of the peak discharge estimations depends on the reliability of scar
738 heights (Ballesteros-Cánovas et al., 2016). The distribution of scar-flow differences in
739 the study area suggests that trees located on the deposits of the cone and in the terrace
740 are the most suitable ones for palaeoflood reconstruction, whereas those standing in the
741 slopes are the less useful ones.

742 The present study is a new step for palaeoflood reconstruction in ungauged small
743 basins. Even if peak discharges obtained by hydrodynamic modelling may be
744 overestimated because of not considering the sediment load, at least they allow
745 estimating the order of magnitude of past events. Such a multidisciplinary approach
746 could be very useful for basins where detailed dendrogeomorphological studies could
747 not be carried out (few or lack of riverbank trees) or the application of hydrologic-
748 hydraulic models presents great limitations (scarce meteorological data and/or not
749 accurate DEMs).

750 5.2. Limitations of the data sources

751 ~~The topographic data used for the generation of the TIN presents the following~~
752 ~~drawbacks: (i) temporal difference between detailed field topography (2014-2016) and~~
753 ~~airborne LiDAR data (2011); (ii) change of the alluvial cone topography, characterised~~
754 ~~by accumulation during high discharge events and erosion between them; (iii) the use of~~
755 ~~the same DEM for hydrodynamic modelling of different years; and (iv) low accuracy of~~
756 ~~LiDAR data in forested or densely vegetated areas. Temporal changes of terrain along~~
757 ~~the alluvial cone indicates that scars in trees located upstream from this area are more~~
758 ~~reliable for palaeoflood discharge estimations, but they are scarce.~~

759 Geomorphic positions of trees could have changed in time, because the assigned
760 present-day landform, element or facet to each tree could not be exactly the same as
761 when the flood occurred and the scar was formed; at least for geomorphic forms close to
762 the river channel and especially for older dendrogeomorphological damages or FDE.
763 This limitation in data sources is very difficult to solve, due to the lack of previous
764 geomorphological maps or detailed aerial photographs ~~in this forested area.~~

765 ~~Dendrogeomorphological studies are usually carried out in rivers with many trees~~
766 ~~showing external disturbances (Ballesteros-Cánovas et al., 2015). In the Portainé~~
767 ~~stream, all the affected trees were analysed and they provided information for the dating~~
768 ~~of 15 past events prior to 2012 (Génova et al., under review). Scars and injuries were~~
769 ~~used as palaeostage indicators (PSI), considering that their maximum height indicates~~
770 ~~the minimum water table of the flow and is close to high water marks (HWM), as~~
771 ~~demonstrated by previous works (Ballesteros et al., 2011; Ballesteros-Cánovas et al.,~~
772 ~~2010). Nevertheless, this approximation involves some uncertainties and error sources:~~
773 ~~(i) PSI can be higher than HWM if the scar was formed by material accumulated~~
774 ~~upstream from a tree, leading to a discharge overestimation (Ballesteros-Cánovas et al.,~~
775 ~~2010); (ii) PSI can be lower than HWM when the scar is partially closed, and therefore,~~
776 ~~the discharge would be underestimated (Guardiola-Albert et al., 2015); and (iii) PSI can~~

777 be lower than HWM when the scar has been produced by sediment load in the lower
778 part of the water column (bedload transport, e.g. saltation), and not by the impact of
779 floating load (large wood), so the discharge could be underestimated (Ballesteros et al.,
780 2010). The trial-and-error technique was applied to compare the height of the PSI
781 (height of the scars) and the modelled water stage in each cross section (Yanosky and
782 Jarrett, 2002). Despite the few number of trees, ~~we had multiple scars to simulate~~
783 ~~the number of scars was considered enough for simulating~~ the flow of 2008 (18 scars) and
784 2010 events (6 scars). Moreover, the existing technical reports that describe the 2008
785 and 2010 events (IGC, 2010a, 2010b), especially upstream, seem to be in accordance
786 with the obtained results about the magnitude of these events.

787 The topographic data presented the following drawbacks: (i) temporal difference
788 between detailed field topography (2014) and airborne LiDAR data (2011); (ii) the use
789 of the same DEM for hydrodynamic modelling of different years; and (iii) low accuracy
790 of LiDAR data in forested or densely vegetated areas. Temporal changes of terrain in
791 the alluvial cone indicates that scars in trees located upstream from this area are more
792 reliable for palaeoflood discharge estimations, but they are scarce. So, main topographic
793 limitations were overcome by acquiring high-accuracy data along multiple cross
794 sections coinciding with the location of the damaged trees.

795 5.3. Limitations of the methods

796 Tree-ring analysis is a very useful tool for data acquisition on past flood events
797 (Ballesteros-Cánovas et al., 2015b; Stoffel and Bollschweiler, 2008). However,
798 dendrogeomorphological methodologies present some ~~limitations and~~ drawbacks (Díez-
799 Herrero et al., 2013a). In our study area, (i) some FDE could correspond to different
800 events occurred in a same year (at least two in 2008 and other two in 2010), and
801 therefore, FDE from a same year could correspond to different intra-annual events; (ii)
802 some scars can be produced by another external factor unrelated to torrential processes,
803 like the impact of a fallen tree during wind gusts or due to human activities. However,
804 in this study, the position, shape, orientation and distribution of the scars were analysed
805 in detail regarding their relation with torrential processes, and the ~~incoherent-doubtful~~
806 ones were dismissed.

807 The hydrodynamic modelling was carried out with the HEC-RAS 1D hydraulic
808 model (USACE, 2008) that works with transversal cross sections. The area between
809 them is lineally interpolated and may involve some errors. This was overcome by
810 acquiring detailed topographic data with a total station in the field and, in few cases,
811 introducing additional sections corresponding to the position of trees showing scars
812 from 2008 or 2010 events. A 2D model was not run due to geometric, hydrodynamic
813 and other factors (see section 3.3.). Moreover, other works like Bodoque et al. (2011)
814 have used 1D hydraulic modelling for peak discharge reconstruction at mountain steep-
815 gradient reaches showing the same configuration and characteristics as the Portainé
816 stream, proving its suitability. ∴ (i) the lack of an accurate enough digital elevation
817 model for an adequate bidimensional hydraulic simulation; (ii) the general
818 unidirectional component of the water flow in high steep torrents like the Portainé
819 stream, in which secondary transversal flows are limited by the narrowness of the valley
820 (not defined floodplain) and the high longitudinal slope (with waterfalls and rapids). A

~~correction factor was not applied as proposed by other authors (Ruiz Villanueva et al., 2010), neither based on the position of the tree with regard to the channel nor for the spatial distribution of the scars, due the little number of scars and their homogeneous distribution along the stream reach.~~ The small differences in peak discharges obtained from the TIN-based cross sections and the field-based cross sections can be explained by the longitudinal variability of the high sediment load flow and the different number of scars for each case.

5.4. Limitations of the results

~~The reconstruction of flooded areas for simulated discharges can present some errors due to the limitations of the 1D hydraulic modelling. Isolated flooded areas could be found when representing the obtained water depth values above the digital elevation model. In this study, this errors were avoided improving the topography of the study area by including topographic data obtained in the field with the total station, by delimiting the channel with levees and by deleting ground points that overcame the established threshold for elevation differences between adjacent points. This process allowed us to obtain a much more accurate TIN for an adequate representation of flooded area.~~

~~Obtained results for flow~~ Flow hydraulics results were not calibrated with real data, because of the lack of flow gauging stations within the basin. Therefore, the palaeodischarges could not be compared and validated with real ~~records~~ observed discharges recorded in the Portainé stream. Nevertheless, the obtained discharges in this study seem reasonable, and their order of magnitude is coherent with the dimensions of the river and the catchment ~~basins~~.

5.5. Further research

Future steps that could improve the characterisation ~~of the dynamics~~ of the Portainé stream and the palaeoflood reconstruction are: (i) the integration of the sediment load and transport, which constitute an important factor for the rheology of torrential and debris floods; (ii) 2D hydrodynamic modelling, to simulate the limited transversal flows and therefore, secondary discharges along the alluvial cone ~~and its channels~~.

Last but not least, the methodology carried out in this study could be applied to other watersheds of similar morphometric and geomorphologic characteristics. The validation of the use of 1D hydraulic models in other small elongated cones in mountainous areas with few source data and relatively few number of trees would corroborate the high potential of such a multidisciplinary analysis for highly torrential problematic settings.

6. Conclusions

~~This paper analyses the palaeohydrology of a small mountain drainage basin with scarce or lack of hydrologic data and limited number of damaged trees. We estimated peak discharges from 2008 and 2010 events, giving an idea of the magnitude of these events, and flow hydraulics and dendrogeomorphology were related. Results of the~~ The palaeohydrological approach presented in this study proves that the flow energy obtained from hydrodynamic modelling of past events, determined by the depth,

863 velocity and stream power, shows a positive correlation with most energetic
864 geomorphic forms (riverbed and low alluvial terrace). However, most of the external
865 disturbances are found in trees located in geomorphic positions of intermediate energy
866 (alluvial cone). ~~This can be explained by the higher percentage of trees in this area and~~
867 ~~the destruction of trees located in the main active channel due to the great energy and~~
868 ~~transport capacity of torrential flows.~~ Trees showing less uncertainty for hydraulic
869 modelling, based on the variability in scar heights, were also located on geomorphic
870 forms formed by intermediate energy processes (high alluvial terrace and deposits of the
871 cone). These findings suggest that the most reliable scarred trees for peak discharge
872 estimations using hydraulic modelling correspond to intermediate flow energy
873 positions.

874 The present work shows the high potential of the combination of techniques for
875 flood assessment in problematic contexts, such as ungauged mountain basins or with
876 scarce hydrological data without gauging stations, densely vegetated areas with poor
877 topographic data, and rivers with few disturbed trees for detailed
878 dendrogeomorphological studies.

879 Acknowledgements

880 This work was funded by the CHARMA project (CGL2013-40828-R) of the
881 Spanish Ministry of Economy, Industry and Competitiveness (MINECO), and by the
882 University of Barcelona (UB). The authors want to thank Dr. Mar Tapia for her advice
883 on statistical analysis. Comments from three anonymous reviewers improved the quality
884 of the manuscript.

885 References

- 886 ~~Abermann, J., Fischer, A., Lambrecht, A., Geist, T., 2010. On the potential of very~~
887 ~~high resolution repeat DEMs in glacial and periglacial environments. Cryosphere 4,~~
888 ~~53–65. doi:10.5194/te-4-53-2010~~
- 889 Arcement, G.J., Schneider, V.R., 1989. Guide for Selecting Manning's Roughness
890 Coefficients for Natural Channels and Flood Plains, United States Geological
891 Survey Water-Supply Paper 2339.
- 892 Bagnold, R.A., 1980. An empirical correlation of bedload transport rate in flumes and
893 natural rivers. Proc. R. Soc. London 372, 453–473. doi:10.1098/rspa.1983.0054
- 894 Baker, V.R., 1987. Paleoflood hydrology and extraordinary flood events. J. Hydrol. 96,
895 79-99. doi:10.1016/0022-1694(87)90145-4
- 896 Baker, V.R., 2008. Paleoflood hydrology: Origin, progress, prospects. Geomorphology
897 101, 1–13. doi:10.1016/j.geomorph.2008.05.016
- 898 Baker, V.R., Kochel, R.C., Patton, P.C., 1988. Flood Geomorphology. John Wiley and
899 Sons, New York, United States. ISBN: 978-0-12-394846-5
- 900 Baker, V.R., Pickup, G., 1987. Flood geomorphology of the Katherine Gorge, Northern
901 Territory, Australia. Geol. Soc. Am. Bull. 98, 635-646. doi:10.1130/0016-
902 7606(1987)98<635:FGOTKG>2.0.CO;2
- 903 ~~Ballesteros, J.A., Bodoque, J.M., Díez Herrero, A., Sanchez-Silva, M., Stoffel, M.,~~
904 ~~2011. Calibration of floodplain roughness and estimation of flood discharge based~~
905 ~~on tree-ring evidence and hydraulic modelling. J. Hydrol. 403, 103–115.~~
906 ~~doi:10.1016/j.jhydrol.2011.03.045~~

- 907 Ballesteros-Cánovas, J.A., Eguibar, M.Á., Bodoque, J.M., Díez-Herrero, A., Stoffel, M.,
908 Gutiérrez-Pérez, I., 2010. Estimating flash flood discharge in an ungauged
909 mountain catchment with 2D hydraulic models and dendrogeomorphic palaeostage
910 indicators. *Hydrol. Process.* 25, 970–979. doi:10.1002/hyp.7888
- ~~911 Ballesteros-Cánovas, J.A., Sanchez-Silva, M., Bodoque, J.M., Díez-Herrero, A., 2013.
912 An Integrated Approach to Flood Risk Management: A Case Study of Navaluenga
913 (Central Spain). *Water Resour. Manag.* 27, 3051–3069. doi:10.1007/s11269-013-
914 0332-1~~
- 915 Ballesteros-Cánovas, J.A., Márquez-Peñaranda, J.F., Sánchez-Silva, M., Díez-Herrero,
916 A., Ruiz-Villanueva, V., Bodoque, J.M., Eguibar, M.Á., Stoffel, M., 2015a. Can
917 tree tilting be used for paleoflood discharge estimations? *J. Hydrol.* 529, 480–489.
918 doi:10.1016/j.jhydrol.2014.10.026
- 919 Ballesteros-Cánovas, J.A., Stoffel, M., St George, S., Hirschboeck, K., 2015b. A review
920 of flood records from tree rings. *Prog. Phys. Geogr.* 29 (6), 1–23.
921 doi:10.1177/0309133315608758
- ~~922 Ballesteros-Cánovas, J.A., Stoffel, M., Spyt, B., Janecka, K., Kaczka, R.J., Lempa, M.,
923 2016. Paleoflood discharge reconstruction in Tatra Mountain streams.
924 *Geomorphology* 272, 92-101. doi:10.1016/j.geomorph.2015.12.004~~
- 925 Barredo, J.I., 2007. Major flood disasters in Europe: 1950–2005. *Nat. Hazards* 42, 125–
926 148. doi:10.1007/s11069-006-9065-2
- 927 Benito, G., Díez-Herrero, A., 2015. Palaeoflood Hydrology: Reconstructing Rare
928 Events and Extreme Flood Discharges, in: Shroder, J.F., Paron, P., Di Baldassarre,
929 G. (Eds.), *Hydro-Meteorological Hazards, Risks, and Disasters*. Elsevier,
930 Amsterdam, The Netherlands, pp. 65-104. ISBN: 978-0-12-394846-5
- 931 Benito, G., Sopena, A., Sánchez-Moya, Y., Machado, M.J., Pérez-González, A., 2003.
932 Palaeoflood record of the Tagus River (Central Spain) during the Late Pleistocene
933 and Holocene. *Quat. Sci. Rev.* 22, 1737–1756. doi:10.1016/S0277-3791(03)00133-
934 1
- 935 Benito, G., Macklin, M.G., Zielhofer, C., Jones, A.F., Machado, M.J., 2015. Holocene
936 flooding and climate change in the Mediterranean. *Catena* 130, 13-33.
937 doi:10.1016/j.catena.2014.11.014
- ~~938 Bizzi, S., Demarchi, L., Grabowski, R.C., Weissteiner, C.J., Van de Bund, W., 2016.
939 The use of remote sensing to characterise hydromorphological properties of
940 European rivers. *Aquat. Sci.* 78, 57–70. doi:10.1007/s00027-015-0430-7~~
- 941 Bodoque, J.M., Eguibar, M.Á., Díez-Herrero, A., Gutiérrez-Pérez, I., Ruiz-Villanueva,
942 V., 2011. Can the discharge of a hyperconcentrated flow be estimated from
943 paleoflood evidence? *Water Resour. Res.* 47, 1–14. doi:10.1029/2011WR010380
- ~~944 Bollschweiler, M., Stoffel, M., 2010. Tree rings and debris flows: Recent developments,
945 future directions. *Prog. Phys. Geogr.* 34, 625–645. doi:10.1177/0309133310370283~~
- ~~946 Bombino, G., Denisi, P., Fortugno, D., Sgrò, A., Tamburino, V., Zema, D.A., 2015.
947 Extreme flood estimation by dendrogeomorphic analysis in small ungauged
948 mountain catchments (Calabria, Italy), in: *AHA 2015 International Mid Term
949 Conference, Naples, Italy.*~~
- 950 Carling, P.A., Hoffmann, M., Blatter, A.S., 2002. Initial Motion of Boulders in Bedrock
951 Channels, in: House, P.K., Webb, R.H, Baker, V.R., Levish, D.R. (Eds.), *Ancient
952 Floods, Modern Hazards: Principles and Applications of Paleoflood Hydrology.*

953 American Geophysical Union, Washington, DC, United States, pp. 147–160.
954 doi:10.1029/WS005p0147

955 Chanson, H., 2004. Environmental Hydraulics of Open Channel Flows, ~~Environmental~~
956 ~~Hydraulics of Open Channel Flows~~. Elsevier, Oxford, United Kingdom. ISBN:
957 978-0-7506-6165-2

958 Chow, V. T., 1959. Open Channel Hydraulics, McGraw-Hill, New York, United States.
959 ISBN: 07-010776-9

960 Church, M., Biron, P., Roy, A., 2012. Gravel Bed Rivers: Processes, Tools,
961 Environments. Wiley-Blackwell, Chichester, United Kingdom. ISBN: 978-0-470-
962 68890-8

963 Cook, E.R., Kairiukstis, L.A., 1990. Methods of Dendrochronology. Applications in the
964 Environmental Sciences. Springer, Dordrecht, Netherlands. doi:10.1007/978-94-
965 015-7879-0

966 Costa, J.E., 1983. Paleohydraulic reconstruction of flash-flood peaks from boulder
967 deposits in the Colorado Front Range. Geol. Soc. Am. Bull. 94, 986–1004.
968 doi:10.1130/0016-7606(1983)94<986:profpf>2.0.co;2

969 ~~Day, D., Jacobsen, K., Passini, R., Quillen, S., 2013. A study on accuracy and fidelity of~~
970 ~~terrain reconstruction after filtering DSMs produced by Aerial images and Airborne~~
971 ~~LiDAR Surveys. ASPRS Annual Conference, Baltimore, United States.~~

972 De las Heras, Á., 2016. Modificación de la respuesta hidrológica en avenidas
973 torrenciales ante los cambios de usos del suelo en una cuenca de montaña
974 (Portainé, Pirineo leridano). Archivo Digital UPM, Master thesis, Universidad
975 Politécnica de Madrid, Spain. Unpublished, available at: <http://oa.upm.es/45430/>

976 Díez-Herrero, A., 2015. Buscando riadas en los árboles: Dendrogeomorfología.
977 Enseñanza las Ciencias la Tierra 23 (3), 272–285. ISSN: 1132-9157

978 Díez-Herrero, A., Ballesteros-Cánovas, J.A., Bodoque, J.M., Ruiz-Villanueva, V.,
979 2013a. A new methodological protocol for the use of dendrogeomorphological data
980 in flood risk analysis. Hydrol. Res. 44.2, 234–247. doi:10.2166/Nh.2012.154

981 ~~Díez-Herrero, A., Ballesteros-Cánovas, J.A., Ruiz-Villanueva, V., Bodoque, J.M.,~~
982 ~~2013b. A review of dendrogeomorphological research applied to flood risk analysis~~
983 ~~in Spain. Geomorphology 196, 211–220. doi:10.1016/j.geomorph.2012.11.028~~

984 ESRI, 2014. ArcGIS 10.2.2 Desktop. Environmental Systems Research Institute,
985 Redlands, United States.

986 ~~Fargas, G., 2015. Datación y caracterización de avenidas torrenciales mediante~~
987 ~~metodologías dendrogeomorfológicas en los Barrancos de Portainé y de Ramiosa~~
988 ~~(Pallars Sobirà, Lérida, España). Dipòsit Digital de la Universitat de Barcelona,~~
989 ~~Spain, available at: <http://hdl.handle.net/2445/102682>~~

990 Ferguson, R.I., 2005. Estimating critical stream power for bedload transport calculations
991 in gravel-bed rivers. Geomorphology 70, 33–41.
992 doi:10.1016/j.geomorph.2005.03.009

993 ~~FGC, ICGC, 2015. Seguiment geològic i geotècnic de la carretera d'accés a Port Ainé,~~
994 ~~24 d'agost de 2015, AP 079/15. Ferrocarrils de la Generalitat de Catalunya and~~
995 ~~Institut Cartogràfic i Geològic de Catalunya, Barcelona, Spain.~~

996 Furdada, G., Génova, M., Guinau, M., Victoriano, A., Khazaradze, G., Díez-Herrero,
997 A., Calvet, J., 2016. Las avenidas torrenciales de los barrancos de Portainé,
998 Reguerals y Ramiosa (Pirineo Central): evolución de las cuencas y dinámica
999 torrencial, in: Durán Valsero, J.J., Montes Santiago, M., Robador Moreno, A.,

- 1000 Salazar Rincón, Á. (Eds.), *Comprendiendo El Relieve: Del Pasado Al Futuro*.
 1001 Instituto Geológico y Minero de España, Madrid, Spain, pp. 315–322. ISBN:978-
 1002 84-9138-013-9
- 1003 García-Oteyza, J., Génova, M., Calvet, J., Furdada, G., Guinau, M., Díez-Herrero, A.,
 1004 2015. Datación de avenidas torrenciales y flujos de derrubios mediante
 1005 metodologías dendrogeomorfológicas (barranco de Portainé, Lleida, España).
 1006 *Ecosistemas* 24, 43–50. doi:10.7818/ECOS.2015.24-2.07
- 1007 Gaume, E., Bain, V., Bernardara, P., Newinger, O., Barbuc, M., Bateman, A.,
 1008 Blaškovičová, L., Blöschl, G., Borga, M., Dumitrescu, A., Daliakopoulos, I.,
 1009 Garcia, J., Irimescu, A., Kohnova, S., Koutroulis, A., Marchi, L., Matreata, S.,
 1010 Medina, V., Preciso, E., Sempere-Torres, D., Stancalie, G., Szolgay, J., Tsanis, I.,
 1011 Velasco, D., Viglione, A., 2009. A compilation of data on European flash floods. *J.*
 1012 *Hydrol.* 367, 70–78. doi:10.1016/j.jhydrol.2008.12.028
- 1013 ~~Génova, M., Díez-Herrero, A., Furdada, G., Guinau, M., Victoriano, A., Under review.~~
 1014 ~~Dendrogeomorphological evidence of possible changes in the torrential floods~~
 1015 ~~periodicity due to anthropic activities (Lleida, Spain).~~
- 1016 Génova, M., Máyer, P., Ballesteros-Cánovas, J.C., Rubiales, J.M., Saz, M.A., Díez-
 1017 Herrero, A., 2015. Multidisciplinary study of flash floods in the Caldera de
 1018 Taburiente National Park (Canary Islands, Spain). *Catena* 131, 22–34.
 1019 doi:10.1016/j.catena.2015.03.007
- 1020 Gob, F., Petit, F., Bravard, J.P., Ozer, A., Gob, A., 2003. Lichenometric application to
 1021 historical and subrecent dynamics and sediment transport of a Corsican stream
 1022 (Figarella River - France). *Quat. Sci. Rev.* 22, 2111–2124. doi:10.1016/S0277-
 1023 3791(03)00142-2
- 1024 Gottesfeld, A.S., 1996. British Columbia flood scars: maximum flood stage indicators.
 1025 *Geomorphology* 14, 319-325. doi:10.1016/0169-555X(95)00045-7
- 1026 Grissino-Mayer, H. D., 2001. Evaluating crossdating accuracy: a manual and tutorial for
 1027 the computer program COFECHA. *Tree-Ring Research* 57 (2), 205–221.
- 1028 Guardiola-Albert, A., Ballesteros-Cánovas, J.A., Stoffel, M., Díez-Herrero, A., 2015.
 1029 How to improve dendrogeomorphic sampling: variogram analyses of wood density
 1030 using XRCT. *Tree-Ring Research* 71 (1), 25-36. doi:10.3959/1536-1098-71.1.25
- 1031 ~~IGC, 2008. Nota tècnica sobre la visita al barranc de Portainé i al barranc des Caners els~~
 1032 ~~dies 1 i 2 d'octubre de 2008 en motiu de la torrentada ocorreguda la matinada del~~
 1033 ~~dia 12 de setembre de 2008, AP-187/08. Institut Geològic de Catalunya, Barcelona,~~
 1034 ~~Spain.~~
- 1035 IGC, 2010a. Estudi de la torrentada de la nit del dia 11 al 12 de setembre de 2008 al
 1036 barranc de Portainé (Pallars Sobirà), AP-019/10. Institut Geològic de Catalunya,
 1037 Barcelona, Spain.
- 1038 IGC, 2010b. Nota de la visita al barranc de Portainé (Pallars Sobirà) arran del episodi de
 1039 pluges dels dies 22 i 23 de juliol de 2010, AP-046/10. Institut Geològic de
 1040 Catalunya, Barcelona, Spain.
- 1041 ~~IGC, 2011. Nota de la visita al barranc de Portainé (Pallars Sobirà) arran de l'episodi de~~
 1042 ~~pluges del dia 5 d'agost de 2011, AP-054/11. Institut Geològic de Catalunya,~~
 1043 ~~Barcelona, Spain.~~
- 1044 IGC, 2013a. Avaluació de la dinàmica torrencial del torrent de Portainé, AP-035/13.
 1045 Institut Geològic de Catalunya, Barcelona, Spain.

1046 ~~IGC, 2013b. Nota de la visita al barranc de Portainé (Pallars Sobirà) arran de l'episodi~~
1047 ~~de pluges del dia 23 de juliol de 2013, AP 091/13. Institut Geològic de Catalunya,~~
1048 ~~Barcelona, Spain.~~

1049 ~~IGC, GEOCAT, FGC, 2013. Informe de visita de terreny de les esllavissades i~~
1050 ~~barrancades a la carretera d'accés a Portainé a juliol de 2013, AP 057/13. Institut~~
1051 ~~Geològic de Catalunya, Gestió de Projectes S.A., and Ferrocarrils de la Generalitat~~
1052 ~~de Catalunya, Barcelona, Spain.~~

1053 ~~Jaboyedoff, M., Oppikofer, T., Abellán, A., Derron, M.H., Loye, A., Metzger, R.,~~
1054 ~~Pedrazzini, A., 2012. Use of LIDAR in landslide investigations: a review. Nat.~~
1055 ~~Hazards 61, 5–28j. doi:10.1007/s11069-010-9634-2~~

1056 Jacob, N., 2003. Les vallées en gorges de la Cévenne vivaraise: montagne de sable et
1057 château d'eau. PhD dissertation, Université Paris-Sorbonne, France.

1058 Keim, R.F., Skaugset, A.E., Bateman, D.S., 1999. Digital terrain modeling of small
1059 stream channels with a total-station theodolite. Adv. Water Resour. 23, 41-48. doi:
1060 10.1016/S0309-1708(99)00007-X

1061 Khazaradze, G., Guinau, M., Calvet, J., Furdada, G., Victoriano, A., Génova, M., 2016.
1062 Debris flow cartography using differential GNSS and Theodolite measurements.
1063 Geophysical Research Abstracts 18, [EGU2016-9696](#). [doi:](#)
1064 [10.13140/RG.2.2.27245.59363](#)

1065 Kochel, R.C., Baker, V.R., 1982. Paleoflood Hydrology. Science 215, 353–361. doi:
1066 10.1126/science.215.4531.353

1067 [Kundzewicz, Z., Stoffel, M., Kaczka, R., Wyźga, B., Niedźwiedz, T., Pińskwar, I.,](#)
1068 [Ruiz-Villanueva, V., Łupikasza, E., Czajka, B., Ballesteros-Cánovas, J.,](#)
1069 [Małarzewski, Ł., Choryński, A., Janecka, A., Mikuś, P., 2014. Floods at the](#)
1070 [northern foothills of the Tatra Mountains-a Polish–Swiss research project. Acta](#)
1071 [Geophys. 62 \(3\), 620–641. doi:10.2478/s11600-013-0192-3](#)

1072 [Lang, M., Fernandez-Bono, J.F., Recking, A., Naulet, R., Grau-Gimeno, P., 2004.](#)
1073 [Methodological guide for paleoflood and historical peak discharge estimation, in:](#)
1074 [Benito, G., Thorndycraft, V.R. \(Eds.\), Systematic, Palaeoflood and Historical Data](#)
1075 [for the Improvement of Flood Risk Estimation: Methodological Guidelines. CSIC,](#)
1076 [Madrid, Spain, pp. 43-53. ISBN:84-921958-3-5](#)

1077 Luis-Fonseca, R., Raïmat, C., Hürlimann, M., Abancó, C., Moya, J., Fernández, J.,
1078 2011. Debris-flow protection in recurrent areas of the Pyrenees. Experience of the
1079 VX systems from output results collected in the pioneer monitoring station in
1080 Spain, in: 5th International Conference on Debris-Flow Hazards Mitigation, Padua,
1081 Italy, pp. 1063–1071.

1082 [Malik, I., Matyja, M., 2008. Bank erosion history of a mountain stream determined by](#)
1083 [means of anatomical changes in exposed tree roots over the last 100 years \(Bila](#)
1084 [Opava River–Czech Republic\). Geomorphology 98, 126-142. doi:](#)
1085 [10.1016/j.geomorph.2007.02.030](#)

1086 Meteocat, 2008. Atlas Climàtic de Catalunya 1961-1990. Servei Meteorològic de
1087 Catalunya, Barcelona, Spain.

1088 Nicholas, A.P., Walling, D.E., 1997. Modelling flood hydraulics and overbank
1089 deposition on river floodplains. Earth Surf. Process. Landforms 22, 59–77.
1090 doi:10.1002/(SICI)1096-9837(199701)22:1<59::AID-ESP652>3.0.CO;2-R

- 1091 O'Connor, J.E., Webb, R.H., 1988. Hydraulic modelling for paleoflood analysis, in:
 1092 Baker, V.C., Kochel, R.C., Patton, P.C. (Eds.), Flood Geomorphology. John Wiley
 1093 & Sons, New York, United States, pp. 393–402. [ISBN:978-0-471-62558-2](#)
- 1094 ~~Ortega, J.A., Garzón, G., 2009. A contribution to improved flood magnitude estimation
 1095 in base of palaeoflood record and climatic implications—Guadiana River (Iberian
 1096 Peninsula). Nat. Hazards Earth Syst. Sci. 9, 229–239. doi:10.5194/nhess-9-229-
 1097 2009~~
- 1098 Ortega, J.A., Garzón, G., 1997. Inundaciones históricas en el río Guadiana: sus
 1099 implicaciones climáticas, in: Rodríguez, J. (Ed.), Cuaternario Ibérico, AEQUA,
 1100 Huelva, Spain, pp. 365–367.
- 1101 ~~Ortuño, M., Marti, A., Martín-Closas, C., Jiménez-Moreno, G., Martinetto, E.,
 1102 Santanach, P., 2013. Palaeoenvironments of the Late Miocene Pruedo Basin:
 1103 implications for the uplift of the Central Pyrenees. J. Geol. Soc. London. 170, 79–
 1104 92. doi:10.1144/jgs2011-121~~
- 1105 ~~Palau, R.M., Hürlimann, M., Pinyol, J., Moya, J., Victoriano, A., Génova, M., Puig-
 1106 Polo, C., 2017. Recent debris flows in the Portainé catchment (Eastern Pyrenees,
 1107 Spain): analysis of monitoring and field data focussing on the 2015 event.
 1108 Landslides 14, 1161–1170. doi:10.1007/s10346-017-0832-9~~
- 1109 ~~Parker, C., Clifford, N.J., Thorne, C.R., 2011. Understanding the influence of slope on
 1110 the threshold of coarse grain motion: Revisiting critical stream power.
 1111 Geomorphology 126, 51–65. doi:10.1016/j.geomorph.2010.10.027~~
- 1112 Portilla, M., Chevalier, G., Hürlimann, M., 2010. Description and analysis of the debris
 1113 flows occurred during 2008 in the Eastern Pyrenees. Nat. Hazards Earth Syst. Sci.
 1114 10, 1635–1645. doi:10.5194/nhess-10-1635-2010
- 1115 ~~Raimat, C., Luis, R., Wendeler, C., 2010. Comportamiento de las barreras VX y
 1116 primeros resultados de la estación de medición pionera en España, Technical
 1117 documentation. Geobruigg Ibérica S.A., Lleida, Spain. Raimat, C., Riera, E., Graf,
 1118 C., Luis-Fonseca, R., Fañanas-Aguilera, C., Hürlimann, M., 2013. Experiencia de la
 1119 aplicación de RAMMS para la modelización de flujo tras la aplicación de las
 1120 soluciones flexibles VX en el Barranc de Portainé, in: VIII Simposio Nacional
 1121 Sobre Taludes Y Laderas Inestables, Mallorca, Spain.~~
- 1122 ~~RinnTech., 2003. TSAP-Win Software for tree-ring measurement, analysis and
 1123 presentation Product Information, v. 0.53. RinnTech, Heidelberg, Germany, 2 pp.~~
- 1124 ~~Roering, J.J., Mackey, B.H., Marshall, J.A., Sweeney, K.E., Deligne, N.I., Booth, A.M.,
 1125 Handwerker, A.L., Cerovski-Darriau, C., 2013. “You are HERE”: Connecting the
 1126 dots with airborne lidar for geomorphic fieldwork. Geomorphology 200, 172–183.
 1127 doi:10.1016/j.geomorph.2013.04.009~~
- 1128 Ruiz-Villanueva, V., Díez-Herrero, A., Stoffel, M., Bollschweiler, M., Bodoque, J.M.,
 1129 Ballesteros, J.A., 2010. Dendrogeomorphic analysis of flash floods in a small
 1130 ungauged mountain catchment (Central Spain). Geomorphology 118, 383–392.
 1131 doi:10.1016/j.geomorph.2010.02.006
- 1132 Sánchez-Moya, Y., Sopeña, A., 2015. Aprendiendo a leer en las estratificaciones
 1133 cruzadas. Enseñanza las Ciencias la Tierra 23 (2), 148–159. ISSN: 1132-9157
- 1134 ~~Sigafoos, R.S., 1964. Botanical evidence of floods and flood-plain deposition. United
 1135 States Geological Survey Professional Paper 485-A.~~
- 1136 Stoffel, M., Bollschweiler, M., 2008. Tree-ring analysis in natural hazards research - an
 1137 overview. Nat. Hazards Earth Syst. Sci. 8, 187–202. doi:10.5194/nhess-8-187-2008

- 1138 | [Stoffel, M., Corona, C., 2014. Dendroecological dating of geomorphic disturbance in](#)
1139 | [trees. *Tree-Ring Research*, 70 \(1\), 3-20. doi:10.3959/1536-1098-70.1.3](#)
- 1140 | Tarolli, P., 2014. High-resolution topography for understanding Earth surface processes:
1141 | Opportunities and challenges. *Geomorphology* 216, 295–312.
1142 | doi:10.1016/j.geomorph.2014.03.008
- 1143 | Terrasolid, 2016. TerraScan User's Guide. Terrasolid Ltd., Helsinki, Finland, 592 pp.
- 1144 | USACE, 2008. HEC-RAS River Analysis System Users's Manual, v. 4.0. Hydrologic
1145 | Engineering Center, Washington, DC, United States, 747 pp.
- 1146 | USACE, 2012. HEC-GeoRAS GIS Tools for Support of HEC-RAS using ArcGIS 10
1147 | User's Manual, v. 10. Hydrologic Engineering Center, Washington, DC, United
1148 | States, 242 pp.
- 1149 | Victoriano, A., Guinau, M., Furdada, G., Calvet, J., Cabré, M., Moysset, M., 2016.
1150 | Aplicación de datos LiDAR en el estudio de la dinámica torrencial y evolución de
1151 | los barrancos de Portainé y Reguerals (Pirineos Centrales), in: Durán Valsero, J.J.,
1152 | Montes Santiago, M., Robador Moreno, A., Salazar Rincón, Á. (Eds.),
1153 | Comprendiendo El Relieve: Del Pasado Al Futuro. Instituto Geológico y Minero de
1154 | España, Madrid, pp. 447–455. ISBN:978-84-9138-013-9
- 1155 | [Webb, R.H., Jarrett, R.D., 2002. One-dimensional estimation techniques for discharges](#)
1156 | [of paleofloods and historical floods, in: House, P.K., Webb, R.H., Baker, V.R.,](#)
1157 | [Levish, D.R. \(Eds.\), *Ancient Floods, Modern Hazards: Principles and Applications*](#)
1158 | [of Paleoflood Hydrology. American Geophysical Union, Washington, DC, pp.](#)
1159 | [111–125. doi:10.1029/WS005p0111](#)
- 1160 | Williams, G.P., 1983. Paleohydrological methods and some examples from Swedish
1161 | fluvial environments. *Geogr. Ann.* 65, 227–243. doi:10.2307/520588
- 1162 | Yanosky, T.M., Jarrett, R.D., 2002. Dendrochronologic evidence for the frequency and
1163 | magnitude of paleofloods, in: House P.K, Webb, R.H., Baker, V.R., Levish, D.R.
1164 | (Eds), *Ancient floods, Modern hazards: Principles and Applications of Paleoflood*
1165 | *Hydrology*. American Geophysical Union, Washington, DC, pp. 77-89.
1166 | doi:10.1029/WS005p0077
- 1167 | [Zielonka, T., Holeksa, J., Ciapala, S., 2008. A reconstruction of flood events using](#)
1168 | [scarred trees in the Tatra Mountains, Poland. *Dendrochronologia* 26, 173-183.](#)
1169 | [doi:10.1016/j.dendro.2008.06.003](#)

1 **Four-topic correlation between flood** 2 **dendrogeomorphological evidence and hydraulic** 3 **parameters (the Portainé stream, Iberian Peninsula)**

4 Ane Victoriano^{a,*}, Andrés Díez-Herrero^b, Mar Génova^c, Marta Guinau^a, Glòria
5 Furdada^a, Giorgi Khazaradze^a, Jaume Calvet^a

6 ^a RISKNAT Group, Geomodels Research Institute, Dpt. de Dinàmica de la Terra i de l'Oceà, Facultat de
7 Ciències de la Terra, Universitat de Barcelona (UB), 08028 Barcelona (Spain).

8 ^b Geological Hazards Division, Geological Survey of Spain (IGME), 28003 Madrid (Spain).

9 ^c Dpto. de Sistemas y Recursos Naturales, Universidad Politécnica de Madrid (UPM), 28040 Madrid
10 (Spain).

11 * Corresponding author

12 *E-mail addresses:* ane.victoriano@ub.edu (A. Victoriano), andres.diez@igme.es (A. Díez-Herrero),
13 mar.genova@upm.es (M. Génova), mguinau@ub.edu (M. Guinau), gloria.furdada@ub.edu (G. Furdada),
14 gkharzar@ub.edu (G. Khazaradze), jcalvet@ub.edu (J. Calvet).

15 **Abstract**

16 Torrential floods are hazardous hydrological phenomena that produce significant
17 economic damage worldwide. Flood reconstruction is still problematic in mountainous
18 ungauged areas due to the lack of systematic real data, so other indirect techniques are
19 required. This paper presents an integrated palaeoflood study of a Pyrenean stream that
20 combines fluvio-torrential geomorphology, dendrogeomorphology, palaeoflood
21 discharges and flow hydraulics. The use of a total station and airborne LiDAR data has
22 allowed obtaining a detailed topography for geomorphological mapping and for running
23 a one-dimensional hydraulic model. Based on the height of scars on several damaged
24 trees, we obtained palaeodischarges of $316 \text{ m}^3\text{s}^{-1}$ and $314 \text{ m}^3\text{s}^{-1}$ for the 2008 and 2010
25 floods. The hydraulic parameters were related to the geomorphic position of trees,
26 showing a positive relation between most energetic geomorphic elements and flow
27 depth and velocity values. The most intensely affected trees are located in intermediate
28 energy geomorphic positions. Analysing variabilities in scar height and flow stage
29 differences, we suggest that most reliable trees for peak discharge estimation correspond
30 to those placed in areas related with fluvio-torrential processes of intermediate energy.
31 This multidisciplinary palaeohydrological study relates flood hydrodynamics with the
32 damages on trees and their geomorphological characteristics, focusing on the hydraulic
33 parameters of the peak flow (depth, velocity and unit stream power), which has never
34 been carried out elsewhere. The proposed approach shows a high potential for
35 palaeoflood analysis in ungauged mountain catchments with scarce non-systematic data.

36 *Keywords:* Dendrogeomorphology, Fluvial geomorphology, Hydraulic modelling,
37 Palaeoflood, Spanish Pyrenees.

38 **1. Introduction**

39 Hydrometeorological phenomena are one of the most recurrent causes of natural
40 disasters worldwide that annually produce significant economic damages and fatalities
41 (Gaume et al., 2009). Flood disasters are increasing in number and damages in the last

42 few decades in Europe (Barredo, 2007). In mountainous areas of Catalonia (Spain),
43 flash floods and debris flows cause severe socioeconomic and geomorphologic impacts
44 due to their sudden occurrence, torrential behaviour and high sediment load involved
45 (Portilla et al., 2010).

46 Flood hazard assessment is often based on conventional statistical magnitude-
47 frequency analyses, which are difficult to apply in areas with scarce rainfall data and
48 lack of flow gauging stations. Palaeohydrology is a useful method in active torrential
49 basins with non-systematic records that consists on the study of past floods especially
50 focusing on ancient extraordinary events, and encompasses different research lines
51 depending on the palaeoflood data and working methodology (Baker, 2008; Benito and
52 Díez-Herrero, 2015; Lang et al., 2004; Webb and Jarrett, 2002). Extreme flood
53 reconstruction has been carried out using a variety of data sources and evidence, such as
54 sedimentological (Benito et al., 2003, 2015; Kochel and Baker, 1982),
55 geomorphological (Baker et al., 1988; Baker and Pickup, 1987), dendrochronological
56 (Ballesteros-Cánovas et al., 2016; Gottesfeld, 1996; Kundzewicz et al., 2014; Malik and
57 Matyja, 2008; Sigafoos, 1964; Yanosky and Jarrett, 2002; Zielonka et al., 2008), and
58 lichenometric indicators (Gob et al., 2003).

59 Many authors have reconstructed palaeoflood using dendrogeomorphology, which
60 provides information about past events recorded in flood dendrogeomorphological
61 evidence (FDE) in riverbed and riverbank trees (see reviews from Ballesteros-Cánovas
62 et al., 2015b and Benito and Díez-Herrero, 2015), but also other hydraulic parameters
63 like flow velocity, depth and power by means of hydrodynamic modelling (Ballesteros-
64 Cánovas et al., 2010, 2015a). Numerous studies relate flood discharges with flow
65 hydraulics with different empirical equations (Bagnold, 1980; Chanson, 2004; Chow,
66 1959; Costa, 1983; Ferguson, 2005). Some other works deal with flow hydraulics and
67 fluvial geomorphology from different perspectives: flood geomorphology (Baker et al.,
68 1988), the stability of geomorphological elements (Nicholas and Walling, 1997; Ortega
69 and Garzón, 1997) or past flood discharges and deposits (Baker, 1987; Kochel and
70 Baker, 1982; Sánchez-Moya and Sopena, 2015). However, dendrogeomorphological
71 evidence have rarely been associated to the geomorphic position of the trees (Ruiz-
72 Villanueva et al., 2010), or other local characteristics of the river reach (Ballesteros-
73 Cánovas et al., 2016).

74 However, these methods tend to have some limitations in mountains areas.
75 Dendrogeomorphological studies are conditioned by the number of trees of the study
76 area, which is limited in some cases. High-resolution geomorphological mapping is
77 difficult to carry out in remote areas. Palaeodischarge reconstructions in ungauged
78 catchments require an adequate topographic data for hydraulic modelling, which is
79 usually scarce in forested mountain catchments. Regarding flow hydrodynamics, the
80 calculation of hydraulic parameters depends on the estimated peak discharge.

81 This paper reconstructs flood events combining all the above mentioned disciplines
82 (Fig. 1). The aim of this paper is to quantify the relation between flood hydrodynamics
83 and the geomorphological characteristics of damaged trees. Flow hydraulics are
84 analysed according to the specific geomorphic position of trees and the obtained stream
85 power from hydraulic modelling is used to estimate the mobilizable particle size, which

86 is compared to field measures to assess its reliability. Such a multidisciplinary analysis
87 specially focusing on hydraulic parameters has never been carried out before in a
88 selected study area, and allows us to obtain an improved knowledge about fluvio-
89 torrential dynamics in areas with few source data.

90 **2. Problematic study area and hazard**

91 The multidisciplinary approach presented in this paper was performed in the 5.72
92 km² Portainé drainage basin (Pallars Sobirà County, Catalonia, Spain), located in the
93 Eastern Pyrenees (Fig. 2a). Maximum altitude is 2439 m a.s.l. (Torreta de l'Orri). Two
94 main streams drain the basin towards the north, the Portainé stream (5.7 km long) and
95 its tributary the Reguerals stream (3 km long). Their confluence is placed at 1285 m
96 a.s.l. and then, the Portainé stream flows until its confluence with the Romadriu River
97 (part of the Ebro River Basin) at 950 m a.s.l. (Fig. 2c). An access road to the Port-Ainé
98 ski station crosses both streams at various points. The climate is Alpine Mediterranean,
99 with a mean annual rainfall of 800 mm and 5-7 °C mean annual temperature (Meteocat,
100 2008).

101 From a geological perspective, the Portainé basin is located in the Pyrenean Axial
102 Zone (Fig. 2b). In the study area, the bedrock is composed of highly folded and
103 fractured Cambro-Ordovician metapelites and sandstones with quartzite intercalations.
104 Wide surficial colluvial materials irregularly cover large parts of the terrain. Due to the
105 highly fractured bedrock and the unconsolidated surficial deposits, materials are easily
106 eroded and mobilized along the streams. Geomorphologically, the catchment can be
107 divided in two sectors (IGC, 2013). The southern one corresponds to the headwaters and
108 shows lower gradients (less than 25°, but usually around 10-20°) and a poorly
109 entrenched drainage network. The northern sector shows higher gradients (more than
110 25°) stronger entrenched streams (Fig. 2c).

111 The Portainé and the Reguerals streams are characterized by a high torrential
112 activity especially since 2006, as debris flood, hyperconcentrated flow and/or debris
113 flow events produce significant losses in infrastructures, mainly where the road crosses
114 the streams. From 2006 to 2015, ten events have occurred in this area (IGC, 2013; Palau
115 et al., 2017), even without extraordinary rainfall values. In addition,
116 dendrogeomorphological studies have proved the occurrence of previous torrential
117 events, even if their frequency is much lower (Furdada et al., 2016; García-Oteyza et al.,
118 2015). In order to reduce these impacts, 15 sediment retention barriers were installed
119 along the channels since 2009 as a hydrological correction measure (Luis-Fonseca et al.,
120 2011). However, the problem remains and the increasingly entrenched streams show a
121 significant erosive tendency (Victoriano et al., 2016).

122 The specific study area corresponds to the most downstream 500 m-long reach of
123 the Portainé stream. In the confluence with the Romadriu River, an alluvial elongated
124 debris cone has formed, mainly composed of sub-rounded to sub-angular decimetric
125 boulders. High sediment load torrential events change the morphology of the mobile
126 riverbed easily, also affecting the riverbank trees. In general, the vegetation of the area
127 constitutes a deciduous broadleaf forest with a variety of species.

128 **3. Material and methods**

129 The methodological approach of this study is synthetized in Fig. 3, showing each
130 research topic and the integration of the methods for final results.

131 *3.1. Geomorphological mapping and analysis*

132 A detailed geomorphological study and mapping of the features was carried out.
133 This analysis had two steps, (i) topographic and geomorphological fieldwork, and (ii)
134 GIS mapping.

135 Detailed topographic data acquisition was carried out in March 2014 using a Leica
136 TC 1700 total station. This taquimetric survey was focused on localizing and defining
137 topographic sharp changes (breaklines) of geomorphic elements and tree positions in
138 order to collect a complete point dataset (Keim et al., 1999) consisting of 1118 points
139 (853 ground points and 265 tree points) in a 4850 m² area. In addition, in places where
140 trees showing external FDE were identified we also obtained detailed topographic cross
141 sections. Differential RTK GNSS methods were carried out to accurately measure the
142 absolute coordinates of certain control points (Khazaradze et al., 2016) used to
143 georeference the dense measurements obtained with the total station. Regarding
144 geomorphological mapping, during the mentioned topographic field survey, main
145 geomorphological elements were identified following the proposal of Church et al.
146 (2012) and their limits were measured with the total station. Main geomorphological
147 elements and deposits were roughly classified as: functional channel, distributary
148 channels of the cone, gravels and boulders; in addition, alluvial terraces were identified,
149 as well as other features like levees, escarpments and flow paths. During subsequent
150 field surveys carried out in March 2015, September 2015 and June 2016, morphological
151 changes in landforms, elements and facets (different parts of the elements) were
152 recognized, which mainly occurred along the channels and did not alter the position of
153 riverbed and riverbank trees.

154 The deposits and forms were mapped using the ArcGIS 10.2.2 software (ESRI,
155 2014), creating a detailed geomorphological map.

156 *3.2. Dendrogeomorphological analysis*

157 Dendrogeomorphology is a palaeohydrological data source that provides
158 information about past torrential events recorded in trunks, branches and roots of
159 riverbed and riverbank trees (Díez-Herrero, 2015). Tree-ring analysis been widely
160 applied for fluvio-torrential processes in flood studies (see reviews from Ballesteros-
161 Cánovas et al., 2015b and Benito and Díez-Herrero, 2015). The
162 dendrogeomorphological study carried out in Portainé is divided in three
163 complementary tasks, (i) dendrochronological sampling, (ii) tree-ring analysis and FDE
164 dating, and (iii) geomorphological analysis of the tree positions.

165 Dendrochronological sampling was carried out in March 2014, March 2015 and
166 September 2015, and the strategy was based on the field recognition of external
167 disturbances. The selected trees were those showing evidence most probably produced
168 by the impact of boulders and/or large wood transported by the flow, mainly injured,
169 decapitated and tilted trees (Fig. 4), but also few trees with exposed roots. Trees were
170 sampled following dendrogeomorphological procedures (Stoffel & Bollschweiler, 2008;
171 Díez-Herrero et al., 2013, Stoffel & Corona, 2014). The geographic position of each tree

172 was measured using a total station, and also the height of scars and decapitation nodes.
173 Additional information was also collected, such as an identifier code, sampling date,
174 species, description of the tree (height and perimeter), description of the FDE (type,
175 height and size), description of the sample (height) and photos of the tree. Cylindrical
176 samples (cores) were obtained using a Pressler increment borer of 5 mm diameter. Some
177 wedges were also extracted from overgrowing callus in scarred trees and cross sections
178 were cut in some death trees. We analysed 57 trees from 9 different species (151
179 samples) providing a multievidence population of *Populus tremula* L. (common aspen),
180 *Populus nigra* L. (black poplar), *Fraxinus excelsior* L. (ash), *Prunus avium* L. (wild
181 chery), *Quercus petraea* (Matt.) Liebl. (sessile oak), *Tilia platyphyllos* Scop. (largeleaf
182 linden), *Juglans regia* L. (common walnut), *Acer campestre* L. (field maple) and *Salix*
183 *caprea* L. (goat willow).

184 In this study, we only considered external evidence on trees. In the laboratory, tree-
185 ring analysis of cores, wedges and sections consisted in (Génova et al., 2015): (i)
186 sample air-drying, cutting or sanding; (ii) tree-ring width measuring using a LINTAB
187 table (with 1/100 mm accuracy) and the associated software TSAPWin (RinnTech,
188 2003); (iii) cross-dating using visual and statistical techniques (Cook and Kairiukstis,
189 1990); and (iv) quality check using the Cofecha software (Grissino-Mayer, 2001). This
190 process let us to date scars in tree-ring series and consequently, torrential events. The
191 last ring of dead trees was dated by comparing tree-ring series with other living trees of
192 the same species. For palaeoflood reconstruction, the scars' formation year (dated
193 following the mentioned procedure) and their height (measured in the field) were used.
194 Additionally we considered the location of decapitated trees, tilted trees and exposed
195 roots for the geomorphic analysis. This information was compiled within a
196 dendrogeochronological database.

197 The inclusion of the dendrogeochronological database into a GIS environment,
198 using ArcGIS 10.2.2 software (ESRI, 2014), allowed to study the geomorphological
199 setting of disturbed trees. Based on the geomorphological mapping and tree positions,
200 geomorphic features were reclassified according to their formation energy (Ruiz-
201 Villanueva et al., 2010). This lead to a considerably more elaborated classification of
202 the geomorphic forms, elements and facets. Moreover, the detailed geomorphic position
203 of each tree was determined in the field, and trees were classified according to the
204 geomorphic form (e.g. riverbed), element (e.g. gravel bar) or facet (e.g. bar tail) in
205 which they were located, obtaining the spatial distribution of de FDE according to the
206 formation energy of the geomorphic form on which they locate. Other
207 geomorphological characteristics (e.g. channel reach morphology and tree exposure to
208 the flow) were not considered in this study because they were equal for all the scarred
209 trees (straight channel and exposed trees). Therefore, the geomorphic position according
210 to geomorphic units was the best evidence to relate flow hydrodynamics and FDE
211 formation.

212 3.3. Palaeodischarge estimations and hydraulic modelling

213 Palaeofloods were reconstructed using the one-dimensional hydraulic simulation
214 software HEC-RAS 4.0 from the US Army Corps of Engineers (USACE, 2008). This
215 model was used to obtain palaeoflood discharges and other hydraulic parameters as

216 stage, water depth, velocity and stream power. It was run a 1D model instead of a 2D
217 one due to the following groups of factors: a) channel geometric characteristics (lack of
218 high-resolution and high-accuracy 2D topographic data; detailed cross-sections
219 coinciding with tree locations measured with total station; narrow valley with
220 length/width ratio $>3:1$; and lack of anthropic features, such as bridges or culverts,
221 along the channel); b) hydrodynamic factors (unidirectional flow patterns during floods;
222 limited secondary transversal flows due to the narrowness of the valley and the steep
223 gradient with waterfalls and rapids); and c) other evidence (scar height-riverbed
224 parallelism suggesting a sub-uniform to gradually variable flow). The required
225 parameters and conditions to run the hydraulic model were: (i) geometric data, (ii)
226 boundary conditions, and (iii) discharges.

227 Regarding geometric data, HEC-RAS works with transversal cross sections (XS
228 sections). Topographic data from two different sources were available for the study
229 area: total station and airborne LiDAR (Light Detection and Ranging). Total station data
230 was acquired in the field (see section 3.1.) and provided high accuracy but slightly low
231 point-density. LiDAR data was collected with the aircraft Cessna Caravan 208B and the
232 topographic LiDAR sensor Leica ALS50-II, owned by the Cartographic and Geological
233 Institute of Catalonia (ICGC), and the point cloud was georeferenced and filtered using
234 the TerraScan software (Terrasolid, 2016). The potential of LiDAR data creating high-
235 resolution elevation models has been widely accepted (Tarolli, 2014). However, in our
236 mountain study area with steep slopes and dense vegetation, the LiDAR dataset
237 provided a good coverage but a low elevation accuracy (about 50 cm RMSE) and not
238 very high-resolution topography (0.63 ground point/m²). Taking into account the
239 mentioned strengths and limitations of data sources, two hydraulic models with
240 different geometric data were run. The first one, manually introducing the cross sections
241 measured with the total station in the field (23 XS sections). The second one, combining
242 both topographic data. LiDAR points were added into the total station dataset and
243 carefully analysed in order to assess its suitability. Some adjacent points showed
244 significant differences in elevation, which were attributed to (i) small but detectable
245 erosion and accumulation between the 2011 LiDAR and 2014 total station data; and (ii)
246 the real morphology of the steep terrain (e.g. stream entrenchment, escarpments and
247 steep slopes). In order to overcome these limitations, a manual point editing process was
248 carried out using objective criteria of congruence and acceptability, consisting in
249 detecting erroneous points by comparing their coordinates with the surrounding points.
250 This was done by creating 0.5 m (in steep areas) or 1 m (in flat area) buffers for total
251 station points and intersected with LiDAR ground points. Establishing a maximum
252 tolerance threshold of 0.5 m for the differences on elevation between both topographic
253 data sources, incoherent LiDAR points were deleted. Finally, a bare-earth Triangulated
254 Irregular Network (TIN) was created with the selected terrain points and sections were
255 extracted from it (35 XS sections), using HEC-GeoRAS 10.2 extension (USACE, 2012)
256 for ArcGIS. The advantage of the TIN-based model is that it allowed the input of
257 additional transversal profiles, but its weakness is that LiDAR data can distort and
258 smooth the detailed sharp topography obtained in the field. In addition, the stream
259 centreline, banks and levees were added. The limits of the riverbanks were defined
260 coinciding with roughness changes, so that a Manning's n value for the left bank,

261 channel and right bank was established for each cross section. The roughness coefficient
262 was obtained from field observations, based on Arcement and Schneider (1989).

263 Boundary conditions upstream and downstream from the modelled reach were
264 critical depth because both boundary sections correspond to small waterfalls (more than
265 2 m high) in stable bedrock riverbed, identified in the field. These are hydraulic jumps
266 with a critical flow (Froude number = 1) especially during flood events, so they are
267 suitable for the critical-depth method (Bodoque et al., 2011). The model was run as a
268 steady flow, as the input were peak discharge values; and the flow regime modelled as
269 supercritical.

270 Palaeodischarges were calculated using external scars as palaeostage indicators
271 (PSIs). These evidence provide the most precise information of both the date and the
272 magnitude of the event, as they allow knowing both the precise year in which they were
273 formed by dendrochronological dating and the minimum water depth of the flow by
274 measuring the height of the scar and/or its absolute altitude. In our study, we dated
275 external scars from 2000 (4 scars), 2006 (1 scar), 2008 (19 scars) and 2010 (6 scars)
276 events. Scars from 2000 were almost closed and did not provide information about the
277 water stage. Regarding the trees scarred in 2006, there was a unique evidence so it was
278 not considered enough as a palaeostage indicator. Therefore, only 2008 and 2010 events
279 could be reconstructed, as they provided a representative number of scars and their
280 height could be reliably measured in the field; but are also the last most destructive
281 documented events. Although two high discharge events occurred in 2008 (September
282 and November) and two others in 2010 (July and August), we assume that the scars
283 were formed by a unique event for each year. In fact, scars from 2008 were all formed
284 in the high-magnitude torrential flood occurred in September, which produced
285 documented damages in a bridge located just upstream of the study reach (IGC, 2013),
286 whereas the low-magnitude event occurred in November did not produce any effect at
287 that point. Regarding scars from 2010, the one in July did not transport material along
288 the study reach because it was accumulated in recently emplaced sediment retention
289 barriers (IGC, 2010b); so, the scars would correspond to the August event when the
290 barriers were filled and the flow transported high sediment load. We selected the trees
291 showing scars corresponding to those events years (25 trees). For each year, we carried
292 out a normality test to height differences (d ; Eq. 3) in order to detect outliers, comparing
293 the samples with a normal or Gaussian distribution. This process allowed us to detect an
294 anomalous scar for 2008, which indeed, showed an odd shape in the field. Therefore, its
295 origin may not be torrential and it was deleted before simulating the discharge values.
296 At last, 18 scars (6 *P. tremula*, 6 *P. nigra*, 2 *F. excelsior*, 2 *P. avium*, 1 *Q. petraea* and 1
297 *A. campestre*) were considered for 2008 modelling (9 of them dated from wedges) and 6
298 scars (2 *P. tremula*, 2 *F. excelsior*, 1 *Q. oetraea* and 1 *T. platyphyllos*) for 2010 (1 dated
299 from a wedge). Peak discharges for analysed palaeofloods were calculated using the
300 step-backwater method (Ballesteros-Cánovas et al., 2010; O'Connor and Webb, 1988),
301 by increasingly introducing peak discharge input values in the model and finding the
302 best fit water surface elevation for the height of the scars. For each event and each input
303 geometric data (XS section), the trial-and-error technique was used to estimate the peak
304 discharge (with a precision of $1 \text{ m}^3\text{s}^{-1}$), by finding the value that showed the minimum
305 mean absolute error (σ or MAE) and mean squared error (MSE) in the heights
306 (difference between scar altitude and modelled water stage), defined as

(1)

(2)

$$\sigma = \frac{\sum_i^n d_i}{n}$$

$$MSE = \frac{\sum_i^n d_i^2}{n}$$

307 where n is the number of scars and d is the absolute value of the difference between the
308 height of the scar and the water stage, estimated by the expression

$$d = |Z_{FDE} - Z_Q| \quad (3)$$

309 where Z_{FDE} is the altitude of the scar in meters (m) and Z_Q is the water surface elevation
310 for the modelled peak discharge in meters (m), both measured in the cross section where
311 the scar is located.

312 The peak discharges were finally calculated as the weighted arithmetic mean
313 between the discharges obtained from the two geometric data, which was estimated by
314 the following equation:

$$Q_{2008} = \frac{\left(\frac{1}{\sigma_{TIN}^2} Q_{TIN}\right) + \left(\frac{1}{\sigma_{TS}^2} Q_{TS}\right)}{\frac{1}{\sigma_{TIN}^2} + \frac{1}{\sigma_{TS}^2}} \quad (4)$$

315 σ_{TIN} and σ_{TS} being the absolute error of the TIN-based model and the one with total
316 station data respectively, and Q_{TIN} and Q_{TS} being the estimated peak discharges in $m^3 s^{-1}$.

317 As the flow in the alluvial cone can be difficult to simulate using a 1D model, we
318 also calculated the minimum peak discharge for bank overflow. This is the threshold for
319 cone flooding and consequently, marks a change in the distribution of the flow
320 discharge. This critical overflow discharge was obtained from the cross section located
321 in the cone apex.

322 3.4. Flow hydrodynamics

323 We extracted other hydraulic parameters from HEC-RAS results for each cross
324 section, such as water depth, velocity and total stream power. These parameters were
325 then obtained for the specific position of each tree containing a scar used for the
326 hydrodynamic modelling. Depth was calculated subtracting the elevation of the base of
327 the tree from the water surface elevation. For the velocity value, we considered the
328 value of the cross section part in which the tree was located (left bank, channel or right
329 bank). The unit stream power was obtained dividing the total stream power obtained by
330 the active width of the flow at the specific cross section part.

331 The knowledge of flow hydraulics allowed us to estimate the particle size that might
332 be mobilized by the flow. These calculations were carried out for the 2008 event and in
333 the deposit of the alluvial cone, because discharge estimation is more reliable and
334 accurate than for 2010 event. We also measured in the field the maximum (length),
335 medium (width) and minimum (height) axes of a representative population of boulders
336 deposited in the alluvial cone, allowing us to compare the results obtained by empirical
337 relations with the real deposited material. The diameter of the transported boulders was
338 calculated using different empirical equations. The mobilizable particle size is a

339 function of the critical unit stream power, so the hydraulic parameters needed for these
340 equations were obtained from the upstream cross section of the alluvial cone because
341 the flow in the study site is supercritical. The three applied relations were:

$$\omega_c = a \cdot D^b$$

342 where ω_c is the critical unit stream power in W/m^2 , a and b are numerical constants
343 depending on the author (Costa, 1983; Gob et al., 2003; Jacob, 2003; Williams, 1983),
344 and D is the particle diameter in millimeters (mm),

$$\omega_c = c_1 \cdot D^{1.5} \cdot \log_{10} \left(\frac{c_2 \cdot d}{D} \right) \quad (6)$$

345 d being the water depth and c_1 and c_2 being numerical constants determined by different
346 authors (Bagnold, 1980; Ferguson, 2005), and

$$C_d = \left(\frac{0.6}{\left(\frac{d}{H}\right)\left(\frac{L}{B}\right)} \right) + 0.9 \quad (7)$$

347 where C_d is the drag coefficient, assumed to be 0.95, and H , B and L are the diameters
348 corresponding to the main three main axes of the particles: height (minimum), width
349 (intermediate) and length (maximum), respectively (Carling et al., 2002). In fact, this
350 equation assumes the morphometry of the particle being dependent on the water depth.
351 They propose that the mobilized boulders should be considered as relation of the three
352 axes, which depends on several factors, such as the lithology, internal structure and
353 fractures of the material.

354 **4. Results**

355

356 *4.1. Geomorphological mapping and geomorphic forms*

357 A geomorphological map of the torrential system was obtained based on the March
358 2014 topography. Multi-temporal field campaigns (2014-2016) showed that the
359 distribution and morphology of the geomorphological elements and deposits changes in
360 time, especially those associated to the riverbed, and therefore the Portainé stream is
361 very dynamic. These changes are mostly visible in the functional channel and in the
362 lowest level of alluvial terraces. In general, the stream shows an erosive tendency,
363 which is reflected on the backward motion of the bank escarpments that delimit the
364 channel. In the alluvial cone area, the flow tends to deposit the boulders transported
365 during debris flow and flood events.

366 13 types of geomorphic forms, elements and facets were identified and mapped,
367 which are ordered according to their formation energy as: in-channel (functional active
368 channel), gravel bars, terrace 1 (low terrace), terrace 2 (high terrace), natural levee,
369 main inactive channel of cone, secondary inactive channels of cone, upper deposits of
370 cone, middle deposits of cone, lower deposits of cone, artificial levee (dyke), left-side
371 slope and right-side slope (Table 1 and Fig. 5).

372 *4.2. Dendrogeomorphological evidence*

373 Regarding external disturbances we identified 10 decapitations, 41 external scars, 25
374 tilted trees and 3 trees with exposed roots.

375 The determination of the geomorphic position of the trees allows relating the spatial
376 distribution of FDE along the torrent with the geomorphological elements (Fig. 5).
377 Table 1 shows the geomorphic position of all the analysed trees and of the scarred trees
378 used for hydraulic modelling. Analysed trees locate on 12 different geomorphic forms,
379 indeed, on all of the identified forms except for natural levees. Most of them are located
380 in the alluvial cone (58%), alluvial terraces (16%) and slopes (14%).

381 *4.3. Flood discharges*

382 The obtained peak discharges for 2008 and 2010 are presented in Table 2. For each
383 case, the value that minimized both absolute and mean squared error was considered.
384 For 2008, the calculated discharges were $300 \text{ m}^3\text{s}^{-1}$ from the TIN topography (Fig. 6)
385 and $321 \text{ m}^3\text{s}^{-1}$ from the total station topography. These results were weighted according
386 to their errors (Eq. 4), obtaining a peak discharge of $316 \text{ m}^3\text{s}^{-1}$ ($\sigma = 0.18 \text{ m}$). Given that
387 for 2010 there were only 4 scars corresponding to cross sections measured with total
388 station, the $314 \text{ m}^3\text{s}^{-1}$ discharge ($\sigma = 0.7 \text{ m}$) obtained from the TIN-based model was
389 considered as the most reliable peak discharge value.

390 For the critical overflow discharge, we obtained a $43 \text{ m}^3\text{s}^{-1}$ value of initial overbank
391 and formation of crevasse splays, named partial overbank discharge. However, the
392 complete flooding of the cone does not occur until the flow exceeds the total critical
393 overbank discharge, estimated to be $58 \text{ m}^3\text{s}^{-1}$. Therefore, higher peak discharges
394 produce the inundation of the debris cone. These are considered extraordinary events,
395 like those in 2008 and 2010.

396 *4.4. Hydraulic parameters and mobilized particle size*

397 Considering the discharge values obtained for 2008 and 2010 events, the flow
398 hydraulics was similar in both cases. Fig. 7 shows the flooded area and the water depth
399 in the most downstream part of the study area for 2008 event. This past flood produced
400 almost the total flooding of the alluvial cone, generating scars in trees due to the impact
401 of boulders and floating large wood.

402 The hydraulic parameters obtained from hydrodynamic modelling are water depth
403 (d), flow velocity (v) and unit stream power (ω) for the left bank, channel, and right
404 bank of each cross section (see results in supplementary material Table 1). *In situ*
405 hydraulic parameters for the specific position of each scarred tree are shown in Table 3.

406 For the empirical equations for particle size estimation, the water depth and unit
407 stream power values were those corresponding to left bank of the section at the apex of
408 the cone (section U-Uc'), for the 2008 peak discharge. These values were 1.03 m and
409 5221.92 Nm^{-2} . The boulder size mobilized by the flow and deposited in the cone was
410 also obtained from the measures of the three axes (Table 4). This allowed us
411 establishing the following field-based diameter relationships: $B=0.74L$, where B is
412 width and L length; and $H=0.43L$, H being height. Table 5 collects the particle

413 diameters calculated for the Portainé alluvial cone, considering the relations proposed
414 by different authors.

415 *4.5. Relation between geomorphic forms, FDE and flow hydraulics*

416 All the aspects analysed in the previous sections have been linked together to obtain
417 a more complete knowledge of the hydrodynamics of the Portainé stream, the behaviour
418 of the riverbank trees and the morphology of the area.

419 The formation of dendrogeomorphological disturbances depends on the geomorphic
420 position of the trees. 103 disturbances (decapitations, scars, stem tilting and root
421 exposure) in 12 geomorphic positions were analysed in our study area from 57 different
422 trees. The number of evidence per tree was calculated for each geomorphic form (total
423 FDE / number of trees for each geomorphic position), shown in Fig. 8 (see results in
424 supplementary material Table 2). There are few FDE in the riverbed trees (in-channel
425 and gravel bars), although these are the most energetic positions. This is due to the
426 lower number of trees in these geomorphic positions and therefore, little number of
427 samples for dendrochronological analysis. Most FDEs locate in the alluvial cone, both
428 in the main or secondary inactive channels (2.7 FDE per tree) or in the deposit area (2
429 FDE per tree). Therefore, in the Portainé study area, the most intensely damaged trees
430 concentrate on the geomorphological elements related to processes of intermediate
431 energy (second terrace and alluvial cone).

432 The geomorphological features of the valley bottom are also related to flow
433 hydraulics, and in this specific case, the stability of geomorphic forms associated to
434 torrential processes depends on the energy of the water. The hydrodynamic modelling
435 allowed us to determine the specific velocity and water depth values for the scarred
436 trees. These hydraulic parameters were then associated to the geomorphic element in
437 which each tree was located. Fig. 9 is the representation of the relation between the
438 energy of flow, affectation on trees and geomorphology. Higher velocity and depth
439 values indicate areas where torrential processes are more intense, and therefore
440 correspond to energetic geomorphic forms. These most energetic geomorphological
441 elements are close to the riverbed (in-channel and gravel bars). Far from the riverbed,
442 there is a decrease on the flow energy, both in terms of hydraulic parameters and in the
443 intensity of the torrential processes associated to the geomorphic features (Fig. 9). In
444 addition, the largest number of scars are located in the alluvial cone, which corresponds
445 to torrential processes of intermediate intensity. Taking into account that every scarred
446 tree of the study area was sampled, the number of samples does not condition the
447 concentration of scars in the alluvial cone and it represents the geomorphic form where
448 more trees are affected during torrential events.

449 The relation of scars, geomorphic forms and flow hydrodynamics can be assessed
450 by comparing the differences between scar height and the modelled water stage (Eq. 3)
451 of the trees according to their geomorphic position. We analysed the 2008 event because
452 it provided a larger population of scars and lower errors in discharge estimation, and we
453 obtained mean height differences for each geomorphic form: 0.07 m in-channel (1 tree),

454 0.49 m in gravel bars (1 tree), 0.53 m in terrace 1 (3 trees), 0.26 m in terrace 2 (2 trees),
455 0.44 m in secondary channels of the cone (2 trees), 0.17 m in middle deposits of the
456 cone (5 trees), 0.01 m in artificial levees (1 tree) and 0.63 m in right-side slopes (3
457 trees). The lowest variability in scar heights was located inside the channel and in an
458 artificial levee, but these geomorphic forms only contain one tree. If we consider
459 geomorphic positions with more than a single tree, the lowest variabilities corresponded
460 to trees located on terrace 2 or middle deposits of the cone, which are intermediate
461 energy positions. Highest variabilities occurred in the right-side slope.

462 **5. Discussion**

463

464 *5.1. Discussion on the results and new contributions*

465 This paper presents a detailed palaeoflood multidisciplinary approach in an
466 ungauged mountain stream (Portainé, Spanish Pyrenees) based on the four-topic
467 correlation of geomorphology, dendrogeomorphology, flood discharge and flow
468 hydrodynamics.

469 Detailed geomorphological mapping from total station data contributed to a good
470 correlation between damaged trees and geomorphic forms. The formation of different
471 dendrogeomorphological evidence (FDE) depends on the geomorphic position of the
472 trees. Usually the most energetic disturbances are found in trees located in energetic
473 geomorphic forms (Ruiz-Villanueva et al., 2010). Nonetheless, in our study area, most
474 FDE locate in geomorphic positions of intermediate energy. This is explained by (i) the
475 scarcity of trees on the riverbed (most energetic positions) because high discharge
476 events with significant stream power, pull and transport them, and (ii) the scarcity of
477 external disturbances on slopes (less energetic positions) due to the flow not having
478 enough energy to produce damages on those trees farther from the active channel, or
479 even the flow not reaching those areas.

480 The estimation of peak discharges was possible thanks to the detailed cross sections
481 measured in the field. LiDAR data was not accurate enough for the application of
482 hydraulic models due to the dense vegetation and therefore, insufficient and inaccurate
483 ground points. The methodology for palaeodischarge calculation for 2008 and 2010 was
484 adapted from Ballesteros-Cánovas et al. (2010). Comparing the two reconstructed years
485 it seems that their magnitudes were similar; but the 2008 event has been reported as the
486 most severe one (IGC, 2013). This discrepancy could be explained by the difference in
487 the real pre-event topography, as we used the same topographic data for hydraulic
488 modelling in both cases, which includes boulder accumulation in the alluvial cone
489 during extraordinary events. Therefore, the pre-2008 topography would be lower than
490 the pre-2010 one, and the water stage for scar formation higher, leading to an
491 underestimation of the 2008 event.

492 Overbank critical discharges calculated at the apex of the alluvial cone indicate the
493 minimum discharge for the overflow of the left bank. However, this minimum discharge
494 not necessarily involves water flowing all along the cone, as it may return to the
495 functional channel. In order to validate the estimations, we checked for the discharge
496 that, apart from overflowing the bank, showed water continuity along the distributary

497 channels of the cone. Therefore, two overbank flow discharges were estimated: partial
498 overbank critical discharge associated to levee breach and formation of crevasse splays
499 ($43 \text{ m}^3\text{s}^{-1}$), and total overbank critical discharge and cone flooding ($58 \text{ m}^3\text{s}^{-1}$).

500 Peak discharges for different return periods were calculated for the Portainé basin by
501 other authors using hydrologic modelling (de las Heras, 2016). Comparing those results
502 with palaeodischarge values obtained in this study for 2008 ($316 \text{ m}^3\text{s}^{-1}$) and 2010 (314
503 m^3s^{-1}), both events would correspond to return periods higher than 500 years. This
504 makes no sense, as torrential or debris events are recorded almost every year since 2006.
505 Moreover, the obtained overbank critical discharge in the downstream part of the
506 Portainé stream would correspond to about 500-year return period. This means that (i)
507 the discharges estimated in this study may be overestimated; and (ii) the discharges with
508 different return periods from de las Heras (2016) could be underestimated. In our study,
509 this is due to the high sediment load not considered in the palaeohydrologic and
510 palaeohydraulic analyses. As outlined by Bodoque et al. (2011), the estimated peak
511 discharges are the result of the combination, not only the sum, of water and sediment
512 load. This is very common in steep mountain streams with high torrential activity.

513 Regarding the calculation of the particle size transported for a specific flow, the best
514 approach is the one proposed by Carling et al. (2002) because we adapted it for the
515 study case. The obtained relation of maximum, medium and minimum diameters of
516 boulders is in agreement with the typology of the bedrock, which is composed of highly
517 fractured metapelites. This leads to the formation of boulders with two similar axes and
518 a considerably shorter one. However, results obtained from Carling et al. (2002)
519 correspond to the most common size of deposited boulders (medium size in the study
520 area), as the relation between diameter axes was established for the average of the field
521 measurements. Bagnold (1980) also considers the most common size, so the obtained
522 results are clearly overestimated. All the other authors come up with equations for the
523 intermediate axis estimation of the maximum transported boulder, so the obtained
524 results should be compared with the width of biggest boulders identified in the field
525 (Table 4, boulder number 2). Among these equations, the one proposed by Costa (1983)
526 for coarse material is considered the most suitable in our case. In general, the results
527 obtained for the Portainé alluvial cone using empirical relations (Table 5) are higher
528 than the boulder size measured in the field (Table 4). The causes for this can be that: (i)
529 they are empirical relations calculated for biphasic flows with Newtonian behavior, and
530 some debris flows are uniphase; (ii) equations work with the mobilizable particle size,
531 but boulders of this dimension are not always available to be moved in the river bottom,
532 in part due to the lithology of the source area (even though this does not seem to occur
533 in the study case), or because they could be fragmented during the transport; (iii) stream
534 power values are averaged for the channel or margins (using a 1D hydraulic model that
535 only distinguishes three zones in each cross section), but they could not be
536 representative of some specific positions; and (iv) the model works with Newtonian
537 flows of clean water so the calculated discharges may be overestimated due to the
538 higher viscosity of the more dense real flow (which includes sediment), leading to a real
539 transport capacity of smaller boulders. Considering these limitations, the results
540 obtained by empirical relations are coherent with real torrential processes in the Portainé
541 study area. The equation proposed by Williams (1983) is the exception and does not
542 work for the studied stream.

543 The uncertainty of the peak discharge estimations depends on the reliability of scar
544 heights (Ballesteros-Cánovas et al., 2016). The distribution of scar-flow differences in
545 the study area suggests that trees located on the deposits of the cone and in the terrace
546 are the most suitable ones for palaeoflood reconstruction, whereas those standing in the
547 slopes are the less useful ones.

548 The present study is a new step for palaeoflood reconstruction in ungauged small
549 basins. Even if peak discharges obtained by hydrodynamic modelling may be
550 overestimated because of not considering the sediment load, at least they allow
551 estimating the order of magnitude of past events. Such a multidisciplinary approach
552 could be very useful for basins where detailed dendrogeomorphological studies could
553 not be carried out (few or lack of riverbank trees) or the application of hydrologic-
554 hydraulic models presents great limitations (scarce meteorological data and/or not
555 accurate DEMs).

556 *5.2. Limitations of the data sources*

557 Geomorphic positions of trees could have changed in time, because the assigned
558 present-day landform, element or facet to each tree could not be exactly the same as
559 when the flood occurred and the scar was formed; at least for geomorphic forms close to
560 the river channel and especially for older dendrogeomorphological damages or FDE.
561 This limitation in data sources is very difficult to solve, due to the lack of previous
562 geomorphological maps or detailed aerial photographs.

563 Scars were used as palaeostage indicators (PSI), considering that their maximum
564 height indicates the minimum water table of the flow and is close to high water marks
565 (HWM). Nevertheless, this approximation involves some uncertainties and error
566 sources: (i) PSI can be higher than HWM if the scar was formed by material
567 accumulated upstream from a tree, leading to a discharge overestimation (Ballesteros-
568 Cánovas et al., 2010); (ii) PSI can be lower than HWM when the scar is partially closed,
569 and therefore, the discharge would be underestimated (Guardiola-Albert et al., 2015);
570 and (iii) PSI can be lower than HWM when the scar has been produced by sediment
571 load in the lower part of the water column (bedload transport, e.g. saltation), and not by
572 the impact of floating load (large wood), so the discharge could be underestimated
573 (Ballesteros et al., 2010). The trial-and-error technique was applied to compare the
574 height of the PSI (height of the scars) and the modelled water stage in each cross section
575 (Yanosky and Jarrett, 2002). Despite the few number of trees, we had multiple scars to
576 simulate the flow of 2008 (18 scars) and 2010 events (6 scars). Moreover, the existing
577 technical reports that describe the 2008 and 2010 events (IGC, 2010a, 2010b),
578 especially upstream, seem to be in accordance with the obtained results about the
579 magnitude of these events.

580 The topographic data presented the following drawbacks: (i) temporal difference
581 between detailed field topography (2014) and airborne LiDAR data (2011); (ii) the use
582 of the same DEM for hydrodynamic modelling of different years; and (iii) low accuracy
583 of LiDAR data in forested or densely vegetated areas. Temporal changes of terrain in
584 the alluvial cone indicates that scars in trees located upstream from this area are more
585 reliable for palaeoflood discharge estimations, but they are scarce. So, main topographic

586 limitations were overcome by acquiring high-accuracy data along multiple cross
587 sections coinciding with the location of the damaged trees.

588 *5.3.Limitations of the methods*

589 Tree-ring analysis is a very useful tool for data acquisition on past flood events
590 (Ballesteros-Cánovas et al., 2015b; Stoffel and Bollschweiler, 2008). However,
591 dendrogeomorphological methodologies present some drawbacks (Díez-Herrero et al.,
592 2013). In our study area, (i) some FDE could correspond to different events occurred in
593 a same year (at least two in 2008 and other two in 2010), and therefore, FDE from a
594 same year could correspond to different intra-annual events; (ii) some scars can be
595 produced by another external factor unrelated to torrential processes, like the impact of
596 a fallen tree during wind gusts or due to human activities. However, in this study, the
597 position, shape, orientation and distribution of the scars were analysed in detail
598 regarding their relation with torrential processes, and the doubtful ones were dismissed.

599 The hydrodynamic modelling was carried out with the HEC-RAS 1D hydraulic
600 model (USACE, 2008) that works with transversal cross sections. The area between
601 them is lineally interpolated and may involve some errors. This was overcome by
602 acquiring detailed topographic data with a total station in the field and, in few cases,
603 introducing additional sections corresponding to the position of trees showing scars
604 from 2008 or 2010 events. A 2D model was not run due to geometric, hydrodynamic
605 and other factors (see section 3.3.). Moreover, other works like Bodoque et al. (2011)
606 have used 1D hydraulic modelling for peak discharge reconstruction at mountain steep-
607 gradient reaches showing the same configuration and characteristics as the Portainé
608 stream, proving its suitability. The small differences in peak discharges obtained from
609 the TIN-based cross sections and the field-based cross sections can be explained by the
610 longitudinal variability of the high sediment load flow and the different number of scars
611 for each case.

612 *5.4.Limitations of the results*

613 Flow hydraulics results were not calibrated with real data, because of the lack of
614 flow gauging stations within the basin. Therefore, the palaeodischarges could not be
615 compared and validated with real records. Nevertheless, the obtained discharges in this
616 study seem reasonable, and their order of magnitude is coherent with the dimensions of
617 the river and the catchment.

618 *5.5.Further research*

619 Future steps that could improve the characterisation of the Portainé stream and the
620 palaeoflood reconstruction are: (i) the integration of the sediment load and transport,
621 which constitute an important factor for the rheology of torrential and debris floods; (ii)
622 2D hydrodynamic modelling, to simulate the limited transversal flows and therefore,
623 secondary discharges along the alluvial cone.

624 Last but not least, the methodology carried out in this study could be applied to
625 other watersheds of similar morphometric and geomorphologic characteristics. The
626 validation of the use of 1D hydraulic models in other small elongated cones in
627 mountainous areas with few source data and relatively few number of trees would

628 corroborate the high potential of such a multidisciplinary analysis for torrential
629 problematic settings.

630 **6. Conclusions**

631 The palaeohydrological approach presented in this study proves that the flow energy
632 obtained from hydrodynamic modelling of past events, determined by the depth,
633 velocity and stream power, shows a positive correlation with most energetic
634 geomorphic forms (riverbed and low alluvial terrace). However, most of the external
635 disturbances are found in trees located in geomorphic positions of intermediate energy
636 (alluvial cone). Trees showing less uncertainty for hydraulic modelling, based on the
637 variability in scar heights, were also located on geomorphic forms formed by
638 intermediate energy processes (high alluvial terrace and deposits of the cone). These
639 findings suggest that the most reliable scarred trees for peak discharge estimations using
640 hydraulic modelling correspond to intermediate flow energy positions.

641 The present work shows the high potential of the combination of techniques for
642 flood assessment in problematic contexts, such as ungauged mountain basins or with
643 scarce hydrological data, densely vegetated areas with poor topographic data, and rivers
644 with few disturbed trees for detailed dendrogeomorphological studies.

645 **Acknowledgements**

646 This work was funded by the CHARMA project (CGL2013-40828-R) of the
647 Spanish Ministry of Economy, Industry and Competitiveness (MINECO), and by the
648 University of Barcelona (UB). The authors want to thank Dr. Mar Tapia for her advice
649 on statistical analysis. Comments from three anonymous reviewers improved the quality
650 of the manuscript.

651 **References**

- 652 Arcement, G.J., Schneider, V.R., 1989. Guide for Selecting Manning's Roughness
653 Coefficients for Natural Channels and Flood Plains, United States Geological
654 Survey Water-Supply Paper 2339.
- 655 Bagnold, R.A., 1980. An empirical correlation of bedload transport rate in flumes and
656 natural rivers. *Proc. R. Soc. London* 372, 453–473. doi:10.1098/rspa.1983.0054
- 657 Baker, V.R., 1987. Paleoflood hydrology and extraordinary flood events. *J. Hydrol.* 96,
658 79-99. doi:10.1016/0022-1694(87)90145-4
- 659 Baker, V.R., 2008. Paleoflood hydrology: Origin, progress, prospects. *Geomorphology*
660 101, 1–13. doi:10.1016/j.geomorph.2008.05.016
- 661 Baker, V.R., Kochel, R.C., Patton, P.C., 1988. *Flood Geomorphology*. John Wiley and
662 Sons, New York, United States. ISBN: 978-0-12-394846-5
- 663 Baker, V.R., Pickup, G., 1987. Flood geomorphology of the Katherine Gorge, Northern
664 Territory, Australia. *Geol. Soc. Am. Bull.* 98, 635-646. doi:10.1130/0016-
665 7606(1987)98<635:FGOTKG>2.0.CO;2
- 666 Ballesteros-Cánovas, J.A., Eguibar, M.Á., Bodoque, J.M., Díez-Herrero, A., Stoffel, M.,
667 Gutiérrez-Pérez, I., 2010. Estimating flash flood discharge in an ungauged
668 mountain catchment with 2D hydraulic models and dendrogeomorphic palaeostage
669 indicators. *Hydrol. Process.* 25, 970–979. doi:10.1002/hyp.7888

670 Ballesteros-Cánovas, J.A., Márquez-Peñaranda, J.F., Sánchez-Silva, M., Díez-Herrero,
671 A., Ruiz-Villanueva, V., Bodoque, J.M., Eguibar, M.Á., Stoffel, M., 2015a. Can
672 tree tilting be used for paleoflood discharge estimations? *J. Hydrol.* 529, 480–489.
673 doi:10.1016/j.jhydrol.2014.10.026

674 Ballesteros-Cánovas, J.A., Stoffel, M., St George, S., Hirschboeck, K., 2015b. A review
675 of flood records from tree rings. *Prog. Phys. Geogr.* 29 (6), 1–23.
676 doi:10.1177/0309133315608758

677 Ballesteros-Cánovas, J.A., Stoffel, M., Spyt, B., Janecka, K., Kaczka, R.J., Lempa, M.,
678 2016. Paleoflood discharge reconstruction in Tatra Mountain streams.
679 *Geomorphology* 272, 92–101. doi:10.1016/j.geomorph.2015.12.004

680 Barredo, J.I., 2007. Major flood disasters in Europe: 1950–2005. *Nat. Hazards* 42, 125–
681 148. doi:10.1007/s11069-006-9065-2

682 Benito, G., Díez-Herrero, A., 2015. Palaeoflood Hydrology: Reconstructing Rare
683 Events and Extreme Flood Discharges, in: Shroder, J.F., Paron, P., Di Baldassarre,
684 G. (Eds.), *Hydro-Meteorological Hazards, Risks, and Disasters*. Elsevier,
685 Amsterdam, The Netherlands, pp. 65–104. ISBN: 978-0-12-394846-5

686 Benito, G., Sopeña, A., Sánchez-Moya, Y., Machado, M.J., Pérez-González, A., 2003.
687 Palaeoflood record of the Tagus River (Central Spain) during the Late Pleistocene
688 and Holocene. *Quat. Sci. Rev.* 22, 1737–1756. doi:10.1016/S0277-3791(03)00133-
689 1

690 Benito, G., Macklin, M.G., Zielhofer, C., Jones, A.F., Machado, M.J., 2015. Holocene
691 flooding and climate change in the Mediterranean. *Catena* 130, 13–33.
692 doi:10.1016/j.catena.2014.11.014

693 Bodoque, J.M., Eguibar, M.Á., Díez-Herrero, A., Gutiérrez-Pérez, I., Ruiz-Villanueva,
694 V., 2011. Can the discharge of a hyperconcentrated flow be estimated from
695 paleoflood evidence? *Water Resour. Res.* 47, 1–14. doi:10.1029/2011WR010380

696 Carling, P.A., Hoffmann, M., Blatter, A.S., 2002. Initial Motion of Boulders in Bedrock
697 Channels, in: House, P.K., Webb, R.H, Baker, V.R., Levish, D.R. (Eds.), *Ancient
698 Floods, Modern Hazards: Principles and Applications of Paleoflood Hydrology*.
699 American Geophysical Union, Washington, DC, United States, pp. 147–160.
700 doi:10.1029/WS005p0147

701 Chanson, H., 2004. *Environmental Hydraulics of Open Channel Flows*. Elsevier,
702 Oxford, United Kingdom. ISBN: 978-0-7506-6165-2

703 Chow, V. T., 1959. *Open Channel Hydraulics*. McGraw-Hill, New York, United States.
704 ISBN: 07-010776-9

705 Church, M., Biron, P., Roy, A., 2012. *Gravel Bed Rivers: Processes, Tools,
706 Environments*. Wiley-Blackwell, Chichester, United Kingdom. ISBN: 978-0-470-
707 68890-8

708 Cook, E.R., Kairiukstis, L.A., 1990. *Methods of Dendrochronology. Applications in the
709 Environmental Sciences*. Springer, Dordrecht, Netherlands. doi:10.1007/978-94-
710 015-7879-0

711 Costa, J.E., 1983. Paleohydraulic reconstruction of flash-flood peaks from boulder
712 deposits in the Colorado Front Range. *Geol. Soc. Am. Bull.* 94, 986–1004.
713 doi:10.1130/0016-7606(1983)94<986:profpf>2.0.co;2

714 De las Heras, Á., 2016. Modificación de la respuesta hidrológica en avenidas
715 torrenciales ante los cambios de usos del suelo en una cuenca de montaña

716 (Portainé, Pirineo Ilerdano). Archivo Digital UPM, Spain, available at:
717 <http://oa.upm.es/45430/>

718 Díez-Herrero, A., 2015. Buscando riadas en los árboles: Dendrogeomorfología.
719 Enseñanza las Ciencias la Tierra 23 (3), 272–285. ISSN: 1132-9157

720 Díez-Herrero, A., Ballesteros-Cánovas, J.A., Bodoque, J.M., Ruiz-Villanueva, V., 2013.
721 A new methodological protocol for the use of dendrogeomorphological data in
722 flood risk analysis. *Hydrol. Res.* 44.2, 234–247. doi:10.2166/Nh.2012.154

723 ESRI, 2014. ArcGIS 10.2.2 Desktop. Environmental Systems Research Institute,
724 Redlands, United States.

725 Ferguson, R.I., 2005. Estimating critical stream power for bedload transport calculations
726 in gravel-bed rivers. *Geomorphology* 70, 33–41.
727 doi:10.1016/j.geomorph.2005.03.009

728 Furdada, G., Génova, M., Guinau, M., Victoriano, A., Khazaradze, G., Díez-Herrero,
729 A., Calvet, J., 2016. Las avenidas torrenciales de los barrancos de Portainé,
730 Reguerals y Ramiosa (Pirineo Central): evolución de las cuencas y dinámica
731 torrencial, in: Durán Valseo, J.J., Montes Santiago, M., Robador Moreno, A.,
732 Salazar Rincón, Á. (Eds.), *Comprendiendo El Relieve: Del Pasado Al Futuro*.
733 Instituto Geológico y Minero de España, Madrid, Spain, pp. 315–322. ISBN:978-
734 84-9138-013-9

735 García-Oteyza, J., Génova, M., Calvet, J., Furdada, G., Guinau, M., Díez-Herrero, A.,
736 2015. Datación de avenidas torrenciales y flujos de derrubios mediante
737 metodologías dendrogeomorfológicas (barranco de Portainé, Lleida, España).
738 *Ecosistemas* 24, 43–50. doi:10.7818/ECOS.2015.24-2.07

739 Gaume, E., Bain, V., Bernardara, P., Newinger, O., Barbuc, M., Bateman, A.,
740 Blaškovičová, L., Blöschl, G., Borga, M., Dumitrescu, A., Daliakopoulos, I.,
741 Garcia, J., Irimescu, A., Kohnova, S., Koutroulis, A., Marchi, L., Matreata, S.,
742 Medina, V., Preciso, E., Sempere-Torres, D., Stancalie, G., Szolgay, J., Tsanis, I.,
743 Velasco, D., Viglione, A., 2009. A compilation of data on European flash floods. *J.*
744 *Hydrol.* 367, 70–78. doi:10.1016/j.jhydrol.2008.12.028

745 Génova, M., Máyer, P., Ballesteros-Cánovas, J.C., Rubiales, J.M., Saz, M.A., Díez-
746 Herrero, A., 2015. Multidisciplinary study of flash floods in the Caldera de
747 Taburiente National Park (Canary Islands, Spain). *Catena* 131, 22–34.
748 doi:10.1016/j.catena.2015.03.007

749 Gob, F., Petit, F., Bravard, J.P., Ozer, A., Gob, A., 2003. Lichenometric application to
750 historical and subrecent dynamics and sediment transport of a Corsican stream
751 (Figarella River - France). *Quat. Sci. Rev.* 22, 2111–2124. doi:10.1016/S0277-
752 3791(03)00142-2

753 Gottesfeld, A.S., 1996. British Columbia flood scars: maximum flood stage indicators.
754 *Geomorphology* 14, 319-325. doi:10.1016/0169-555X(95)00045-7

755 Grissino-Mayer, H. D., 2001. Evaluating crossdating accuracy: a manual and tutorial for
756 the computer program COFECHA. *Tree-Ring Research* 57 (2), 205–221.

757 Guardiola-Albert, A., Ballesteros-Cánovas, J.A., Stoffel, M., Díez-Herrero, A., 2015.
758 How to improve dendrogeomorphic sampling: variogram analyses of wood density
759 using XRCT. *Tree-Ring Research* 71 (1), 25-36. doi:10.3959/1536-1098-71.1.25

760 IGC, 2010a. Estudi de la torrentada de la nit del dia 11 al 12 de setembre de 2008 al
761 barranc de Portainé (Pallars Sobirà), AP-019/10. Institut Geològic de Catalunya,
762 Barcelona, Spain.

- 763 IGC, 2010b. Nota de la visita al barranc de Portainé (Pallars Sobirà) arran del episodi de
764 pluges dels dies 22 i 23 de juliol de 2010, AP-046/10. Institut Geològic de
765 Catalunya, Barcelona, Spain.
- 766 IGC, 2013. Avaluació de la dinàmica torrencial del torrent de Portainé, AP-035/13.
767 Institut Geològic de Catalunya, Barcelona, Spain.
- 768 Jacob, N., 2003. Les vallées en gorges de la Cévenne vivaraise: montagne de sable et
769 château d'eau. PhD dissertation, Université Paris-Sorbonne, France.
- 770 Keim, R.F., Skaugset, A.E., Bateman, D.S., 1999. Digital terrain modeling of small
771 stream channels with a total-station theodolite. *Adv. Water Resour.* 23, 41-48. doi:
772 10.1016/S0309-1708(99)00007-X
- 773 Khazaradze, G., Guinau, M., Calvet, J., Furdada, G., Victoriano, A., Génova, M., 2016.
774 Debris flow cartography using differential GNSS and Theodolite measurements.
775 *Geophysical Research Abstracts* 18, 9696. doi: 10.13140/RG.2.2.27245.59363
- 776 Kochel, R.C., Baker, V.R., 1982. Paleoflood Hydrology. *Science* 215, 353–361. doi:
777 10.1126/science.215.4531.353
- 778 Kundzewicz, Z., Stoffel, M., Kaczka, R., Wyzga, B., Niedźwiedz, T., Pińskwar, I.,
779 Ruiz-Villanueva, V., Łupikasza, E., Czajka, B., Ballesteros-Cánovas, J.,
780 Małarzewski, Ł., Choryński, A., Janecka, A., Mikuś, P., 2014. Floods at the
781 northern foothills of the Tatra Mountains-a Polish–Swiss research project. *Acta*
782 *Geophys.* 62 (3), 620–641. doi:10.2478/s11600-013-0192-3
- 783 Lang, M., Fernandez-Bono, J.F., Recking, A., Naulet, R., Grau-Gimeno, P., 2004.
784 Methodological guide for paleoflood and historical peak discharge estimation, in:
785 Benito, G., Thorndycraft, V.R. (Eds.), *Systematic, Palaeoflood and Historical Data*
786 *for the Improvement of Flood Risk Estimation: Methodological Guidelines*. CSIC,
787 Madrid, Spain, pp. 43-53. ISBN:84-921958-3-5
- 788 Luis-Fonseca, R., Raïmat, C., Hürlimann, M., Abancó, C., Moya, J., Fernández, J.,
789 2011. Debris-flow protection in recurrent areas of the Pyrenees. Experience of the
790 VX systems from output results collected in the pioneer monitoring station in
791 Spain, in: *5th International Conference on Debris-Flow Hazards Mitigation*, Padua,
792 Italy, pp. 1063–1071.
- 793 Malik, I., Matyja, M., 2008. Bank erosion history of a mountain stream determined by
794 means of anatomical changes in exposed tree roots over the last 100 years (Bila
795 Opava River–Czech Republic). *Geomorphology* 98, 126-142. doi:
796 10.1016/j.geomorph.2007.02.030
- 797 Meteocat, 2008. *Atlas Climàtic de Catalunya 1961-1990*. Servei Meteorològic de
798 Catalunya, Barcelona, Spain.
- 799 Nicholas, A.P., Walling, D.E., 1997. Modelling flood hydraulics and overbank
800 deposition on river floodplains. *Earth Surf. Process. Landforms* 22, 59–77.
801 doi:10.1002/(SICI)1096-9837(199701)22:1<59::AID-ESP652>3.0.CO;2-R
- 802 O'Connor, J.E., Webb, R.H., 1988. Hydraulic modelling for paleoflood analysis, in:
803 Baker, V.C., Kochel, R.C., Patton, P.C. (Eds.), *Flood Geomorphology*. John Wiley
804 & Sons, New York, United States, pp. 393–402. ISBN:978-0-471-62558-2
- 805 Ortega, J.A., Garzón, G., 1997. Inundaciones históricas en el río Guadiana: sus
806 implicaciones climáticas, in: Rodríguez, J. (Ed.), *Cuaternario Ibérico*, AEQUA,
807 Huelva, Spain, pp. 365–367.
- 808 Palau, R.M., Hürlimann, M., Pinyol, J., Moya, J., Victoriano, A., Génova, M., Puig-
809 Polo, C., 2017. Recent debris flows in the Portainé catchment (Eastern Pyrenees,

Spain): analysis of monitoring and field data focussing on the 2015 event. Landslides 14, 1161-1170. doi:10.1007/s10346-017-0832-9

Portilla, M., Chevalier, G., Hürlimann, M., 2010. Description and analysis of the debris flows occurred during 2008 in the Eastern Pyrenees. *Nat. Hazards Earth Syst. Sci.* 10, 1635–1645. doi:10.5194/nhess-10-1635-2010

RinnTech., 2003. TSAP-Win Software for tree-ring measurement, analysis and presentation Product Information, v. 0.53. RinnTech, Heidelberg, Germany, 2 pp.

Ruiz-Villanueva, V., Díez-Herrero, A., Stoffel, M., Bollschweiler, M., Bodoque, J.M., Ballesteros, J.A., 2010. Dendrogeomorphic analysis of flash floods in a small ungauged mountain catchment (Central Spain). *Geomorphology* 118, 383–392. doi:10.1016/j.geomorph.2010.02.006

Sánchez-Moya, Y., Sopeña, A., 2015. Aprendiendo a leer en las estratificaciones cruzadas. *Enseñanza las Ciencias la Tierra* 23 (2), 148–159. ISSN: 1132-9157

Sigafoos, R.S., 1964. Botanical evidence of floods and flood-plain deposition. United States Geological Survey Professional Paper 485-A.

Stoffel, M., Bollschweiler, M., 2008. Tree-ring analysis in natural hazards research - an overview. *Nat. Hazards Earth Syst. Sci.* 8, 187–202. doi:10.5194/nhess-8-187-2008

Stoffel, M., Corona, C., 2014. Dendroecological dating of geomorphic disturbance in trees. *Tree-Ring Research*, 70 (1), 3-20. doi:10.3959/1536-1098-70.1.3

Tarolli, P., 2014. High-resolution topography for understanding Earth surface processes: Opportunities and challenges. *Geomorphology* 216, 295–312. doi:10.1016/j.geomorph.2014.03.008

Terrasolid, 2016. TerraScan User's Guide. Terrasolid Ltd., Helsinki, Finland, 592 pp.

USACE, 2008. HEC-RAS River Analysis System Users's Manual, v. 4.0. Hydrologic Engineering Center, Washington, DC, United States, 747 pp.

USACE, 2012. HEC-GeoRAS GIS Tools for Support of HEC-RAS using ArcGIS 10 User's Manual, v. 10. Hydrologic Engineering Center, Washington, DC, United States, 242 pp.

Victoriano, A., Guinau, M., Furdada, G., Calvet, J., Cabré, M., Moysset, M., 2016. Aplicación de datos LiDAR en el estudio de la dinámica torrencial y evolución de los barrancos de Portainé y Reguerals (Pirineos Centrales), in: Durán Valsero, J.J., Montes Santiago, M., Robador Moreno, A., Salazar Rincón, Á. (Eds.), *Comprendiendo El Relieve: Del Pasado Al Futuro*. Instituto Geológico y Minero de España, Madrid, pp. 447–455. ISBN:978-84-9138-013-9

Webb, R.H., Jarrett, R.D., 2002. One-dimensional estimation techniques for discharges of paleofloods and historical floods, in: House, P.K., Webb, R.H., Baker, V.R., Levish, D.R. (Eds.), *Ancient Floods, Modern Hazards: Principles and Applications of Paleoflood Hydrology*. American Geophysical Union, Washington, DC, pp. 111–125. doi:10.1029/WS005p0111

Williams, G.P., 1983. Paleohydrological methods and some examples from Swedish fluvial environments. *Geogr. Ann.* 65, 227–243. doi:10.2307/520588

Yanosky, T.M., Jarrett, R.D., 2002. Dendrochronologic evidence for the frequency and magnitude of paleofloods, in: House P.K, Webb, R.H., Baker, V.R., Levish, D.R. (Eds), *Ancient floods, Modern hazards: Principles and Applications of Paleoflood Hydrology*. American Geophysical Union, Washington, DC, pp. 77-89. doi:10.1029/WS005p0077

856 Zielonka, T., Holeksa, J., Ciapala, S., 2008. A reconstruction of flood events using
857 scarred trees in the Tatra Mountains, Poland. *Dendrochronologia* 26, 173-183.
858 doi:10.1016/j.dendro.2008.06.003

Highlights

- Geomorphology, dendrochronology, flood discharges and flow hydraulics are related.
- Palaeofloods were reconstructed using a 1D hydraulic model and dendro-evidences.
- Dendro-evidences were related to the in-situ hydraulic parameters.
- Most damaged trees locate in geomorphic positions of intermediate flow energy.

Table 1. Geomorphic position of the trees analyzed and dated by dendrochronological techniques and the number of trees with external scars used for hydrodynamic modelling of 2008 and 2010 events.

Geomorphic form		Trees with FDE	Scarred trees
Riverbed	In-channel	1	1
	Gravel bar	1	1
Alluvial terraces	Terrace 1	4	3
	Terrace 2	5	4
Levees	Natural levee	0	0
	Artificial levee	5	1
Alluvial cone	Main channel	3	0
	Secondary channel	3	2
	Upper deposits	14	1
	Middle deposits	8	6
	Lower deposits	5	2
Slope	Left-side	4	0
	Right-side	4	3

Table 2. Estimation of flood peak discharges using hydraulic modelling based on scars as dendrogeomorphological palaeostage indicators.

Year	Geometric data source	Peak discharge, Q_p ($m^3 s^{-1}$)	Absolute error, σ (m)	Mean squared error, MSE (m)	Variance (m)
2008	TIN	300	0.35	0.23	0.11
	Total station	321	0.21	0.08	0.04
2010	TIN	314	0.7	0.35	0.04
	Total station	-	-	-	-

Table3

[Click here to download Table: Table3.docx](#)**Table 3.** Hydraulic parameters calculated for the specific location of the trees.

Tree			Hydraulic parameters			
Cross section	Bank location	Elevation	Scar date	Water depth (m)	Velocity (ms ⁻¹)	Unit stream power (Wm ⁻²)
M-M'	Right	1029.42	2008	2.17	12.18	4542.02
K-K'	Channel	1019.13	2008	1.32	15.07	3291.31
Kb-Kb'	Channel	1015.45	2008	1.75	14.52	6403.48
Kc-Kc'	Right	1015.24	2008	0.96	6.15	1775.85
Kd-Kd'	Channel	1013.60	2008	1.43	14.02	5338.19
Ke-Ke'	Channel	1012.49	2008	1.21	13.55	3541.88
P-P'	Left	1008.98	2008	1.65	5.15	1899.26
O-O'	Channel	1007.51	2008	1.88	14.98	7375.25
O-O'	Left	1007.98	2010	1.48	6.02	1826.440
O-O'	Left	1007.98	2010	1.48	6.02	1826.440
Nb-Nb'	Right	1007.11	2008	1.22	4.37	362.72
Y-Y'	Left	995.25	2008	0.27	4.81	1365.61
Xb-Xb'	Left	993.14	2008	0.55	4.35	1294.98
Uc-Uc'	Left	985.80	2010	0.75	12.12	5476.54
Jb-Jb'	Left	978.70	2010	1.10	11.02	915.50
D-D'	Left	977.53	2008	1.12	9.08	592.94
F-F'	Left	976.75	2008	0.70	8.13	886.59
F-F'	Left	976.21	2008	1.24	8.13	886.59
C-C'	Left	975.75	2008	1.32	7.75	539.47
C-C'	Left	975.51	2008	1.56	7.75	539.47
G-G'	Left	975.19	2008	0.30	8.74	753.42
G-G'	Left	974.88	2008	0.61	8.74	753.42
A-A'	Left	973.75	2010	0.73	6.91	336.96
A-A'	Left	973.18	2010	1.30	6.91	336.96

Table 4. Field measurements and relationships among the length (L), width (B) and height (H) of boulders accumulated in the alluvial cone.

Boulder number	Relative size	Length (m)	Width (m)	Height (m)	B/L ratio	H/L ratio
1	Big	0.67	0.48	0.3	0.72	0.45
2	Very big	1.52	0.88	0.92	0.58	0.61
3	Big	0.54	0.32	0.15	0.59	0.28
4	Medium	0.26	0.17	0.05	0.65	0.19
5	Medium	0.27	0.13	0.08	0.48	0.30
6	Small	0.17	0.15	0.08	0.88	0.47
7	Small	0.15	0.15	0.05	1.00	0.33
8	Very small	0.09	0.07	0.06	0.78	0.67
9	Medium	0.21	0.18	0.08	0.86	0.38
10	Medium	0.21	0.17	0.13	0.81	0.62
Average	Medium	0.29	0.21	0.12	0.74	0.43

Table 5. Estimation of the mobilized particle size, obtained from equations proposed by different authors. Costa, Williams, Jacob and Gob et al.: intermediate axis of maximum boulders; Bagnold: intermediate axis of mode size (medium) boulders; Carling et al: maximum axis of average size (medium) boulders.

Author	Equation	Numerical constants	Particle diameter (m)
Costa (1983)	Eq. 5	$a=0.09$ $b=1.686$	2.62
Costa (1983) for coarse material	Eq. 5	$a=0.03$ $b=1.686$	1.28
Williams (1983)	Eq. 5	$a=0.079$ $b=1.27$	6.24
Jacob (2003)	Eq. 5	$a=0.025$ $b=1.647$	1.70
Gob et al. (2003)	Eq. 5	$a=0.0253$ $b=1.62$	1.91
Bagnold (1980), adapted by Ferguson (2005)	Eq. 6	$c_1=2860.5$ $c_2=12$	1.63
Carling et al. (2002)	Eq. 7	$C_d=0.95$ $L-H-B$ (field)	0.27

Figure1
[Click here to download high resolution image](#)

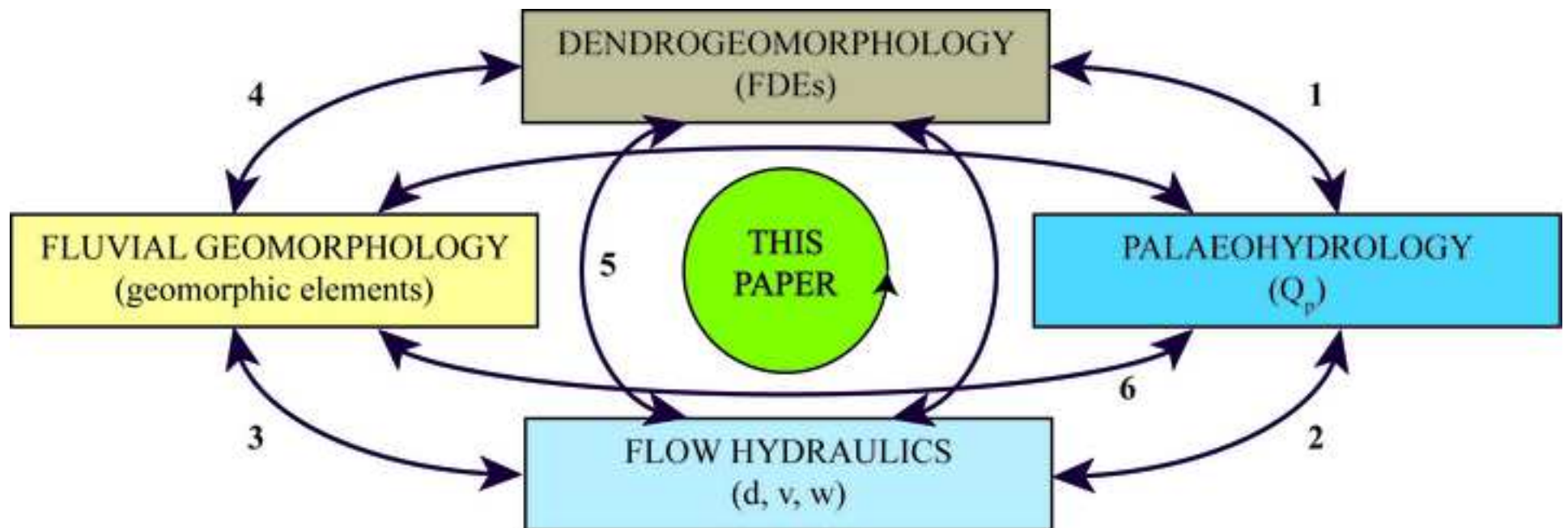


Figure2

[Click here to download high resolution image](#)

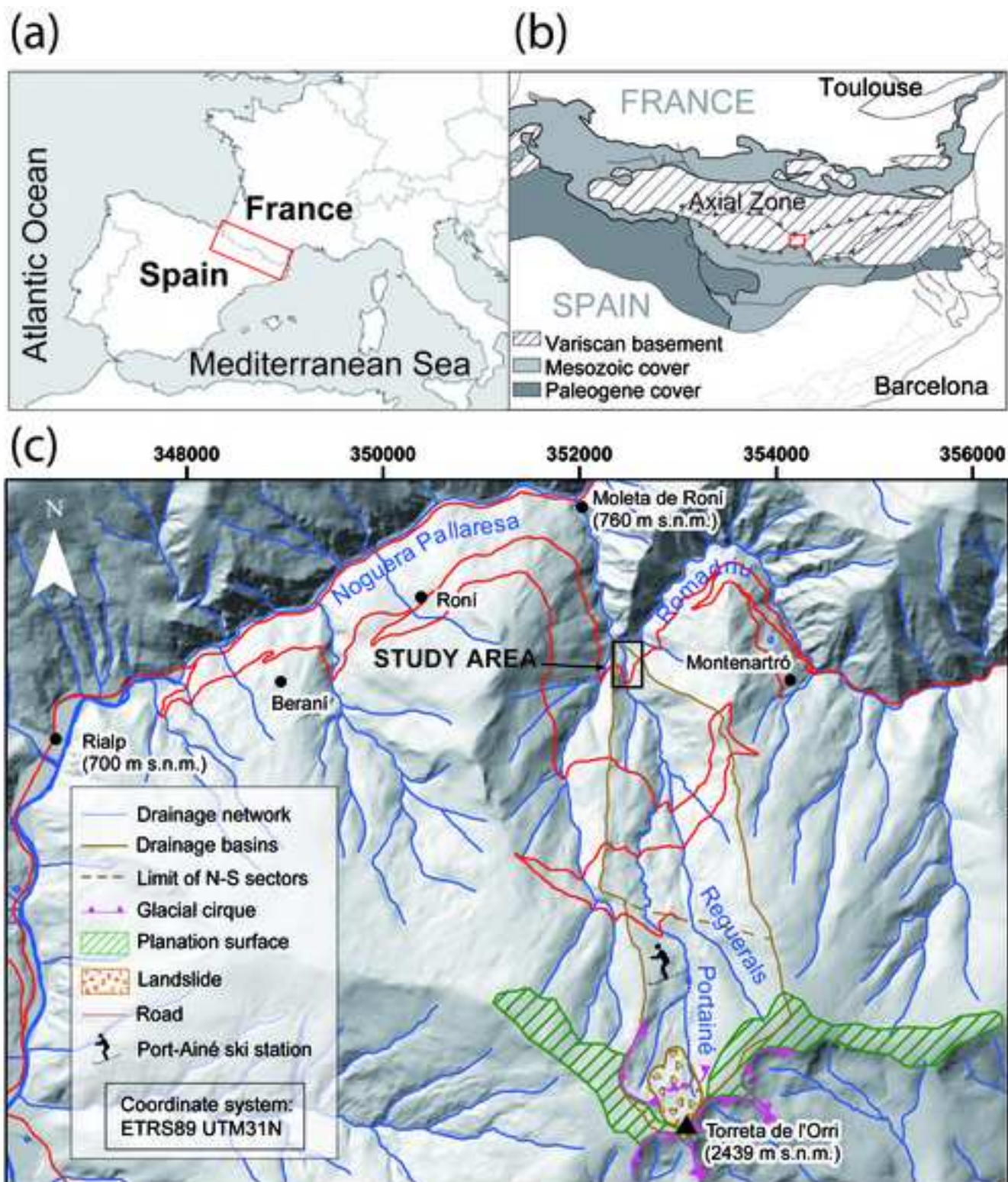


Figure3
[Click here to download high resolution image](#)

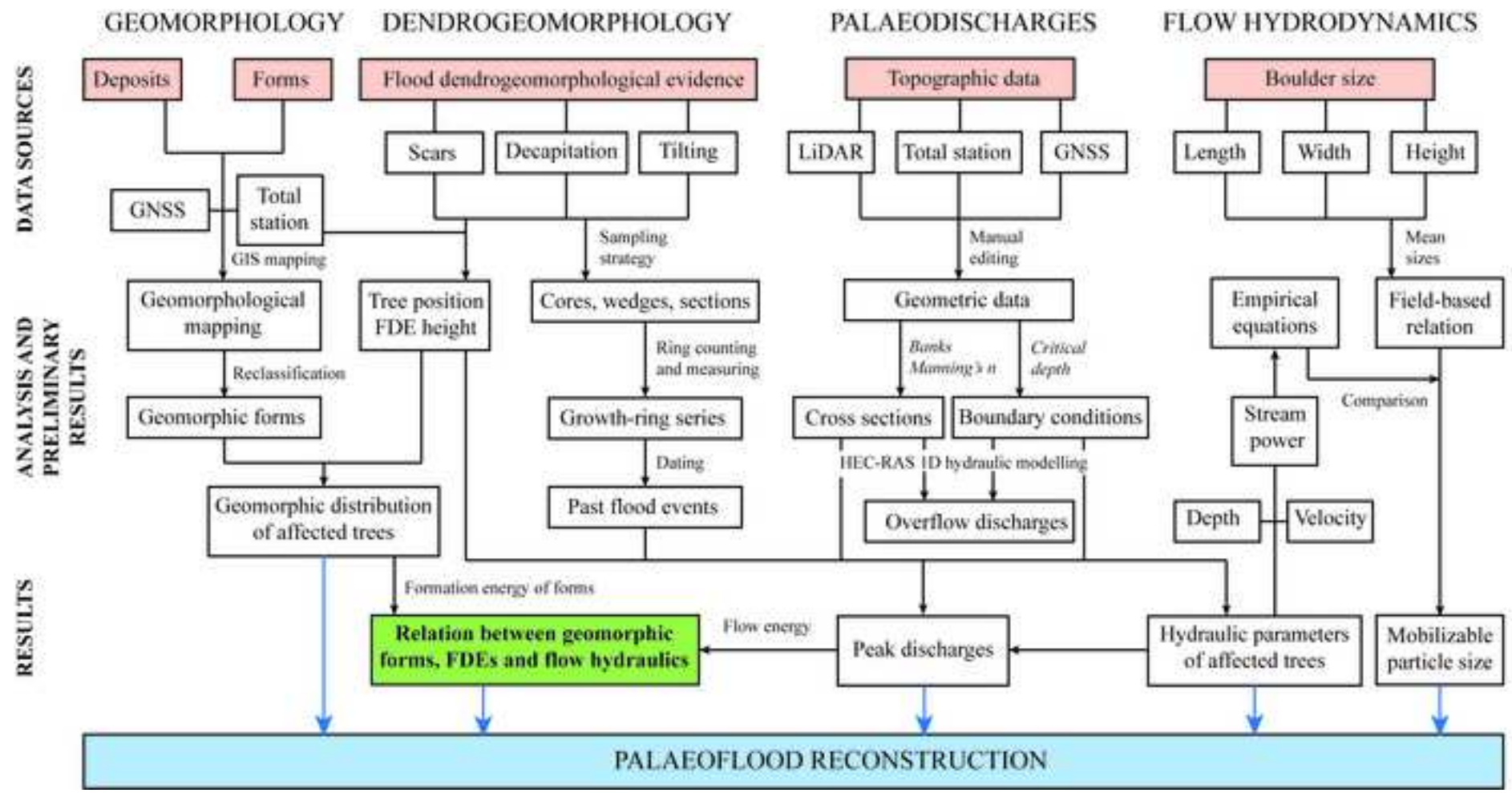


Figure4
[Click here to download high resolution image](#)



(a)



(b)



(c)

Figure 5
[Click here to download high resolution image](#)

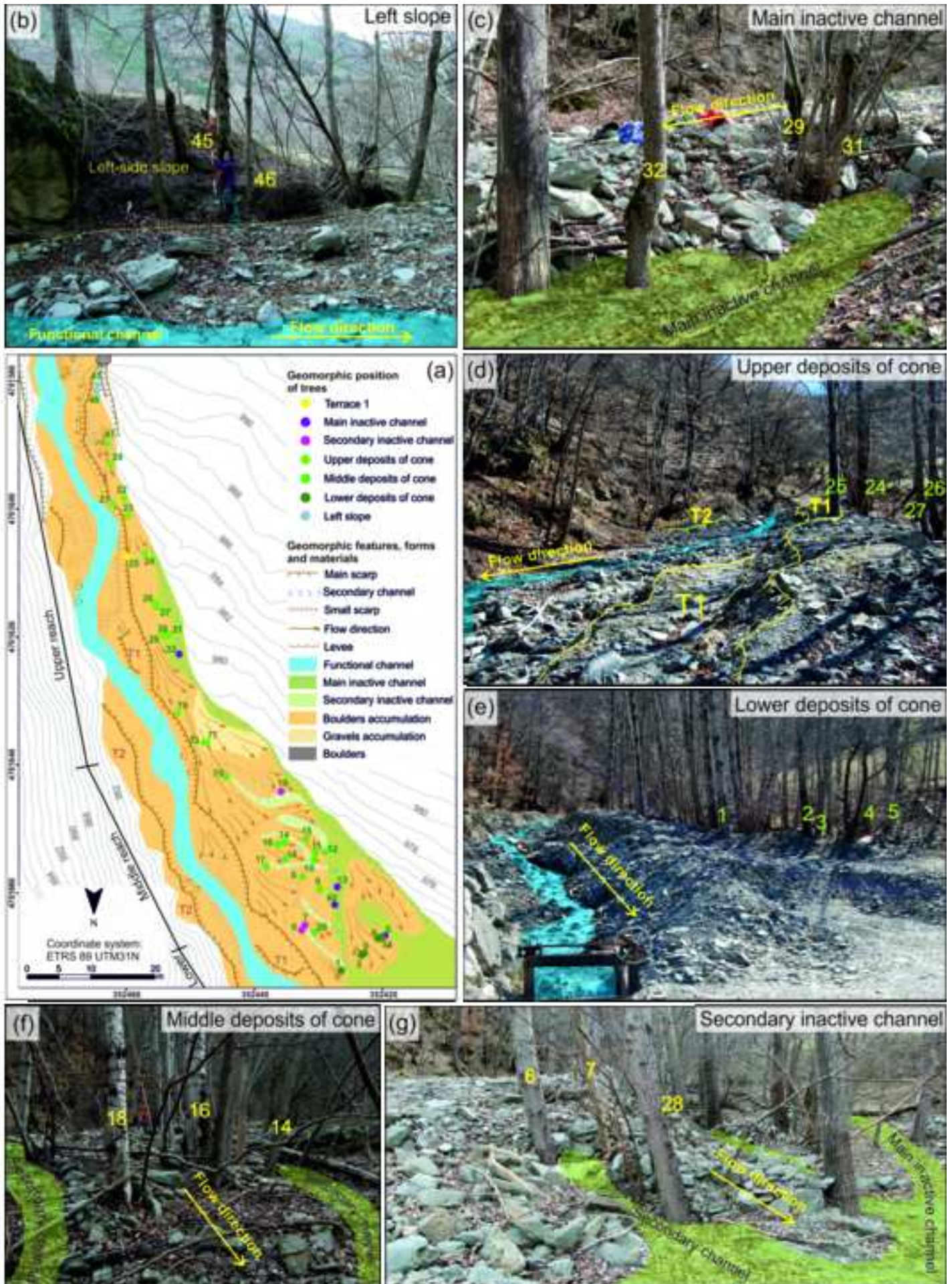


Figure6

[Click here to download high resolution image](#)

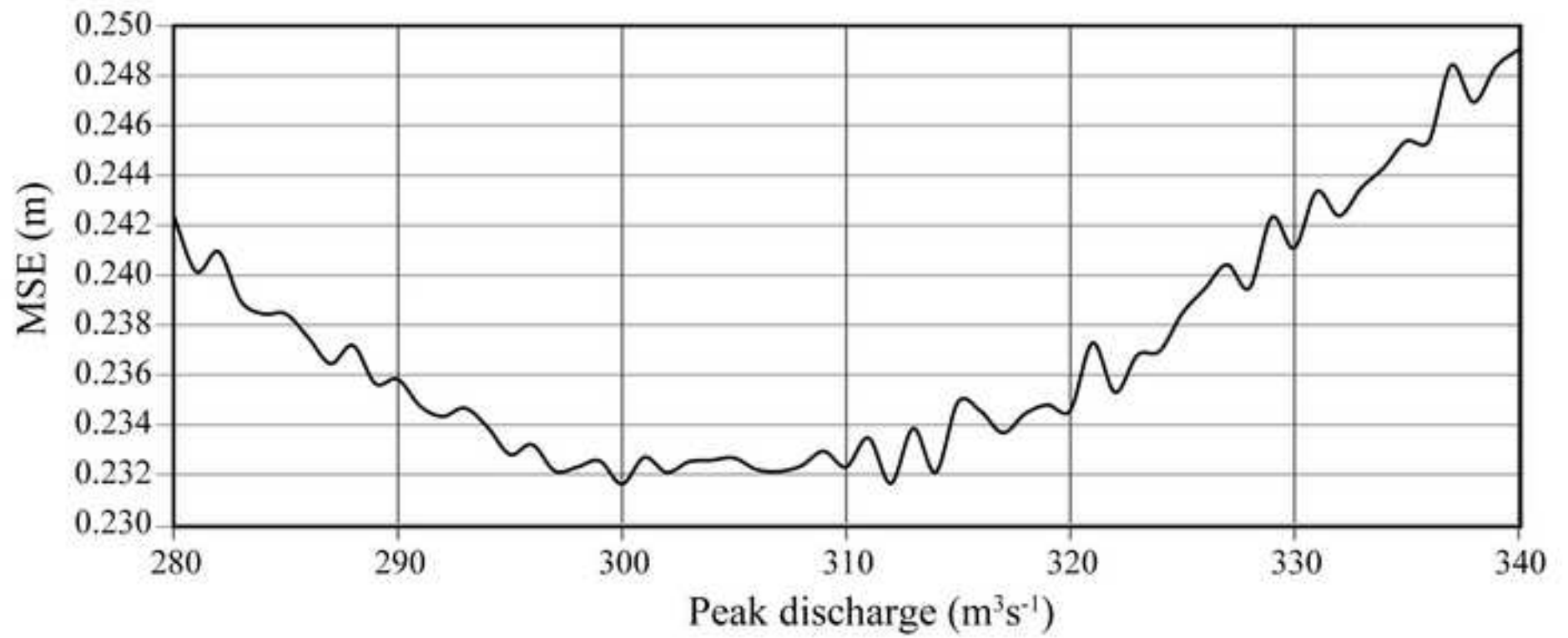


Figure7
[Click here to download high resolution image](#)

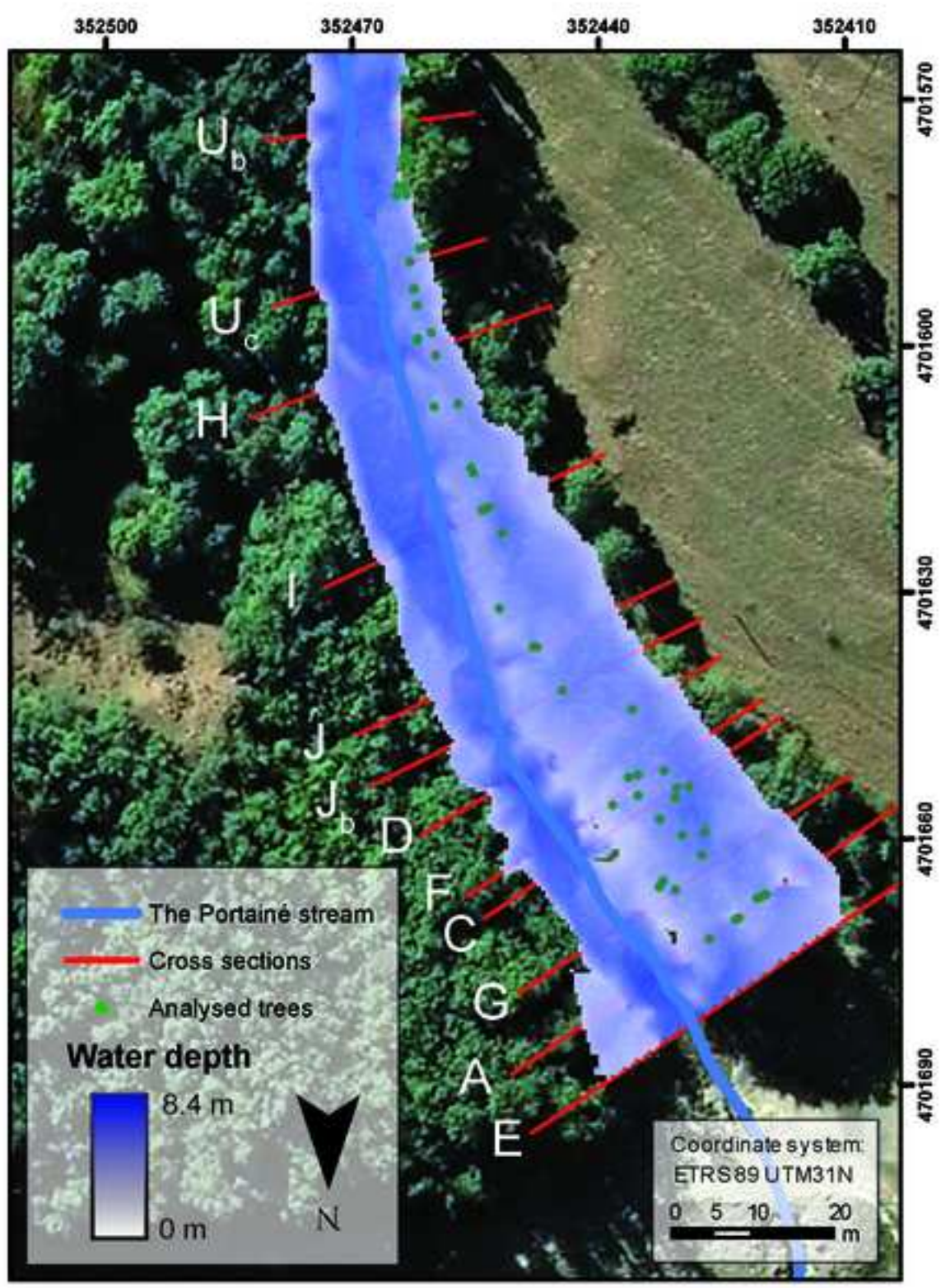


Figure8

[Click here to download high resolution image](#)

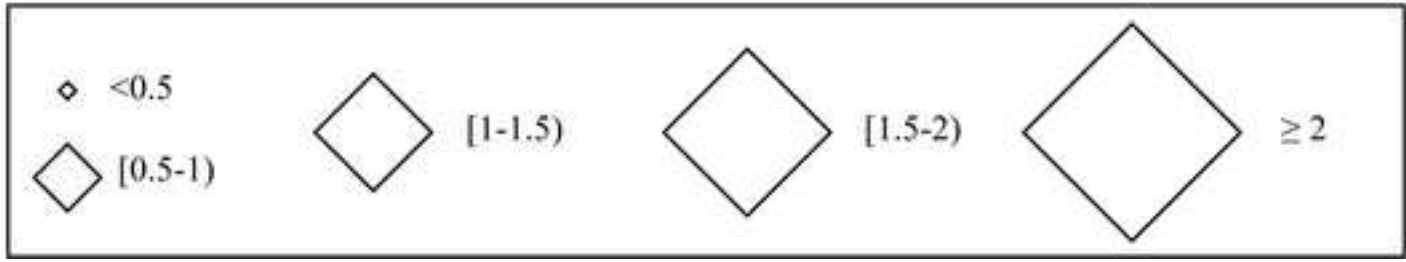
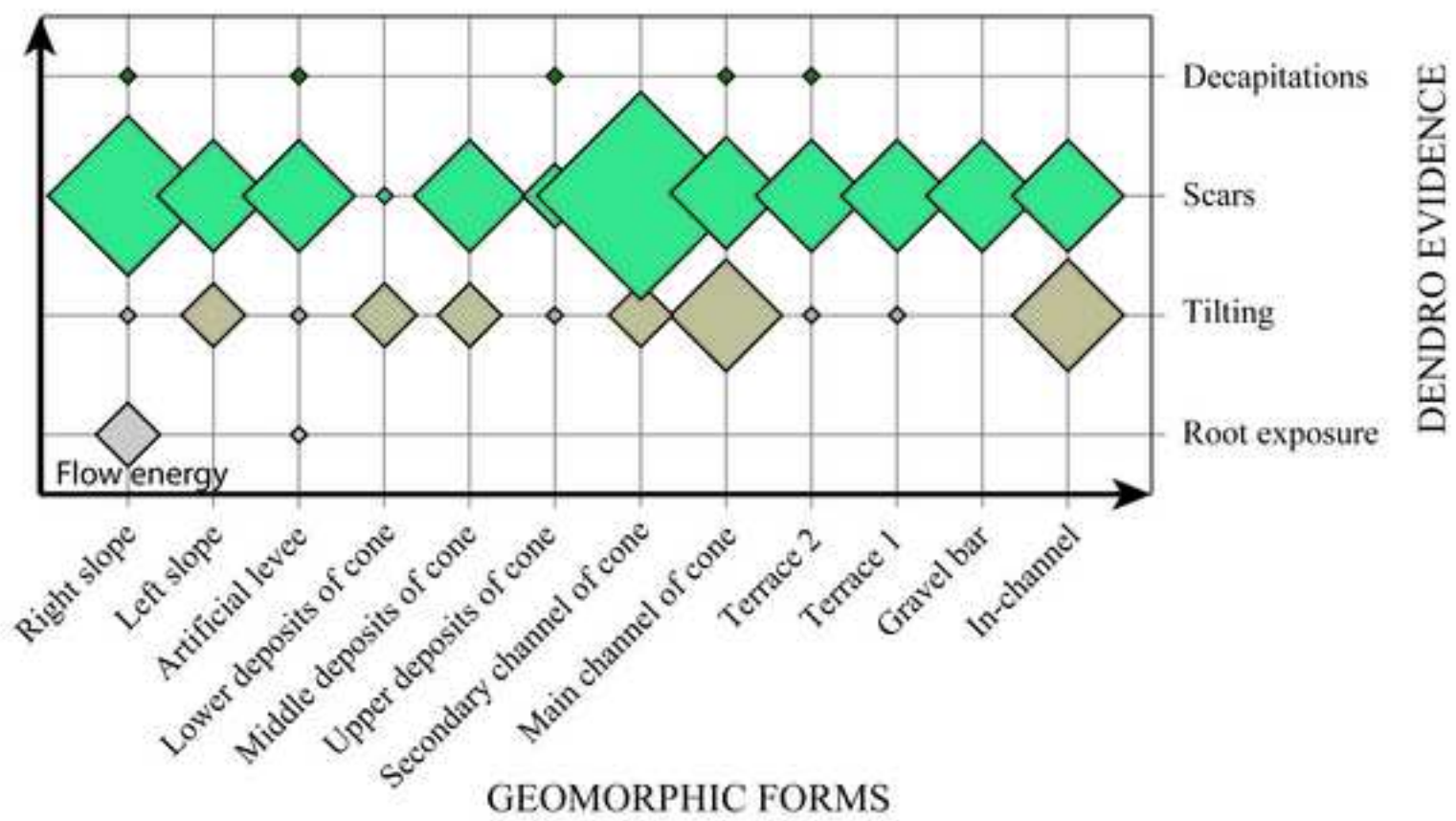


Figure9

[Click here to download high resolution image](#)

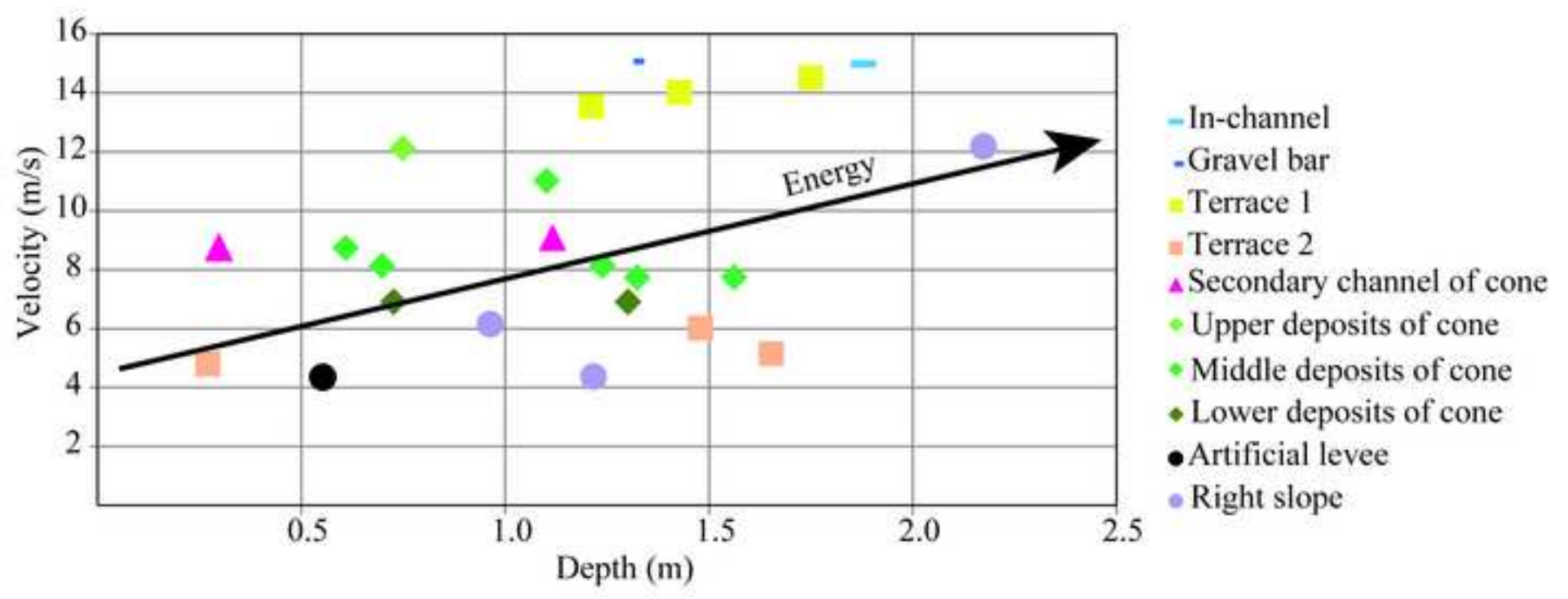


Figure 1. Conceptual diagram of the disciplines and methods combined in the present study. Numbers indicate some of the groups of existing studies relating different research topics: 1, Dendrogeomorphology vs Palaeohydrology (see reviews from Ballesteros-Cánovas et al., 2015b, and Benito and Díez-Herrero, 2015); 2, Palaeohydrology vs Flow Hydraulics (Bagnold, 1980; Chanson, 2004; Chow, 1959; Costa, 1983; Ferguson, 2005); 3, Flow Hydraulics vs Fluvial Geomorphology (Nicholas and Walling, 1997; Ortega and Garzón, 1997; Sánchez-Moya and Sopena, 2015); 4, Fluvial Geomorphology vs Dendrogeomorphology (Ballesteros-Cánovas et al., 2016; Ruiz-Villanueva et al., 2010); 5, Dendrogeomorphology vs Flow Hydraulics (Ballesteros-Cánovas et al., 2010, 2015a); 6, Palaeohydrology vs Fluvial Geomorphology (Baker, 1987; Baker et al., 1988; Kochel and Baker, 1982).

Figure 2. (a) Geographic setting, with the Pyrenees marked with a red square. (b) Geological setting of the study area, located in the Axial Pyrenees, and the area of Fig. 2c marked with a red square. (c) Geomorphological context of the Portainé basin and the specific study area marked with a black square, corresponding to the most downstream reach.

Figure 3. Flow diagram showing the multidisciplinary methodology applied in this study for palaeoflood reconstruction, from data sources to results, following four main disciplines: geomorphology, dendrogeomorphology, paleodischarge estimation and flow hydrodynamics.

Figure 4. External disturbances on trees located in the riverbanks of the Portainé stream. (a) Scar formed in 2008. (b) Stem tilting. (c) Decapitated tree.

Figure 5. (a) Detailed geomorphological mapping (September 2015) of the alluvial cone showing the main geomorphological features, forms, deposits and the position of the trees that have been sampled for the dendrogeomorphological analysis; where trees are colored by the geomorphic position. (b), (c), (d), (e), (f), (g) Pictures showing examples of different geomorphic positions identified in the study area.

Figure 6. Peak discharge estimation for 2008 from the TIN-based hydraulic modelling. The accepted value corresponds to the minimum mean squared error obtained from the average of the squared errors of 18 tree scars.

Figure 7. Bathymetric map of the flooded area for the 2008 event, corresponding to the alluvial cone.

Figure 8. Relation between dendrogeomorphological evidence and geomorphic forms, organized by the increase of the flow energy. The size of the symbols represents the number of FDE per tree.

Figure 9. Flow velocity – depth diagram for the formation of scars, classified by the geomorphic form in which they are located. The arrow indicates the increase of the flow energy.

Supplementary material 1

[Click here to download Supplementary material for on-line publication only: Table_1.docx](#)

Supplementary material 2

[Click here to download Supplementary material for on-line publication only: Table_2.docx](#)